

FABRICATION OF WELL-ORGANIZED PLASMONIC INTERFACES BY
NANOSPHERE LITHOGRAPHY

A THESIS SUBMITTED TO
THE GRADUATE SCHOOL OF NATURAL AND APPLIED SCIENCES
OF
MIDDLE EAST TECHNICAL UNIVERSITY

BY

YUSUF KASAP

IN PARTIAL FULFILLMENT OF THE REQUIREMENTS
FOR
THE DEGREE OF MASTER OF SCIENCE
IN
PHYSICS

FEBRUARY 2016

Approval of the Thesis:

**FABRICATION OF WELL-ORGANIZED PLASMONIC INTERFACES BY
NANOSPHERE LITHOGRAPHY**

submitted by **YUSUF KASAP** in partial fulfillment of the requirements for the degree
of **Master of Science in Physics Department, Middle East Technical University**
by,

Prof. Dr. Gülbin Dural Ünver
Dean, Graduate School of **Natural and Applied Sciences**

Prof. Dr. Mehmet T. Zeyrek
Head of Department, **Physics**

Assoc. Prof. Dr. Alpan Bek
Supervisor, **Physics Dept., METU**

Examining Committee Members:

Assoc. Prof. Dr. Serhat Çakır
Physics Dept., METU

Assoc. Prof. Dr. Alpan Bek
Physics Dept., METU

Assist. Prof. Dr. Halil Berberoğlu
Physics Dept., Gazi University

Assist. Prof. Dr. Selçuk Yerci
Electrical & Electronics Engineering Dept., METU

Assist. Prof. Dr. Emre S. Taşçı
Physics Engineering Dept., Hacettepe University

Date: 05.02.2016

I hereby declare that all information in this document has been obtained and presented in accordance with academic rules and ethical conduct. I also declare that, as required by these rules and conduct, I have fully cited and referenced all material and results that are not original to this work.

Name, Lastname: Yusuf Kasap
Signature :

ABSTRACT

FABRICATION OF WELL-ORGANIZED PLASMONIC INTERFACES BY NANOSPHERE LITHOGRAPHY

Kasap, Yusuf

M.S., Department of Physics

Supervisor: Assoc. Prof. Dr. Alpan Bek

February 2016, 101 pages

In this thesis, we propose to design plasmonic metal nanostructures by utilizing lithography with nanospheres of various diameters. When deposited at a high surface coverage, nanospheres form closed-pack trigonal lattices on surfaces, leaving concave triangular gaps in-between. After evaporation of thin metal films and lifting-off the nanospheres, metal islands which support plasmonic resonances and of the gap shape are fabricated in a trigonal periodicity on the substrate material. Depending on nanosphere diameter, the size of the triangular shaped nanostructures can be rearranged.

In addition to classical nanosphere lithography (NSL) method, the physical influences that affect the fabrication method were also be considered in order to move beyond one step further. In other words, using annealing and physical etching mechanisms; size, shape of nanostructures and total surface coverage parameters were taken under control without deforming the system.

Using these, our aim is to produce metal nanoparticle in desired shape and periodicity for plasmonic applications. Moreover, another goal is to prove that nanosphere lithography is a powerful tool especially for surface modification. In order to show that, how close-pack structure can be used is discussed by giving examples of different lithographic modifications.

In this thesis work, we focus on experimental details of NSL and its extensions. After defining stages of production, we also show that NSL can be used to fabricate periodic metal structures with identical geometry and size, plasmonic interfaces with adjustable surface coverage, microlens arrays, and capability for generating 3D photonic crystals and adaptability with different lithography methods. In order to show them, we have used Scanning Electron Microscope (SEM), Raman Spectroscopy, total reflection techniques to characterize the nanostructures. Thanks to Comsol simulations and Gwyddion image analysis, experimental results are analyzed.

Keywords: Nanosphere Lithography, Metal Nanoparticles, Plasmonic interface, Electric field enhancement

ÖZ

İYİ DÜZENLENMİŞ PLAZMONİK ARAYÜZEYLERİN, NANOKÜRE LİTOGRAFI YÖNTEMİ İLE ÜRETİMİ

Kasap, Yusuf
Yüksek Lisans, Fizik Bölümü
Tez Yöneticisi: Doç. Dr. Alpan Bek

Şubat 2016, 101 sayfa

Bu tezde, değişik çaplardaki nanokürelerle litografiden istifade ederek plazmonik metal nano parçacıklarını dizayn etmeyi önermekteyiz. Nanoküreler geniş bir yüzey kapsamında çökertildiğinde, ortalarında üçgensel aralıklar bırakacak şekilde kapalı-paket üçgensel kafessel bölgeler oluşturur. İnce metal filmlerin buharlaştırılmasından ve nano kürelerin kaldırılmasından sonra plazmonik rezonansları destekleyen ve nanoküreler arasındaki şeklini belirleyen metal adalar üçgensel bir dönemsellikte substrat materyalin üzerinde üretilir. Nanoküre çapına bağlı olarak üçgensel nanoparçacıkların boyutu ayarlanabilmektedir.

Klasik Nanoküre Litografisinin yanı sıra, sisteme etki eden bazı fiziksel etkilerin nasıl klasik yöntemi bir adım öteye götüreceği ele alınmıştır. Farklı bir deyişle, fırınlama ve fiziksel aşındırma mekanizmaları kullanılarak nanoparçacık boyutu, şekli ve yüzey dağılımı parametreleri system yapısını bozmadan kontrol altına alınabilmektedir.

Bunlar kullanılarak, plazmonik uygulamalar için kullanılacak olan metal nanoparçacıkların istenilen şekil ve periyodik yapıda üretmeyi hedeflemekteyiz. Ayrıca diğer bir hedefimiz, nanoküre litografinin özellikle yüzey modifikasyonu için neden önemli olduğu kanıtlamaktır. Bunun için farklı litografi tekniklerinden örnekler verilerek kapalı paketler halinde oluşturulan yapının nasıl kullanılabilineceği tartışılacaktır.

Bu tez çalışmasında, nanoküre litografi ve uzantılarının deneysel detayları üzerinde durulacaktır. Üretim aşamalarının tanımlanmasından sonra ise bu metodun eş geometri ve boyuttaki metal yapıların üretimi, yüzey kapsaması ayarlanabilir plazmonik arayüzler, mikrolens dizilimleri, 3D fotonik kristal üretim kabiliyeti ve farklı litografi metodlarına adapte olabilesi kanıtlamaktayız. Bunu göstermek amacıyla, taramalı elektron mikroskobu, raman spektroskopisi ve yansıma tekniklerini nanaoyapıların karakterizasyonu için kullandık. Comsol simulasyon ve Gwyddion resim analizi yardımıyla deneysel veriler analiz edilmektedir.

Anahtar kelimeler: Nanoküre litografisi, Metal nanoparçacıklar, Plazmonik arayüz, Elektrik alan güçlendirilmesi

To my family

ACKNOWLEDGEMENTS

I would like to express my deep gratitude to my master thesis advisor, Assoc. Prof. Dr. Alpan Bek. I've acquired many theoretical and experimental knowledge since I became his student. He share his time providing useful suggestions about my study. I want to present my appreciation to Prof. Dr. Rařit Turan and Prof. Dr. Mehmet Parlak giving me opportunities to work in their laboratories.

It is a great pleasure for me to thank Mona Zolfaghariborra, İbrahim Murat Öztürk, Arezoo Hosseini, Tahir Çolakođlu, Musa Kurtuluř Abak for their supports during my studies.

I am thankful to Hande Çiftpınar, Hasan Hüseyin Güllü, Ergi Dönerçark, Yasin Ergunt, Fırat Es, Salar Sedani, Hisham Nasser, Mustafa Ünal, Merve Pınar Kabukçuođlu, Engin Özkol, Mete Günöven, Yiđit Ozan Aydın, Seda Kayra Güllü, Bilge Can Yıldız, Özden Bařar Balbařı, Zeynep Demirciođlu, Olgu Demirciođlu, Serra Altınoluk, Zeynep Nilüfer Güven, Mehmet Karaman and all other GUNAM family that I forgot to mention.

I am grateful to thank my close friends; Burak Aydemir, Masum Deniz, Bayram Kaya, Eray Canlı, Sedat Çapar, Deniz Kennedy, Onur Oktay, Cenk Türkođlu, Cořkun Marangoz, and Neslihan Dođan Aydemir keeping me motivated all the time.

I kindly acknowledge financial support from TUBİTAK under project no: 113F239

Finally, I would like to express my endless thanks and motivation to my family supporting me throughout all my life.

TABLE OF CONTENTS

ABSTRACT.....	v
ÖZ.....	vii
ACKNOWLEDGEMENTS.....	x
TABLE OF CONTENTS.....	xi
LIST OF TABLES.....	xiv
TABLE OF FIGURES.....	xv
CHAPTERS	
1. INTRODUCTION.....	1
2. OPTICAL AND CHEMICAL INTERACTIONS OF SUBMICRON PARTICLES	5
2.1 OPTICAL INTERACTION.....	5
2.1.1 Introduction.....	5
2.1.2 Maxwell's Equations.....	7
2.2.1 Vector solutions.....	9
2.2.2 Recurrence equations.....	10
2.2.3 Expansion Coefficients.....	11
2.1.3 Mie Theory.....	13
2.1.4 Plasmonics.....	16
2.1.4.1 Lorentz Model.....	17
2.1.4.2 Drude Model.....	19
2.1.5 Photonic Crystals.....	21
2.2 Chemical Particle Interaction.....	22
2.2.1 Van de Waals Interaction.....	23
2.2.2 Electrostatic Interaction.....	24

2.2.3 DVLO Theory	26
3.NANOLITHOGRAPHY	29
3.1 Top-Down Approach.....	31
3.1.1 Photolithography Technique	34
3.1.2 X-Ray Lithography Technique	35
3.1.3 NanoImprint Lithography	37
3.1.4 Electron Beam Lithography Technique	39
3.2 Bottom-Up Approach	41
3.2.1 Self-Assembly of Nanoparticles	42
3.2.2 Chemical Vapor Deposition.....	43
4. NANOSPHERE LITHOGRAPHY	47
4.1 Introduction	47
4.2 Nanosphere Lithography Method (NSL) and History.....	48
4.3 Pattern Formation Equipments	51
4.3.1 Cleanroom environment.....	51
4.3.2 Surface cleaning and treatment chemicals	51
4.3.3 Nanosphere solution.....	51
4.3.4 Centrifuge.....	52
4.3.5 Thermal evaporation coating system.....	52
4.3.6 Oxygen plasma device	52
4.3.7 Furnace	53
4.4 Procedure And Results	53
4.4.1 Nanosphere Selection.....	53
4.4.2 Surface Treatment and Cleaning	55
4.4.3 Nanosphere Deposition	56
4.4.3.1 Drop Casting.....	56

4.4.3.2	Langmuir Blodgett Like	61
4.4.4	Thin Film Deposition	63
4.4.5	Lift –Off	66
4.5	Beyond the Capabilities of Classical Nanosphere Lithography	68
4.5.1	Double Layer Structures	68
4.5.2	Annealing Nanoparticles	70
4.5.3	Oxygen Plasma Treatment	72
4.5.4	Annealing Nanospheres	74
4.6	Image Analysis	77
4.7	Numerical Calculation.....	81
4.8	Optical Measurements	88
4.8.1	Surface Enhanced Raman Measurement.....	88
4.8.2	Reflection Measurement	91
5.	CONCLUSIONS.....	93
	REFERENCES.....	97

LIST OF TABLES

TABLES

Table 3. 1 Comparison between Top-Down lithography methods with respect to minimum size feature, pattern, area, cost, time and industry	33
Table 3. 2 Different technologies using a mold.....	38

TABLE OF FIGURES

FIGURES

Figure 2. 1 Schematic of surface plasmonic resonance where the free conduction electrons in the metal nanoparticle are driven into oscillation due to strong coupling with incident light.	17
Figure 2. 2 Two identical flat plate	23
Figure 2. 3 Distance and concentration dependency of Stern Model	25
Figure 2. 4 Total interaction potential of two spheres.....	27
Figure 3. 1 Nanoparticle generation by means of top-down and bottom-up approach	31
Figure 3. 2 Schematic diagram of top-down approach	32
Figure 3. 3 Process steps of Photolithography by using positive and negative photoresist material	35
Figure 3. 4 X-ray proximity lithography with a collimated light source	37
Figure 3. 5 Schematic diagram of Thermoplastic Nanoimprint lithography and Photo Nanoimprint Lithography.....	37
Figure 3. 6 Electron Beam Lithography.....	39
Figure 3. 7 Snowflake like structure produced by Electron Beam Lithography.....	40
Figure 3. 8 Schematic diagram of Bottom-up approach	41
Figure 3. 9 Examples of self-assembled magnetic nanoparticles.....	43
Figure 3. 10 Schematic drawing of Chemical Vapor Deposition System.....	44
Figure 4. 1 The convergence of top-down and bottom-up approaches.....	48
Figure 4. 2 Schematic process diagram of NSL.....	49
Figure 4. 3 Schematic diagram of particle distance and size calculation.....	53
Figure 4. 4 Surface coverage of close-pack nanosphere structure	54
Figure 4. 5 Low concentration single layer nanosphere array	58

Figure 4. 6 Formation of single drop of water on hydrophilic and hydrophobic surface	59
Figure 4. 7 Single layer non close-pack nanosphere stucture	60
Figure 4. 8 Monolayer hexagonal close pack nanosphere structure.....	61
Figure 4. 9 Process steps of Langmuir Blodgett like surface coating	62
Figure 4. 10 Monolayer hexagonal close-pack nanosphere structure created by Langmuir Blodgett Like method	63
Figure 4. 11 Schematic diagram of thermal evaporation coating system	65
Figure 4. 12 Triangular silver lattices with defects	66
Figure 4. 13 Chemical nanosphere mask removal process	67
Figure 4. 14 Well-ordered triangular silver nanoparticles after lift-off.....	68
Figure 4. 15 Double layer well-ordered hexagonal close-pack nanosphere structure	69
Figure 4. 16 Schematic diagram of double layer structure and transformation of gap between nanospheres.....	70
Figure 4. 17 Rounded shape silver nanoparticles after annealing at 200 °C for 1 hour	71
Figure 4. 18 Reduction in size of 400 nm polystyrene nanosphere after oxygen plasma treatment.....	73
Figure 4. 19 Size distribution of 400 nm polystyrene nanosphere after oxygen plasma treatment.....	74
Figure 4. 20 Close-pack structure of 750 nm polystyrene nanosphere before annealing	75
Figure 4. 21 Close-pack structure of 750 nm polystyrene nanosphere after annealing at 120 °C for 5 min	76
Figure 4. 22 Close-pack structure of 750 nm polystyrene nanosphere after annealing at 120 °C for 8 min	76
Figure 4. 23 Close-pack structure of 750 nm polystyrene nanosphere after annealing at 120 °C for 12 min	77
Figure 4. 24 Gwyddion particle selection of spherical particles after annealing triangular ones	79
Figure 4. 25 Particle size distribution of Figure 4.24.....	80

Figure 4. 26 Gwyddion particle selection of spherical particles after reducing triangular gaps and annealing triangular ones.....	80
Figure 4. 27 Particle size distribution of Figure 4.26.....	81
Figure 4. 28 Normalized electric field distribution caused by the interaction between 120 nm spherical single nanoparticle and x polarized electric field propagating along y direction.....	84
Figure 4. 29 Normalized electric field distribution caused by the interaction between two 120 nm spherical nanoparticles and x polarized electric field propagating along y direction.....	85
Figure 4. 30 Coupling and normalized electric field distribution caused by the interaction between two 120 nm spherical nanoparticles and x polarized electric field propagating along y direction.....	85
Figure 4. 31 Normalized electric field distribution caused by the interaction between 200 nm triangular single nanoparticle and x polarized electric field propagating along y direction.....	86
Figure 4. 32 Coupling and normalized electric field distribution caused by the interaction between two 200 nm triangular nanoparticles and x polarized electric field propagating along y direction.....	87
Figure 4. 33 Refraction of light from air-silicon interface.....	88
Figure 4. 34 Raman measurement of silicon wafer and 200 nm triangular silver nanoparticle coated silicon wafer.....	89
Figure 4. 35 Raman measurement of silicon wafer and 120 nm spherical silver nanoparticle coated silicon wafer.....	90
Figure 4. 36 Reflection measurement of uncoated and close-pack nanosphere coated silicon wafer.....	92

CHAPTER 1

INTRODUCTION

Nanotechnology is a technology which is conducted on nanoscale and new technological advances can be mastered in this science. Nanotechnology is defined as the design, characterization, production and application of structures, devices and systems by controlling shape and size at nanometer scale (The Royal Society & The Royal Academy of Engineering, 2004a). A nanometer (nm) is one thousand millionth of a meter in which materials behave differently, showing characteristics that vary physically, chemically, and biologically from their larger counterparts. Nanomaterials can be employed in variety of applications ranging from optics to electronics and biomedical fields.

A nanoparticle is the substantial part in the fabrication of a nanostructure. General size of a nanoparticle spans the range between 1 and 100 nm. Nanoparticles are larger than individual atoms and molecules but they are smaller than bulk solid. Even though they can be generated by bulk material and expected to exhibit same characteristic, they can be different. For instance, metallic nanoparticles can present variable physical and chemical characteristics from bulk metals such as lower melting points, higher specific surface areas and specific optical properties. Furthermore, the optical property is one of the fundamental attractions and a characteristic of a nanoparticle. Due to the different properties, the quantum chemistry or classical physics laws are not thoroughly expected in the structure of nanoparticles. These differences occur because of two separate phenomena.

The first phenomenon referred to the fact that when the size of a crystal is decreased, the number of atoms at the surface of the crystal will be ascended. Therefore, the high dispersity can be observed in nanocrystalline systems.

The second phenomenon can be observed in metals and semiconductors. The size of a nanoparticle is similar to the de Broglie wavelength of its charge carriers which is

called size quantization effect. The valance and conduction bands of nanoparticles are divided into quantized levels. These electronic levels are comparable to the ones that exist in atoms and molecules [1].

The splitting of levels and the bandgap can be enhanced by reducing the particle size. The increase in the coulombic interaction between electron hole pairs are responsible for this effect. Because, an electron hole pair will be located close to each other by decreasing the size. In large bandgap materials, more energy is needed for the excitement process. Therefore, light with a higher frequency or shorter wavelength would be absorbed.

Nanotechnology can be considered as an interdisciplinary approach. The concept of nanotechnology was first noted by Richard P. Feynman at his speech by the name of “There's Plenty of Room at the Bottom”[2]. This classic talk was in 1959. After that, in a short time later, many scientists in different fields got attracted to this new concept and implemented it to their research area. Not only nanotechnology found many answers to today’s challenges but also there can be lots of innovations and new sights in it. The area of nanotechnology is so wide, therefore selected applications including nanoparticles are presented in following parts. One of the most commonly applicable area of nanotechnology is for electronic devices. Besides, having smaller sizes in devices require less raw material. This means, with these small electronic devices, new forms of electronic circuit boards and computer memories were offered.

In nano scale, the properties of materials are changed; due to this fact the application of nanoparticles as fillers have been presented in the composite materials. As an illustration, ceramics can be obtained softer and metals tougher. In addition to that, solar energy collection or photovoltaics are described as widely used areas of nanotechnology. With the help of it, it is possible to get flexible, thinner and cost effective solar cells with high efficiency. There is a vast usage of this technology with nanoparticles in medicine. There are sensors and tools for medical diagnostics. Furthermore In medical approaches in order to repair and replace damaged cells, skin, bone, tissue, the idea of combination of nanotechnology and biotechnology makes a great result. Besides, through neuronavigation, which is one of the advantages of

nanotechnology, serious scars for the surgery will be reduced in the future. Drug delivery is another application field in medicine. The possibility of manipulation of nanoparticles for delivering drugs makes this field so attractive. For example, the drug can be carried by nanoparticles and released as fixed doses of the drug over specified period of time [3].

All of these areas are supported by nanotechnological investigations that need controllable procedures. For this reason, such nanotechnologic devices and systems require nanometer scale resolution that makes nanotechnology to proceed for this purpose. With changing size, materials get new physical and chemical identities that are distinct from bulk. This circumstance creates an opportunity for such areas like optics, magnetism, chemistry ...etc [4].

In addition to suitable and desired nanostructure production, the goal of ideal fabrication technique based on cost effective, flexible and easily controllable generation with respect to size and periodicity. Even though most of the commercial methods have capability to produce intended size, shape and inter-particle distance structures, like resolution, special equipment requirement or long process time, the limitations restrict the area of usage of most lithographic methods. For example, photolithography is one of the most used commercial method for large area production of electronic and semiconductor devices but diffraction limit of UV source prevent to reach nanometer scale. Considering Electron Beam Lithography which is well-known method due to its high resolution is not suitable for large area manufacturing because of its long process time. Special equipment requirement makes it also expensive. For these reasons, researchers move towards on well-organized self-assembled processes since two decades. Thanks to investments in new physical and chemical synthesis methods, self-assembly approach can be applied in a more controllable way than before. One of the most powerful techniques known for its cost effectiveness, high resolution capability and adaptability to most lithography methods is NSL [5].

In this thesis, the main concern is to stand on surface nano structuring by means of NSL techniques. This technique can be described as the combination of top-down and bottom-up approaches. In other words, top-down approach takes built pieces of material and transforms it into small pieces. On the contrary, bottom-up approach uses small pieces and create bigger structure by joining them together. Both methods

include different type of structuring methods. Each methods have their own capabilities. However, it is possible to face with some restrictions such as large area usage, cost effectiveness, resolution or time while focusing on one simple method. For this reason, NSL is used for its cost effectiveness, small particle size contribution and time saving properties to produce plasmonic metal nanostructures for large areas. Large scale nanosphere size provides to bring out desired size structures for metals and non-metals. Furthermore, mono dispersity and stable size distribution producibility adjust well-oriented periodicity. In addition to nanoparticle formation, this method is used for surface modification with the combination of other mechanisms like etching. For instance, it is easy to produce single nanohole or nanowire structures by adding few external steps to NSL. In this thesis, plasmonic metal nanostructure generation will be discussed in detail.

In Chapter 2, brief information will be given to describe what the surface plasmons are. To better understand the concept of surface plasmons, it is essential to make connection between electromagnetic wave and the metal nano particles. The solution of Maxwell's equations with boundary conditions gives satisfactory results for concept of surface plasmons and their electrical and magnetic properties. For this reason, analytic solution of Maxwell's equation will be considered. Moreover, one of most important point for NSL is chemical particle-particle interactions for surface manufacturing. Therefore, the effective chemical forces will be handled.

In Chapter 3, top-down and bottom-up approaches will be discussed. Some convenient methods, their advantages and drawbacks will be mentioned. Then, the position of NSL in nanostructuring processes will be presented by comparing it with other methods.

In Chapter 4, what NSL technique is and its experimental steps will be discussed in detail. Moreover, what makes this technique powerful and how effective it is to produce nanoparticles for plasmonic applications will be deliberated. Then, except from classical method of it, new arrangements and modifications of this technique will be mentioned.

Finally, by using classical and extended version of NSL, results, improvements, future studies and new applications of this study will be given and discussed.

CHAPTER 2

OPTICAL AND CHEMICAL INTERACTIONS OF SUBMICRON PARTICLES

2.1 OPTICAL INTERACTION

2.1.1 Introduction

In chemistry, every matter includes protons and electrons. When these electric charges interact with light that is also described as electromagnetic wave, they exhibit oscillations. These oscillations lead to incident and secondary radiations. While incident radiation are absorbed inside the material, secondary radiations are emitted. The extinguished ones are called as absorbing and the other ones are scattering. Both absorbing and scattering parts are described as complex and real index of refraction respectively. Both radiations bring about the decreasing intensity of the incident light. This total intensity reduction of it is called extinction which is the sum of absorbing and scattering [6].

All of the quantities are explained by the light-matter interaction. Interactions can be divided into two main explanation depending on Mie Theory and Ray Optics. The concept of Mie Theory based on Maxwell's Equations. By applying boundary condition to equations, internal, incident and scattered wave field conditions are calculated. Calculations are mostly supported by vector harmonics. Also, vector harmonics are defined as infinite series expansions. Furthermore, such chemical and physical values affect the interaction between light and matter. These influences are based on the shape of the particle, refractive index of particle depending wavelength and medium and contact angle between incident light and matter.

Size parameter of spherical particle resonance is calculated as

$$\chi = \frac{2\pi a n}{\lambda} \quad (2.1)$$

Where a is particle radius. Also, the wavelength of the incident light changes while transferring one medium to another. Depending on the refractive index comparison,

wavelength shift to higher or lower wavelengths. For this reason, λ/n term describes the new wavelength value inside the surrounding medium. In addition to Mie Theory, ray optics try to explain the reflection and refraction parameters while passing through the particle. By using both parameters, the net forces and energies acting on particle are calculated.

Generally, the calculations are applied with respect to the plane wave or Gaussian wave. When these wave interact with the particle, it loses its own identity and transfer its energy to particle. Then, scattering and absorption appear due to interaction. To better understand the theoretical approach underlying this circumstances, Mie Theory tries to explain.

The first observation about the interaction between the microscopic particle and light are done by Kwata. The experiment consists of 150 mW Nd:YAG laser source and polystyrene and silica particles. Because of Mie Theory study, the particle size should not be so large; on the contrary, it should be small. For this reason, Kwata used micron-sized particles. After Kwata's experiment, Alamaas and Brevik tried to explain experimental results by means of Mie Theory. After that, Waltz worked on Alamaas and Brevik study and tried to clarify it by mean of ray optics. He found that ray optics can only work well in a condition that the particle radius are at least 20 times bigger than incident wavelength. For this reason, Mie theory are very essential due to their large area of usage for most particles sizes.

To describe the Mie Theory, one of the most important point is wave excitation. As mentioned before, plane wave is suitable for general case. Considering an incident wave,

$$\vec{E}_{inc} = E_0 e^{i\beta z} \hat{x} \quad (2.2)$$

To give a more information about the wave, E_0 represents amplitude value of wave which is the scalar quantity. Moreover, the wave propagating along z direction with x direction polarization. β is the propagation constant.

In this study, given plane wave description provide a basis for the solution of the Maxwell's equations. With the help of vector solutions, it is possible to solve it in such coordinate system. Spherical coordinate system will be used due to spherical particle

in this study. It gives more information for both radial and angular parts. While applying such calculations, it is needed to some special functions and polynomials and their recurrence relations like Bessel function Legendre polynomials. Finally, Mie scattering and internal coefficients will be found by applying boundary conditions.

2.1.2 Maxwell's Equations

For Mie theory, Maxwell's Equations should be solved in spherical coordinates. Therefore, the starting point shall be writing Maxwell's equations and finding E and H field

From curl of Electric Field and Magnetic field

$$\nabla \times \vec{E} = i\omega\mu\vec{H} \quad (2.3)$$

$$\nabla \times \vec{H} = -i\omega\epsilon_m\vec{E} \quad (2.4)$$

Then, it can written as

$$\begin{aligned} \nabla \times (\nabla \times \vec{E}) &= \nabla \times (i\omega\mu\vec{H}) = i\omega\mu (\nabla \times H) = i\omega\mu (-i\omega\epsilon_m\vec{E}) \\ &= \omega^2\mu\epsilon_m\vec{E} \end{aligned} \quad (2.5)$$

$$\begin{aligned} \nabla \times (\nabla \times \vec{H}) &= \nabla \times (-i\omega\epsilon_m\vec{E}) = -i\omega\epsilon_m (\nabla \times \vec{E}) = -i\omega\epsilon_m (i\omega\mu\vec{H}) \\ &= \omega^2\mu\epsilon_m\vec{H} \end{aligned} \quad (2.6)$$

By using definition of vector identity

$$\nabla \times (\nabla \times \vec{A}) = \nabla (\nabla \cdot \vec{A}) - \nabla \cdot (\nabla \vec{A}) \quad (2.7)$$

Both equations 2.5 and 2.6 can be written as

$$\omega^2\mu\epsilon_m\vec{E} = \nabla (\nabla \cdot \vec{E}) - \nabla \cdot (\nabla \vec{E}) \quad (2.8)$$

$$\omega^2\mu\epsilon_m\vec{H} = \nabla (\nabla \cdot \vec{H}) - \nabla \cdot (\nabla \vec{H}) \quad (2.9)$$

With the definition of $\nabla (\nabla \cdot \vec{E}) = \nabla (\nabla \cdot \vec{H}) = 0$, both equations can be written as

$$\nabla^2 \vec{E} + \omega^2\mu\epsilon_m\vec{E} = 0 \quad (2.10)$$

$$\nabla^2 \vec{H} + \omega^2\mu\epsilon_m\vec{H} = 0 \quad (2.11)$$

To solve the wave equations, it is essential to solve in spherical coordinates by defining scalar function $\psi_{l,m}$ and vector \vec{r} . Moreover, it is needed vector solutions which are \vec{L} , $\vec{M}_{l,m}$ and $\vec{N}_{l,m}$ for equations 2.10 and 2.11 where,

$$\vec{L} = \nabla\psi_{l,m} \quad (2.12)$$

$$\vec{M}_{l,m} = \nabla \times \vec{r}\psi_{l,m} \quad (2.13)$$

$$\vec{N}_{l,m} = \frac{1}{k_m} \nabla \times \vec{M}_{l,m} \text{ Where } k_m^2 = \omega^2 \mu \epsilon_m \quad (2.14)$$

While $\vec{M}_{l,m}$ and $\vec{N}_{l,m}$ are the selenoidal functions, \vec{L} is defined as longitudinal wave

Main goal is to solve equation in spherical coordinates. For this reason, scalar solution $\psi_{l,m}$ should include R , θ and ϕ dependency. By using the solution of spherical coordinates system as

$$\nabla^2 = \frac{1}{r^2} \frac{\partial}{\partial r} \left(r^2 \frac{\partial}{\partial r} \right) + \frac{1}{r^2 \sin \theta} \frac{\partial}{\partial \theta} \left(\sin \theta \frac{\partial}{\partial \theta} \right) + \frac{1}{r^2 \sin^2 \theta} \frac{\partial^2}{\partial \phi^2} \quad (2.15)$$

Then

$$\begin{aligned} \nabla^2 \psi = \frac{1}{r^2} \frac{\partial}{\partial r} \left(r^2 \frac{\partial \psi}{\partial r} \right) + \frac{1}{r^2 \sin \theta} \frac{\partial}{\partial \theta} \left(\sin \theta \frac{\partial \psi}{\partial \theta} \right) + \frac{1}{r^2 \sin^2 \theta} \frac{\partial^2 \psi}{\partial \phi^2} \\ + k_m^2 \psi = 0 \end{aligned} \quad (2.16)$$

By writing equation $\psi(r, \theta, \phi) = R(r)\theta(\theta)\Phi(\phi)$, scalar function can be solved separately.

By putting R , θ and Φ into equation 2.16, it is found

$$\frac{\partial^2 \Phi}{\partial \phi^2} + m^2 \Phi = 0 \quad (2.17)$$

Then, the solution of equation 2.17 is $\Phi = e^{\pm im\phi}$

Note that, solution of Φ is described as $\cos m\phi$ and $\sin m\phi$ for even and odd functions respectively.

$$(1 - \cos^2 \Theta) \frac{\partial^2 \Theta}{\partial (\cos \Theta)^2} - 2 \cos \Theta \frac{\partial \Theta}{\partial \Theta} + \left[Q - \frac{p^2}{(1 - \cos^2 \Theta)} \right] = 0 \quad (2.18)$$

To make the equation Legendre like, the notation $Q = l(l + 1)$ should be used. Then, Θ function can be found as

$$\Theta = P_l^m(\cos \Theta) = \frac{(1 - \cos^2 \Theta)^{m/2} d^{l+m}(\cos^2 \Theta - 1)^l}{2^l l! d(\cos \Theta)^{l+m}} \quad (2.19)$$

Then, the remaining R equation becomes

$$r^2 \frac{d^2 R}{dr^2} + 2r \frac{dR}{dr} + (k_m^2 r^2 - Q^2) = 0 \quad (2.20)$$

By applying $p = k_m r$ formation, the solution of radial part R can be calculated as

$$R = \sqrt{\frac{2}{\pi}} Z_l(p) \quad (2.21)$$

$Z_l(p)$ value is the combination of radial spherical Bessel function $j_l(p)$ and first order Henkel function $h_l(p)$. The solution of radial spherical function is used to calculate incident and transmitted fields acts whereas Henkel function shows the scattering wave fields.

Finally, combining all radial and angular solutions, scalar wave function $\psi(r, \Theta, \Phi)$ becomes

$$\psi_{l,m,e,o}(r, \Theta, \Phi) = \sqrt{\frac{2}{\pi}} Z_l(p) P_l^m \frac{\cos \Theta}{\sin \Theta} m \phi \quad (2.22)$$

Where e and o notations represent even and odd functions.

2.2.1 Vector solutions

In equation 2.23, vector solution of $\vec{M}_{l,m}$ was described and $\vec{M}_{l,m}(\hat{r}) = 0$. Then, $\vec{M}_{l,m}$ can be represented as even and ode modes as

$$\vec{M}_{l,m,\theta} = \nabla \times \hat{r}(r\psi_{l,m,\theta}) \quad (2.23)$$

$$\begin{aligned} \vec{M}_{l,m,\theta} &= \frac{1}{r \sin \theta} \frac{d(r\psi)}{d\phi} \hat{\theta} - \frac{1}{r} \frac{d(r\psi)}{d\theta} \hat{\phi} \\ &= \pm Z_l \frac{P_l^m}{\sin \theta} \frac{\sin \theta}{\cos \theta} m\phi \hat{\theta} - Z_l \frac{dP_l^m}{d\theta} \frac{\cos \theta}{\sin \theta} m\phi \hat{\phi} \end{aligned} \quad (2.24)$$

In equation (....) $\vec{N}_{l,m,\theta}$ value was described as $\vec{N}_{l,m} = \frac{1}{k_m} \nabla \times \vec{M}_{l,m}$. Then,

$$\begin{aligned} \vec{N}_{l,m,\theta} &= \frac{l(l+1)}{k_m r} \psi_{\theta}^e \hat{r} + \frac{1}{k_m r} \frac{d(r\vec{M}_{l,m,\phi})}{dr} \hat{\theta} + \frac{1}{k_m r} \frac{d(r\vec{M}_{l,m,\theta})}{dr} \hat{\phi} \\ &= \frac{l(l+1)}{k_m r} Z_l P_l^{m \cos} \frac{m\phi}{\sin} \hat{r} + \frac{1}{r} \frac{d(pZ_l)}{dp} \frac{P_l^{m \cos}}{d\theta_{\sin}} m\phi \hat{\theta} \\ &\quad \pm m \frac{1}{p} \frac{d(pZ_l)}{dr} \frac{P_l^{m \cos}}{\sin \theta_{\sin}} m\phi \hat{\phi} \end{aligned} \quad (2.25)$$

2.2.2 Recurrence equations

To make analysis for Mie, several recurrence relations are needed to solve radial and associated Legendre functions.

$$Z_{l+1}(p) = \frac{(2l+1)}{p} j_l(p) - j_{l-1}(p) \quad (2.26)$$

$$[j_{l+1}(p)]' = \frac{1}{l+1} \left[\frac{l}{2l+1} j_{l-1}(p) - (2l+1) j_l(p) \right] \quad (2.27)$$

By using standard Legendre polynomial definition, the relations of associated Legendre polynomials are calculated as

$$P_{l+1}^m = \frac{1}{l-m+1} [(2l+1) \cos \theta P_l^m - (l+m) P_{l-1}^m] \quad (2.28)$$

$$\frac{m P_l^m}{\sin \theta} = \frac{1}{2 \cos \theta} [P_l^{m+1} + (l(l+1) - m(m-1)) P_l^{m-1}] \quad (2.29)$$

$$\frac{dP_l^m}{d\theta} = \frac{1}{2} [(l-m+l(l+m)) P_l^{m-1} - P_l^{m+1}] \quad (2.30)$$

$$\frac{d}{d\theta} = -\sqrt{1 - \cos^2 \theta} \frac{d}{d(\cos \theta)} \quad (2.31)$$

$$P_l^{-m} = (-1)^m \frac{(l-m)!}{(l+m)!} P_l^m \quad (2.32)$$

2.2.3 Expansion Coefficients

By using Biot Savart Rule, the magnetic current B can be defined

$$B(r) = \frac{\mu_0}{4\pi} \int \frac{J(r') \times (r - r')}{|r - r'|^3} d^3 r' \quad (2.33)$$

Then, $\frac{(r-r')}{|r-r'|^3}$ function can be written as a curl function as

$$\frac{(r - r')}{|r - r'|^3} = -\nabla \times \frac{1}{|r - r'|} \quad (2.34)$$

By applying equation (2.34) into equation (2.33) magnetic current can be written

$$B(r) = \frac{\mu_0}{4\pi} \nabla \times \int \frac{J(r')}{|r - r'|} d^3 r' \quad (2.35)$$

The function of $\frac{\mu_0}{4\pi} \int \frac{J(r')}{|r - r'|} d^3 r'$ is defined as vector potential. Therefore,

$$B = \nabla \times A \quad (2.36)$$

If the vector potential is constituted by the combination of vector functions $\vec{M}_{l,m}$ and $\vec{N}_{l,m}$ as

$$\vec{A} = \frac{i}{\omega} \sum_{l,m} [A_{l,m} \vec{M}_{l,m} + B_{l,m} \vec{N}_{l,m}] \quad (2.27)$$

Magnetic field can be written as

$$\begin{aligned} \vec{H}_{inc} &= \frac{1}{i\omega\mu} \nabla \times \vec{A} = -\frac{i}{\omega\mu} \sum [A_{l,m} (\nabla \times \vec{M}_{l,m}) + B_{l,m} (\nabla \times \vec{N}_{l,m})] \\ &= -\frac{ik_m}{\omega\mu} \sum [A_{l,m} \vec{N}_{l,m} + B_{l,m} \vec{M}_{l,m}] \end{aligned} \quad (2.38)$$

By applying same calculation for Electric Field, it is found that

$$\vec{E}_{inc} = \frac{k_m}{\omega^2 \epsilon_m \mu} \sum [A_{l,m} \vec{M}_{l,m} + B_{l,m} \vec{N}_{l,m}] \quad (2.39)$$

Where $A_{l,m}$ and $B_{l,m}$ are incident beam expansion coefficients

$$A_{l,m} = \int M_{l,m}^* \vec{E}_{inc} d\Omega \quad (2.39)$$

$$B_{l,m} = \int N_{l,m}^* \vec{E}_{inc} d\Omega \quad (2.40)$$

For the integral notation, Ω is expressed as the surface area of the sphere that is $4\pi r^2$. As a result of the both $A_{l,m}$ and $B_{l,m}$ integrals, expansion coefficients are calculated separately as

$$A_{l,m} = -i^{l+1} \frac{2l+1}{l(l+1)} \frac{(l-m)!}{(l+m)!} \Pi_{l,m} E_o \quad (2.41)$$

$$B_{l,m} = -i^{l+2} N_m \frac{2l+1}{l(l+1)} \frac{(l-m)!}{(l+m)!} T_{l,m} E_o \quad (2.42)$$

Simplification of both equation (2.41) and (2.42) around $\Theta = 0$ for plane wave. Only $m=1$ term can give result. Other ones goes to zero and can be omitted. Then T term gives result for $m=1$

$$T_{l,1} = \frac{1}{2} l(l+1) \quad (2.43)$$

$$\frac{1}{l(l+1)} \frac{(l-1)!}{(l+1)!} = \frac{1}{l^2(l+1)^2} \quad (2.44)$$

Finally, equation (2.41) and (2.42) are expressed as a simplified form

$$A_{l,1} = i^{l-1} E_o \frac{2l+1}{l(l+1)} \quad (2.45)$$

$$B_{l,1} = i^l E_o \frac{2l+1}{l(l+1)} \quad (2.46)$$

Around $\Theta = 0$, angular dependency of incident wave is not calculated. If it is added into calculation, more excitation can be found that affects the internal and scattering fields' values inside and outside of the particle.

As a result, electric and magnetic field for scattered and internal are found by means of scattering coefficients a_l and b_l , and internal coefficients c_l and d_l

$$\vec{E}_{scat} = \frac{k_m}{\omega^2 \epsilon_m \mu} \sum [A_{l,m} a_l \vec{M}_{l,m} + B_{l,m} b_l \vec{N}_{l,m}] \quad (2.47)$$

$$\vec{H}_{scat} = -\frac{ik_m}{\omega\mu} \sum [A_{l,m}a_l\vec{N}_{l,m} + B_{l,m}b_l\vec{M}_{l,m}] \quad (2.48)$$

$$\vec{E}_{int} = \frac{k_m}{\omega^2\epsilon_m\mu} \sum [A_{l,m}c_l\vec{M}_{l,m} + B_{l,m}d_l\vec{N}_{l,m}] \quad (2.49)$$

$$\vec{H}_{int} = -\frac{ik_m}{\omega\mu} \sum [A_{l,m}c_l\vec{N}_{l,m} + B_{l,m}d_l\vec{M}_{l,m}] \quad (2.50)$$

2.1.3 Mie Theory

The fact which spherical shape particles scatters the light can be observed almost anywhere in real life. Thinking the sunset at the seacoast, one can realize the color of the air or the clouds. Although color mostly is seen as a blue, sometimes it turns into yellow or reddish ones. It is a kind of scattering phenomenon depending on the wavelength of the incident light and radius of particle [7,8].

However, the observation of Gustav Mie is different from the scattering of light on small atmospheric objects. The particle size range changes order of 10 nm to few hundreds nanometer. For this reason, while colorful effect is observed in different size nm scale gold nanoparticles, scattering of light on water droplets does not change the color due to its larger size.

In Gustav Mie's famous paper "*Contributions to the optics of turbid media, particularly colloidal metal suspension*" written in 1908, he tried to explain light scattering by dielectric absorbing spherical particles and their colorful effects related to colloidal gold solutions. Even though this topic was studied Loren and Debye, the results was arranged by Gustav Mie. Therefore, the approximation is called a Mie Theory. The theory can be applied in such physical areas like near field optics or plasmonics.

Mie Theory is the solution of Maxwell Equation with boundary conditions. The region that permittivity and the permeability are isotropic and constant, Maxwell's equations must be satisfied by the electromagnetic fields. Moreover, at the point that separates the region into two, the tangential components of \vec{E} and \vec{H} must satisfy the boundary conditions below.

$$[\vec{E}_{inc} + \vec{E}_{scat} - \vec{E}_{int}] \times \vec{r} = 0 \quad (2.51)$$

$$[\vec{H}_{inc} + \vec{H}_{scat} - \vec{H}_{int}] \times \vec{r} = 0 \quad (2.52)$$

Therefore, the equations become

$$\vec{E}_{inc,\theta} + \vec{E}_{scat,\theta} = \vec{E}_{int,\theta} \quad (2.53)$$

$$\vec{H}_{inc,\theta} + \vec{H}_{scat,\theta} = \vec{H}_{int,\theta} \quad (2.54)$$

$$\vec{E}_{inc,\phi} + \vec{E}_{scat,\phi} = \vec{E}_{int,\phi} \quad (2.55)$$

$$\vec{H}_{inc,\phi} + \vec{H}_{scat,\phi} = \vec{H}_{int,\phi} \quad (2.56)$$

At the point $r=a$, using spherical harmonics gives that

$$j_l(N\chi)c_l + h_l(\chi)b_l = j_l(\chi) \quad (2.57)$$

$$[N\chi j_l(N\chi)]'c_l + [\chi h_l(\chi)]'b_l = [\chi j_l(\chi)]' \quad (2.58)$$

$$Nj_l(N\chi)d_l + h_l(\chi)a_l = j_l(\chi) \quad (2.59)$$

$$[N\chi j_l(N\chi)]'d_l + N[\chi h_l(\chi)]'a_l = N[\chi j_l(\chi)]' \quad (2.60)$$

By solving them, it is found the well-known Mie coefficients as [9]

$$a_l = \frac{N^2 j_l(N\chi)[\chi j_l(\chi)]' - j_l(\chi)[N\chi j_l(N\chi)]'}{N^2 j_l(N\chi)[\chi h_l(\chi)]' - h_l(\chi)[N\chi j_l(N\chi)]'} \quad (2.61)$$

$$b_l = \frac{j_l(N\chi)[\chi j_l(\chi)]' - j_l(\chi)[N\chi j_l(N\chi)]'}{j_l(N\chi)[\chi h_l(\chi)]' - h_l(\chi)[N\chi j_l(N\chi)]'} \quad (2.62)$$

$$c_l = \frac{j_l(\chi)[\chi h_l(\chi)]' - h_l(\chi)[\chi j_l(\chi)]'}{j_l(N\chi)[\chi h_l(\chi)]' - h_l(\chi)[N\chi j_l(N\chi)]'} \quad (2.63)$$

$$d_l = \frac{Nj_l(\chi)[\chi h_l(\chi)]' - Nh_l(\chi)[\chi j_l(\chi)]'}{N^2 j_l(N\chi)[\chi h_l(\chi)]' - h_l(\chi)[N\chi j_l(N\chi)]'} \quad (2.64)$$

While a_l and b_l are described as scattering coefficients, c_l and d_l are the internal fields. When denominator of four equation goes to zero, a_l , b_l , c_l and d_l values diverge. In this circumstances, the solution of equations give resonance peaks due to particle diameter. For this reason, it is called as structural or morphology-dependent resonant. In addition to the size of the particles, sphere indices N_s and surrounding medium N_m have affect the behavior of the coefficients.

To find the net energy change rate, the complex Poynting vector law should be used

$$S = E \times H \quad (2.65)$$

Then, the scattered and the extinction energies are calculated as

$$W_{scat} = \frac{1}{2} Re \int_0^{2\pi} \int_0^\pi (E_{scat} \times H_{scat}^*) dV \quad (2.66)$$

$$\begin{aligned} &= \frac{1}{2} Re \int_0^{2\pi} \int_0^\pi (E_{scat,\theta} \times H_{scat,\phi}^* \\ &\quad - E_{scat,\phi} \times H_{scat,\theta}^*) dV \\ W_{ext} &= \frac{1}{2} Re \int_0^{2\pi} \int_0^\pi (E_{inc} \times H_{scat}^*) dV \\ &= \frac{1}{2} Re \int_0^{2\pi} \int_0^\pi (E_{inc,\phi} \times H_{scat,\theta}^* - E_{inc,\theta} \times H_{scat,\phi}^* \\ &\quad - E_{scat,\theta} \times H_{inc,\phi}^* - E_{scat,\phi} \times H_{inc,\theta}^*) dV \end{aligned} \quad (2.67)$$

After putting the energy values into equations,

$$C_{scat} = \frac{W_{scat}}{I_{inc}} \quad (2.68)$$

$$C_{ext} = \frac{W_{ext}}{I_{inc}} \quad (2.69)$$

I_{inc} is intensity value of incident light. The cross sections of scattered and extinction are calculated as

$$C_{scat} = \frac{2\pi}{k_m^2} \sum_{l=1}^{\infty} (2l+1)(a_l |H_{l,m}|^2 + b_l |F_{l,m}|^2) \quad (2.28)$$

$$C_{ext} = \frac{2\pi}{k_m^2} Re \sum_{l=1}^{\infty} (2l+1)(a_l |H_{l,m}|^2 + b_l |F_{l,m}|^2) \quad (2.71)$$

$F_{l,m}$ and $H_{l,m}$ values can be described in terms of angular term $\Pi_{l,m}$ and $T_{l,m}$

$$F_{l,m} = \frac{2}{l(l+1)} \sum_{m=-l}^l \frac{(l-m)!}{(l+m)!} |\Pi_{l,m}|^2 \quad (2.72)$$

$$H_{l,m} = \frac{2}{l(l+1)} \sum_{m=-l}^l \frac{(l-m)!}{(l+m)!} |T_{l,m}|^2 \quad (2.73)$$

Where $\Pi_{l,m} = m \frac{P_l^m}{\sin\theta}$ and $T_{l,m} = \frac{dP_l^m}{d\theta}$

Considering plane wave excitation, only $m=1$ value gives result. Finally, scattered and extinction cross sections are found as

$$C_{scat} = \frac{2\pi}{k_m^2} \sum_{l=1}^{\infty} (2l+1)(|a_l|^2 + |b_l|^2) \quad (2.74)$$

$$C_{ext} = \frac{2\pi}{k_m^2} Re \sum_{l=1}^{\infty} (2l+1)(a_l + b_l) \quad (2.75)$$

The absorption value can be calculated by

$$C_{abs} = C_{ext} - C_{scat} \geq 0 \quad (2.76)$$

To find the dimensionless cross section value, both scattering and extinction values should be divided by πr^2 .

2.1.4 Plasmonics

The basis of electromagnetic waves and their interaction with particles are mentioned in freshman physics. However, their physical concepts are not described in detail. The only thing handling is that transmission and reflection from metal basis and skin effect in good conductors. The importance of these transmission and reflection properties should not be denied; nevertheless, new physical concepts reveal themselves when incident radiation frequency changes from radio-frequency to higher optical ranges. In other words, the area of usage of the radiation comes from light metal interaction increases especially for medicine, photovoltaic, integrated circuits ...etc. Considering the metal, it includes so many electrons. These electrons are not directly connected to the nuclei. By means of electromagnetic wave, it moves freely depending on the condition of nuclei and electromagnetic wave.

A few decades ago, scientists applied electromagnetic waves to the metal which is placed on dielectric surface. They realized that there exists resonance between electromagnetic wave and metal electrons. Which means coupling is generated between electron and electromagnetic oscillations.

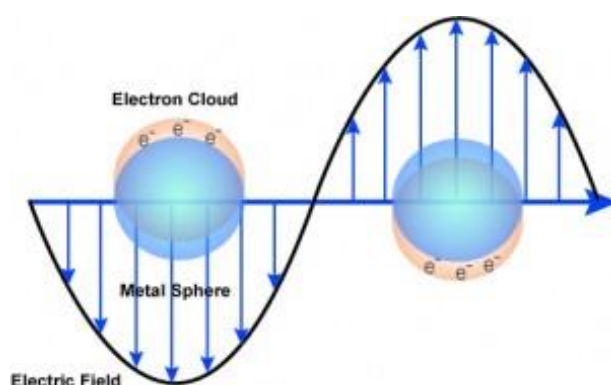


Figure 2. 1 Schematic of surface plasmonic resonance where the free conduction electrons in the metal nanoparticle are driven into oscillation due to strong coupling with incident light.

To better understand the interaction between electromagnetic wave and the metal particle, the action of the metal while electromagnetic radiation coming is essential. In general, materials are classified with respect to their permittivity ϵ and permeability μ properties. Even though these are described for each material, there is no strict value of them. In other words, electrical and magnetic properties of the material is changed by frequency [10]. Frequency dependency of them can be described by two main model which are Lorentz and Drude. Although they are seemed as two different approach, they are connected to each other.

2.1.4.1 Lorentz Model

Linear optical polarizability is related with the electrical property of the molecule. Molecule's orbitals and coupling determine the polarizability property. This property can be explained by special mathematical expressions based on quantum mechanics and perturbation theory. However, in 1900s, H.A Lorentz handled the physical concept behind it by means of classical treatments [53]. After that, it is needed to translate classical terms to the quantum-mechanical like terms. According to past studies, it is shown that harmonic oscillators problem approaching both quantum mechanical and classical exhibits same results and expressions.

Lorentz model solve simple damped harmonic oscillator problem having natural frequency ω_0 . The classical approach give satisfactory results since electric field acts on the electrons and creates small perturbations on it [11].

Then, all of the forces can be written with respect to simple damped harmonic oscillator

$$\text{Driving Force} = -eE_0e^{-i\omega t} \quad (2.77)$$

$$\text{Spring Constant} = -\omega_0^2mx \quad (2.78)$$

$$\text{Damping Force} = -\Gamma m \frac{dx}{dt} \quad (2.79)$$

If take all the forces into calculation and applying the Newton's Second Law $F = m a$. This law describes the acceleration of the object that depends on the net force acting on it and mass of the object. Then, the equation becomes for electron

$$\frac{d^2x}{dt^2} + \Gamma \frac{dx}{dt} + \omega_0^2x = -eE_0e^{-i\omega t}/m \quad (2.80)$$

To find the general solution of Equation (2.80), $x(t)$ assumption is used

$$x(t) = Ae^{-i\omega t} \quad (2.81)$$

By taking first and second derivative of $x(t)$ and putting into equation (2.80), A value can be found as

$$A = -\frac{eE_0}{m} \frac{1}{\omega_0^2 - \omega^2 - i\Gamma\omega} \quad (2.29)$$

Then, $x(t)$ becomes

$$x(t) = \frac{eE_0}{m} \frac{e^{-i\omega t}}{\omega_0^2 - \omega^2 - i\Gamma\omega} \quad (2.30)$$

If multiply the result of one oscillator polarization by the number of the oscillator, total polarization can be found as

$$P = N_0ex = \frac{N_0e^2E_0}{m} \frac{e^{-i\omega t}}{\omega_0^2 - \omega^2 - i\Gamma\omega} = \frac{\omega_p^2}{\omega_0^2 - \omega^2 - i\Gamma\omega} \varepsilon_0E \quad (2.31)$$

Where square of plasma frequency

$$\omega_p^2 = \frac{N_0 e^2}{m \epsilon_0} \quad (2.32)$$

Polarization is also described with respect to the electric field

$$P = \chi \epsilon_0 E \quad (2.33)$$

By equalizing equation (2.84) and (2.86) each other, electric susceptibility and relative permittivity can be found respectively as

$$\chi = \frac{\omega_p^2}{\omega_0^2 - \omega^2 - i\Gamma\omega} \quad (2.34)$$

$$\epsilon_r = 1 + \chi = 1 + \frac{\omega_p^2}{\omega_0^2 - \omega^2 - i\Gamma\omega} = \epsilon_r' + i\epsilon_r'' \quad (2.88)$$

Then, real and imaginary part of equation (2.88) becomes

$$\epsilon_r = 1 + \frac{\omega_p^2 (\omega_0^2 - \omega^2)}{(\omega_0^2 - \omega^2)^2 + \Gamma^2 \omega^2} \quad (2.89)$$

$$\epsilon_i = \frac{\omega_p^2 \Gamma \omega}{(\omega_0^2 - \omega^2)^2 + \Gamma^2 \omega^2} \quad (2.90)$$

If the system have more than one simple harmonic oscillator, the total relative permittivity is calculated by

$$\epsilon_r = 1 + \sum_j \frac{\omega_p^2}{\omega_{0j}^2 - \omega^2 - i\Gamma_j \omega} \quad (2.91)$$

2.1.4.2 Drude Model

Metals are one of the most well-known material with their high electric and thermal conductivity properties. Having many free electron makes metal useful for plasmonics applications. Under electric field, electrons changes their positions. That situation can be explained by Drude Model [12].

According to the paper written by Drude in 1990, electrons are taken as electron gas supposing that kinetic energy value of the each electrons as E_m . In Drude Model, free electrons acts as an electron cloud inside the metal structure. The interaction of ions and electrons protect the thermal stability for the electrons. With the improvement of

the J.J Thompson study, Paul Drude propose that free electrons have an energy E_m . This energy value is expressed as

$$E_m = \frac{3}{2}k_B T \quad (2.92)$$

Also, he found that electrons have average speed v_m and the energy can only be described by kinetical term. This means that, electrons do not have any potential energy. For this reason, electron energy can be rearranged as

$$E_m = \frac{3}{2}k_B T = \frac{mv_m^2}{2} \quad (2.93)$$

Where m is electron mass. In ideal condition, v_m is $v_m = 10^7$ cm/s.

If the electrons does not interact with each other, they acts in linear way. This motion is described by Newton Laws. Applying extra electric field to the system leads to drift velocity. Drift velocity is described as

$$v_d = -\frac{eE}{m}t \quad (2.35)$$

To find the mean free path value, it is need to multiply average quadratic speed v_d by relaxation time which is the time value between two collisions. Then, free path is [13]

$$l_{mfp} = v_m \tau \quad (2.95)$$

Furthermore, classical Drude Model plays an essential role especially for metal permittivity. As mentioned before, metals are electrically conductive. Drude model try to explain to this property. Also, it provides opportunities to find the permittivity and conductivity of metals. If electric field acts to the system, electrons are influenced. In other words, there exists conduction-band electron motion inside metal. Then, Drude Model uses these charge carriers' motion. By solving the equations of motions, it calculates the permittivity.

With impact of electron – stationary ion interaction, there exist frictional damping. This force prevent electrons to move freely inside metal lattice and it is used for permittivity calculation. Normally, Drude model is not interested in electron-electron interaction. However, it is very effective to get permittivity data for metal in a specific frequency.

According to the equation (2.91), dielectric permittivity are calculated for Lorentz Model. As known for metals, electrons and ions are not combined each other by means of spring. For this reason, the resonance frequency ω_0 should be taken into account as 0 by using Lorentz formulation. Then, dielectric function is calculated for Drude Model as

$$\varepsilon_r = 1 - \frac{\omega_p^2}{\omega^2 + i\Gamma\omega} \quad (2.96)$$

By dividing equation (2.96) into two as real and imaginary parts respectively. [12]

$$\varepsilon_r' = 1 - \frac{\omega_p^2}{\omega^2 + \Gamma^2} \quad (2.97)$$

$$\varepsilon_r'' = \frac{\omega_p^2\Gamma}{\omega(\omega^2 + \Gamma^2)} \quad (2.98)$$

If higher frequencies is applied to the system, ε_r'' value goes to zero. This situation means that particle cannot absorb electric field; in other words, becomes transparent. The physical reason of this circumstances exist in high frequencies is that the reaction between electrons and wave are so slow.

2.1.5 Photonic Crystals

Photonic crystals is essential for application that relates to light. As it is also described as dispersion relation or band structure, coupling mode of photons can be identified by it. Even though photonic crystals are the beneficial tool, it does not give data for interfaces. In detail, it describe how light acts inside of the structure. It does not work for interfaces between two different mediums. This circumstance creates controversial issue between crystal structure and light source data. For instance, thinking a symmetrical structure, it is possible get no excitation from some modes. Therefore, it is essential to observe optical properties of band structure by means of its structure. Coupling effect should not be considered.

Depending on the wavelength of light, Wood faced with some unexpected results in diffraction grating system leading to field variations. Ordinary grating theory do not have capability to clarify to physical fact about these intensity changes belonging to

different diffracted spectral orders in specific frequency bands. Low refractive index substrate material and air creates an effective waveguide. Under such condition that it is possible to exist diffraction of guided modes, guided modes cannot be appear anymore inside waveguide. If applied light match with these guided modes on the surface, the resonance happens. That situation causes that each diffracted orders have strong energy values. Moreover, type of the waveguide and refractive index of the substrate have an influence on the resonance spectral positions.

2D photonics crystals are also expressed as surface that acts as diffraction grating. For this reason, Wood's study is important to understand the behavior of different configuration photic crystals [14].

NSL is a kind of special tools that can be used to produce both 2D and 3D photonics crystals. To get that, polystyrene or silica spheres that their sizes alter ranging from tens nanometer to few micrometer, plays an essential role as mask or themselves. By this methods, it is possible to produce well-ordered hole, wire or particle structural arrayetc. These arrays will be discussed in detail in Chapter 4 [15].

2.2 Chemical Particle Interaction

Self-assembly is a kind bottom-up approach that small building units plays an essential role to generate desired structures. Moreover, the stability of these units have influences on how much close the desired pattern can be built. For the colloidal solutions, there are two main forces as particle-substrate and particle-particle forces. However, particle-particle interaction are the main factor that define the stability of the colloidal dispersion [16].

Particle-particle interaction can be divided into two main forces which are Van Der Waals attraction and Electrostatic repulsion. The combination both interaction potential determine particle positions with respect to one to another. This interaction combined in single theory called as DLVO. The name comes from people, Derjaguin and Landau, and Verwey and Overbeek who worked on it. DLVO theory try to explain total interaction potential [17].

2.2.1 Van de Waals Interaction

When the molecules come closer, there exists an interaction between them because of intermolecular dipole. The polarizability of the electron influences on dipoles. This effect shows permanent and induced impact depending on their covalent bonding type. While polar bonding exhibits permanent, non-polar bonding shows adverse effect.

There are three main forces as Keesom, Debye and London describing van der Waals interactions, U_{vdW} .

$$\begin{aligned} U_{vdW} &= U_{Keesom} + U_{Debye} + U_{London} \\ &= -\frac{C_{orient}}{d^6} - \frac{C_{induced}}{d^6} - \frac{C_{disp}}{d^6} = -\frac{C_{AB}}{d^6} \end{aligned} \quad (2.36)$$

A and B represents the two different molecules that their polarizability, dipole moment and the distance d between them are essential for the total van der Waals interactions. C_{AB} is the sum of each individual terms which is not related with distance.

Depending on size of the particle, microscopic and macroscopic approach takes places for the calculation of total van der Waals interactions. In other words, molecular interactions are used to calculate it for microscopic approach while surrounding medium is added to the calculation for macroscopic approach.

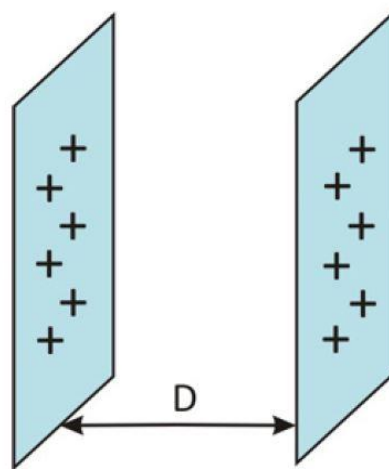


Figure 2. 2 Two identical flat plate

Considering two identical flat planes with distance D , the total van der Waals interactions, U_{plane} is described as total interactions of two planes' molecules. Then, the force that corresponds to unit area can be defined.

$$u_{plane} = \frac{U_{plane}}{Area} = -\frac{\pi\rho_A\rho_B C_{AB}}{12D^2} \quad (2.100)$$

Derjaguin approximation provide a solution to find the reciprocal energy value between different spheres that their radius are R_1 and R_2 respectively. Then, it takes similar calculation for two parallel plates instead of spheres. However, for this simplification distance between to plate should be smaller than each of sphere radius. Therefore, it gives

$$U_{sphere-sphere} = -\frac{\pi^2\rho_A\rho_B C_{AB}}{6D} \frac{R_1 R_2}{(R_1 + R_2)} \quad (2.371)$$

2.2.2 Electrostatic Interaction

If a surface interacts physically or immersed into aqueous solutions, there exists electrostatic interaction and surface get charged. This situation is as a result of surface chemical property, adsorption of ions or dissociation of surface groups. To describe the reasons of this electric field issue, two main models, Helmholtz and Gouy-Chapman, are established. Then, Stern unify the theorem as one part that feature a rigid layer of adsorbed counter-ions in close vicinity of the charged surface and a diffuse layer of non-bound ions at higher distances of the surface.

To show the Stern Model as visual (Figure 2.3)

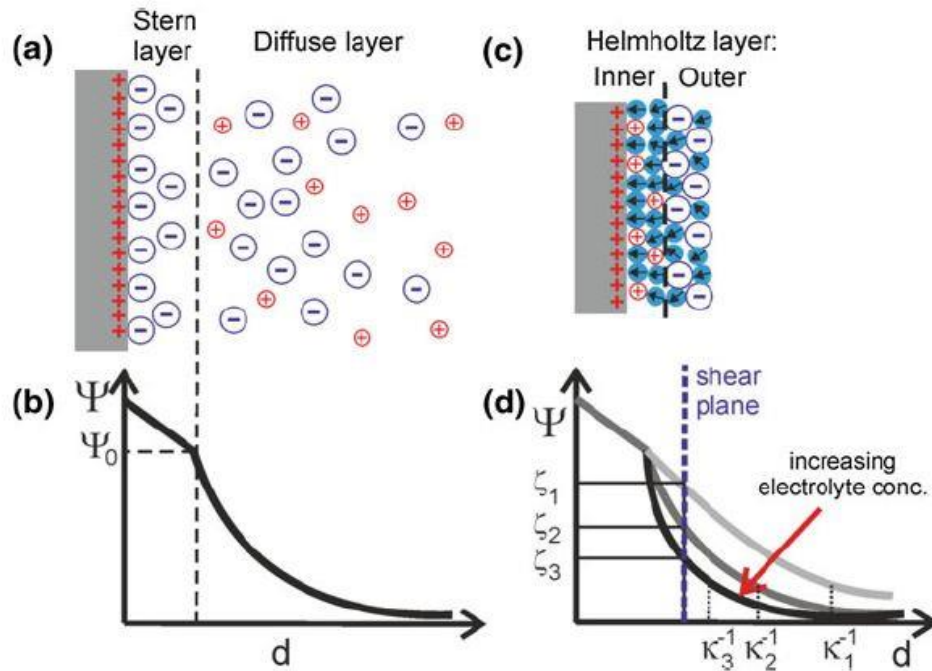


Figure 2. 3 Distance and concentration dependency of Stern Model

According to Figure (2.3-b), with increasing distance, the potential value decreases linearly and exponentially in Stern Layer and Diffuse Layer respectively. Especially for Diffuse Layer, surface potential transform to the bulk electrolyte solution potential due to counter ions. In addition to the single layer Stern layer, the model also is described into two part as inner and outer layer of Helmholtz. In inner layer of Helmholtz, van der Waals forces and surface-charged particle interactions occurs that water molecules and charged ions are connected to the surface strongly. On the other hands, hydrated counter-ions takes place in outer Helmholtz layer.

Moreover, there is one more plane, called shear, which is different than Stern potential Ψ_0 . At this point, there is enough force that makes ions near the surface. According to the Figure (2.3-d), shear plane, or ζ potential, strongly depends on the concentration of the electrolyte concentration. If the concentration is not high enough, the ζ Potential will close the value of the Stern potential. The reason of reduction in ... potential value with higher concentration can be explained by the compression of diffuse layer.

To define exponentially distance dependency of Stern model, Poisson-Boltzmann relation is used. Due to electrostatic interaction and thermal motion, there exists ion distributions over the surface. This surface distribution is calculated by Boltzmann equation. Furthermore, Poisson equation solve surface potential for fixed charges. Except from Stern layer, two particle electrostatic interaction having distance d can be described by the linearization of Poisson-Boltzmann equation as

$$\Psi(d) = \Psi_0 \cdot e^{-\kappa d} \quad (2.102)$$

Where

$$\kappa = \sqrt{\frac{2c_0 e^2}{\varepsilon \varepsilon_0 k_b T}} \quad (2.103)$$

ε and ε_0 are the dielectric constant of electrolyte solution and vacuum while k_b is defined as the Boltzmann constant. Also, c_0 is the ion concentration.

2.2.3 DVLO Theory

DVLO is a theory that investigate van der Waals interaction and Electrostatic force at the same time. As mentioned in Section 2.2.1 and 2.2.2, the distance d between two particles is essential for each forces [18,19]. However, if the distance is smaller than the particles radius, there is one more potential, called Born Repulsion, takes places for DVLO theory. This potential has d^{-12} distance dependency. Therefore, the total interaction energy, DVLO, can be described as

$$U_{DVLO} = U_{vdW}(d) + \Psi(d) + U_{Born}(d) \quad (2.104)$$

$$U_{DVLO} = -\frac{\pi^2 \rho_A \rho_B C_{AB}}{6d} \frac{R_1 R_2}{(R_1 + R_2)} + \Psi_0 \cdot e^{-\kappa d} + \frac{1}{d^{12}} \quad (2.105)$$

By showing all terms of DVLO theory schematically

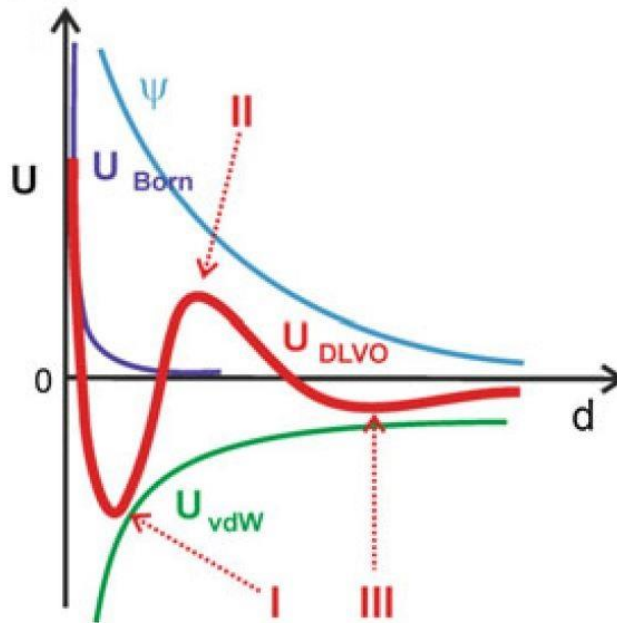


Figure 2. 4 Total interaction potential of two spheres

Figure (2.4) shows that the total energy fluctuates by changing distance d due to impacts of all three forces. By summarizing maximum and minimum points of total energy which is represented by red line, the interconnection between particles can easily be understood. At the first point, the total energy gets its minimum value and is expressed as aggregated state. In other words, it is highly possible to reside particles. At the second point, primary maximum, the aggregation processes occur. To be protected from aggregation, this activation barrier must be exceeded. For this reason, two particles should hit each other. The final state, secondary minimum, is called as flocculated. This point is important to get close contact between particles and should be exceeded this energy barrier for it.

As a result, all of the three forces are effective for the stability. For this reason, generating correct barrier point at primary maximum plays an essential role. To succeed a stability, the value of primary maximum should be higher than $10k_bT$.

CHAPTER 3

NANOLITHOGRAPHY

After one of the most famous lecture “There’s plenty of room at the bottom” by Feynman, the main topic is focusing on micro and nanoscale structures. In this lecture, Feynman talk about possibilities and ways to create atomic scale structures that resulted in extraordinary results. To generate very tiny size machines, he explain some techniques that provide miniature writing, playing with atoms and by doing these, creating miniature devices. With the help of these kind of devices, it is more than imagination to generate effective devices which have smaller components. In other words, it should be expected from future that people have faster computer and smaller size data storage having larger area opportunities. Moreover, this is not the only innovation that miniature devices can do. Ranging from solar cells to biosensors, many application can be accessible by means of this innovation.

To better understand Feynman’s idea, the most important question should be “How do we write small?”. To answer this question, it is necessary to write and generate nanoscale structures. People named this method as nanolithography [20]. The nanolithography terminology is created by three Greek Words, nanos, lithos and graphein. While meaning of nanos is “dwarf”, “lithos” and “graphein” means rock and write simultaneously. In other words, nanolithography can be expressed as building small structures.

Nanolithography, the branch of nanotechnology, focus on nanoscale architectures that dimension of each atom described as nanometer. Almost all nanoresearch scientific researches and productions, nanolithography or nano patterning can be said as one of the best way for structuring. In today’s world, while the most frequently used area seams for electronics devices, it also becomes indispensable for such areas like biomaterial engineering, cellular biology and solar cells. In other words, nanolithography method have extensive usage area. For example, to generate high capability nanoscale computers, it is needed to have nanodiodes, nanoswitches and any

other electronics components. Moreover, these nanosystems is used for medicine and health such as drug synthesis, drug delivery, nanosurgery, nanotheraphy and nanoartificial organ design and implant. All of the areas, we can say that with growing technologies, this technology generate the new world for fabrication and manufacturing of materials and systems. Therefore, it is possible to create safer, eco-friendly, more stable, higher capacity and more efficiency devices [21].

There are so many techniques to build such nanostructures that can be collected into two main title which are “top-down” and “bottom-up” approaches. While “top-down” approaches is described as traditional methods to generate nanoscale builds, “bottom-up” approaches can be expressed as the reverse engineering of “top-down” approach. In details, the main point is starting with bulk material for top down approaches. And, this bulk material is removed step by step until formation of the bulk material to nano-size regime by means special lithography techniques However, for “bottom-up” approaches, the starting point should be atoms and molecules. By using them, nano and micro size structures are generated [22](Figure 3.1).

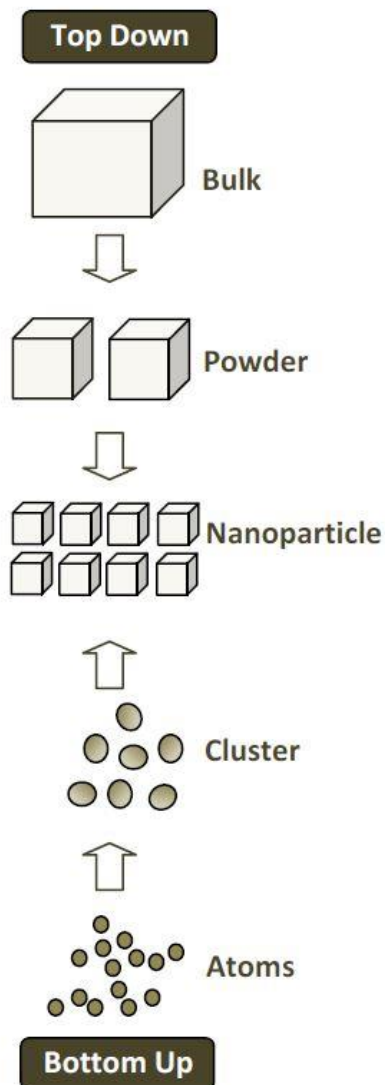


Figure 3. 1 Nanoparticle generation by means of top-down and bottom-up approach

3.1 Top-Down Approach

The top-down approach basically uses large bulk materials (Figure 3.2). For making nano-objects, this bulk materials is shaped into nanoscale structures. In this kind of approach, the fabrication technique consist of three main steps. At first, target materials are coated on substrate. Then, desired shapes are created lithography techniques. This technique can be different depending on feature size and shape.

Finally, desired pattern is formed by means of lift-off process or different selective etching methods [23].

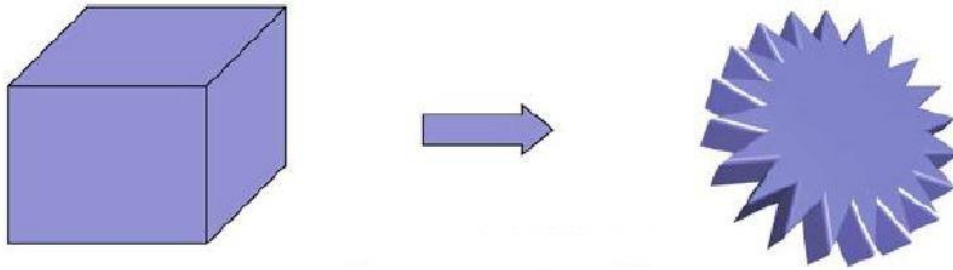


Figure 3. 2 Schematic diagram of top-down approach

More than 30 years, nanodevices can be done with the help of precision engineering and lithography techniques. These kind of techniques especially used for semiconductor industry. Furthermore, finding new subtractive and additive methods create many possibilities for various nanoarchitectures. For this kind of lithography approach, lithographic tools can be divided into two different methods as “parallel writing” and “sequential writing”. Masks are the main tool for parallel writing and whole pattern uses it. In this kind of writing technique, light is applied to expose photoresist coated surfaces. The limitation is the wavelength of light source. To decrease the size of structures, using shorter wavelengths and reducing optics are the main ways. On the contrary, in sequential mode, the pattern is generated point by point on the resist surface. For this reason, sequential mode need special tools and applied in a long period of time. Therefore, it can be more expensive. Except from light sources, to enforce the limitations, deep UV and X-Ray is used but it bring some technical difficulties to control. Comparing these two writing techniques as methods and wavelengths, the resolution of parallel writing is about 1 micron to few 100 micrometers while sequential writing can reach sub-10 nm resolution.

In Table 3.1, there exist some kind of top-down approaches with writings methods as area, cost, time and using area [14].

Table 3. 1 Comparison between Top-Down lithography methods with respect to minimum size feature, pattern, area, cost, time and industry

Technique	Minimum Feature Size	Pattern	Area	Cost	Time	Industry
Deep UV L.	50-100 nm	Parallel Writing	Large	High	Short	Industry
Immersion Deep UV L.	30 nm	Parallel Writing	Large	High	Short	R & D
Extreme UV L.	<50 nm	Parallel Writing	Large	High	Short	R & D
X-Ray L.	20 nm	Parallel Writing	Large	High	Short	R & D
Electron L.	nm	Sequential Writing	Small	High	Long	R & D (Industry)
Soft L.	10 nm	Parallel Writing	Large	Low	Short	R & D (Industry)
Scanning Probe L	<1 nm	Sequential Writing	Small	High	Long	R & D

In the following part, some of the frequently used top-down approach techniques will be mentioned as general forms.

3.1.1 Photolithography Technique

Since microelectronic industry growing day by day, optical lithography techniques takes its position in fabrication of integrated circuits. Because of its resolution and high productivity, photolithography technique is always popular and necessary for microelectronics.

The basic working principle of photolithography depends on transferring pattern on substrate surface. For this transferring process, light source, mask and photoresist material are the main tools. By means of optical system and the mask pattern, UV light is managed and projected onto photoresist coated substrate material. Therefore, the chemical properties of resist material is changed in some specific locations that light can reach. After applying the baking process, exposed places get sensitive or insensitive property depending on positive or negative photoresist type. Finally, developer solution is applied to remove weak pattern parts. Thus, the transferred pattern is generated successfully and ready for etching step. The resist material is durable for ion implant and some etching chemicals. For this reason, the places which is not coated with photoresist can be etched. Finally, the resist material is totally removed over the surface [24](Figure 3.3).

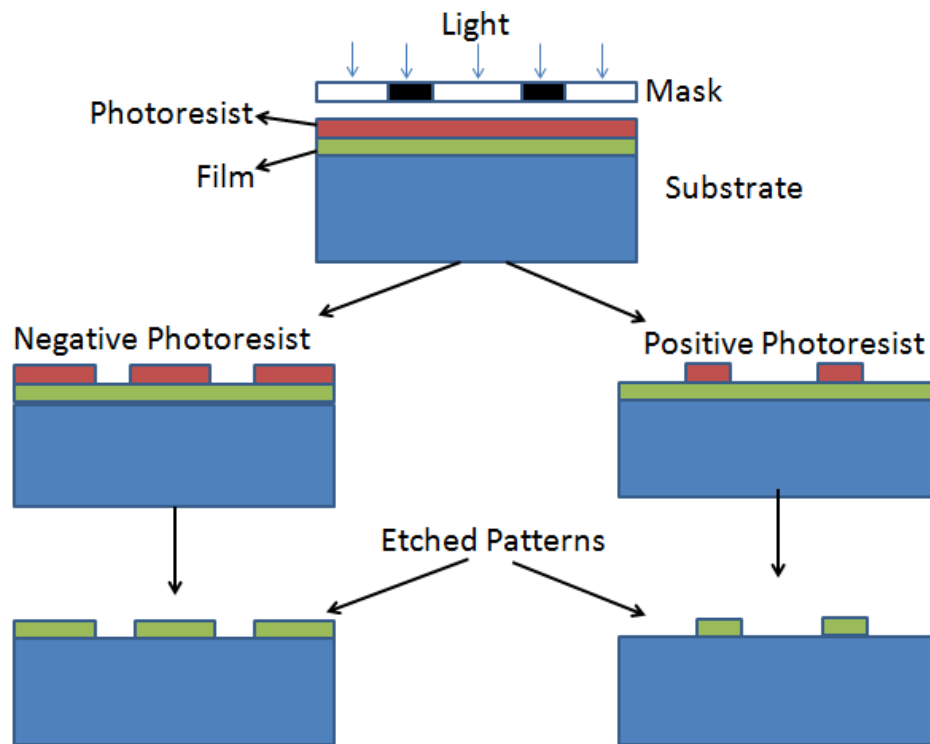


Figure 3. 3 Process steps of Photolithography by using positive and negative photoresist material

Photolithography is one of the well-known and easy way to create desired pattern. The most important factor that changes the structure is UV exposure time and power regardless of mask. Moreover, UV source can be applied over whole surface at the same time. Therefore, photolithography is suitable for large areas. However, there exists some feature size limitation due to diffraction limit of UV light source. The minimum size can be described as close to micrometer.

3.1.2 X-Ray Lithography Technique

The history of the X-ray Lithography technique was beginning in the early of 1970s. When the objective was announced the capability of exceeding the resolution of lithography techniques, it can be used especially in semiconductor technology. In these day, the most popular way in microelectronics technology was photolithography. And,

the resolution scale of this techniques can be described in micrometer. However, with developing technology, it is needed to crate smaller size structures than micrometer. By using UV lithography method, the diffraction barrier limits the size of the structure. Hence, using shorter exposure wavelengths was though as new possible solution for associate with Moore's law. Then, it is decided to use for semiconductor devices.

Of course, using wavelength that is shorter than UV spectrum leads to obstacles. Because, the energy values reaches to 250eV. In that region, most of the materials is not transparent for shorter wavelengths. Moreover, dense materials have capability to absorb X-ray photon energies. For these reasons, people face with finding convenient photomask material for special X-ray systems. However, after Röntgen's discovery on X-ray, it is understood that X-rays have higher penetration depth when X-ray places in a region between soft and hard X-ray. This gives a possibility to use X-ray as a new lithography technique with higher resolution.

X-ray Lithography can be described as parallel writing technique. In other words, structure is not generated directly on the sample surface. All of the structures are built at the same time. For this reason, X-ray lithography is one of the fastest lithography technique. Nevertheless, the design pattern which is used as mask is created over surface than nanoarchitecture is generated by means of design pattern [25].

There are desired pattern on the transparent mask. This E-beam Lithography made mask is absorbing X-ray photon energies that is used for exposure weakly. The working principle of X-ray Lithography depends on copying photomask structure on sample surface by exposing the photoresist coated on sample. Some of the beams is stopped by photomask and the rest of it interact with photoresist material after passing thorough mask. Depending on the type of the resist materials, positive or negative, specific parts of photoresist material can be resolved by developer. If the resist is positive, exposure part removed easily. If it is not, other part is dissolved by developer. In both cases, there is no difference for pattern replication process.

If the nanostructure sizes is described as 100 nm feature size, coherent X-ray radiation can propagate along the gap between mask and the substrate (Figure 3.4). Hence, X-ray Lithography is necessary process to create high complexity structures.

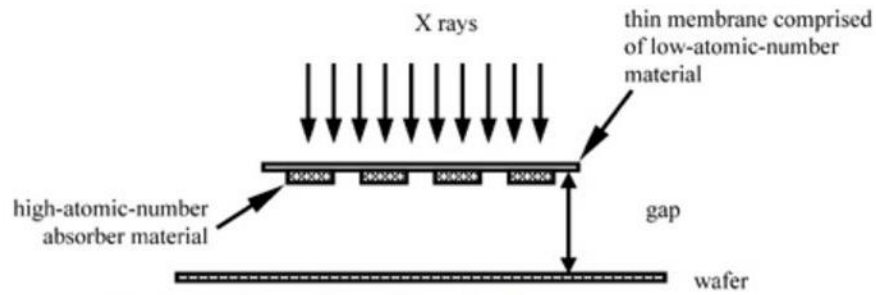


Figure 3. 4 X-ray proximity lithography with a collimated light source

3.1.3 NanoImprint Lithography

The working principle of NanoImprint Lithography based on transferring 2D or 3D generated pattern over the target surface by stamping or molding. Unlike other kind of Lithography methods such as photolithography and X-ray Lithography, NanoImprint Lithography is different from convenient methods. While most of convenient ways use positive or negative photoresist to build desired pattern by means of physical and chemical contrast, topographic contrast and flow of the resist through the stamp’s cavities shapes the pattern [25,26] (Figure 3.5).

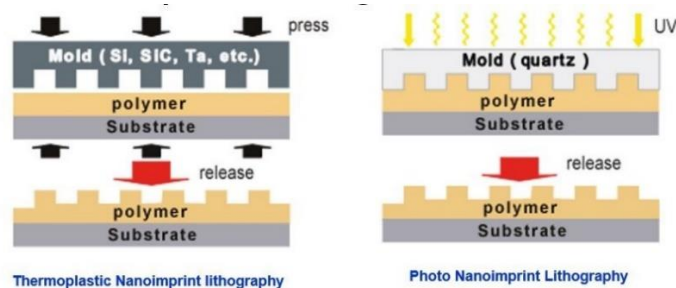


Figure 3. 5 Schematic diagram of Thermoplastic Nanoimprint lithography and Photo Nanoimprint Lithography

This technique can be applied into two main methods as Thermal and UV assisted nanoimprint lithography. Both ways have an impact on generating nanostructures which is important for electronic and biological devices. In thermal ways, liquid or solid states of materials are regenerated or deformed thermally. For the second method, it is given new physical and chemical identity to material by means of UV. Properties of thermal and UV assisted nanoimprint lithography listed in Table 3.2.

Table 3. 2 Different technologies using a mold

Name of The Technique	Specification for the mold	Shaped Materials	Physical principle behind the shaping
Thermal NanoImprint or hot embossing	Hard Soft	Monomers	Constrained flowing
		Polymers	Selective De-wetting
	Sol-gels		
		Hard organic materials or minerals	Constrained flowing
UV assisted NanoImprint Lithography	Soft	Monomers	Capillarity
	Transparent to UV	Polymers	Constrained flowing
	Hard	Monomers	Constrained flowing
	Transparent to UV	Polymers	
		Sol-gels	

3.1.4 Electron Beam Lithography Technique

Electron beam technique of one of most popular way for nanofabrication processes allowing to create sub-10 nm dimension nanostructures. The working principle of this technique based on Scanning Electron Microscope. Instead of UV or X-Ray sources, highly focused electrons beam plays an essential role for exposing the resist material. With the growing technology, the scanning electron microscope system fades to more dedicated systems. Therefore, electron sources and the mechanical design of the systems have high resolution.

The application procedure is very similar to photolithography techniques. At first, resist material is covered on the substrate surface by spin coating method. Then, focused ion sources applied to the resist material step by step to expose it. Finally, with the help of developer, exposed resist material removed [21, 25] (Figure 3.6).

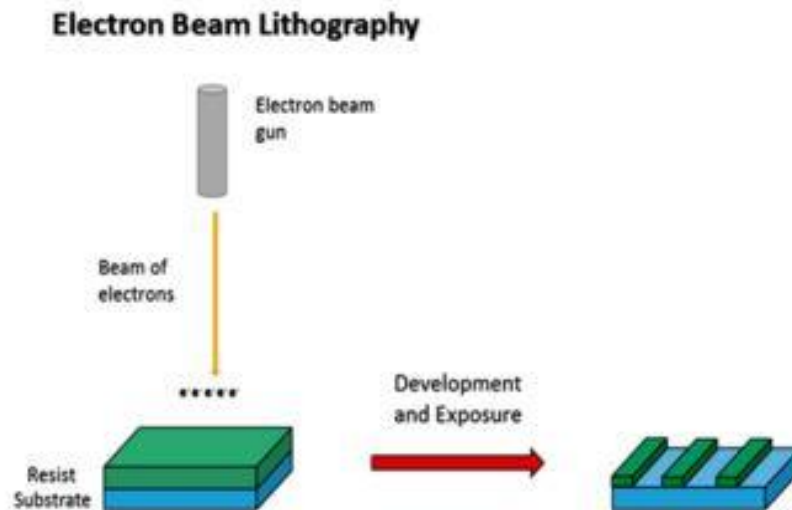


Figure 3. 6 Electron Beam Lithography

This kind of direct writing system have an advantage that the resolution and capability is almost unlimited. Also, because of being maskless application process, electron

beam lithography is suitable especially for complex smaller size nanostructures. However, one of the important disadvantage of this technique is that process takes longer time than commercial methods. So, it is not effective for large area structures. To deal with this problem, instead of single beams, parallel beam is used.

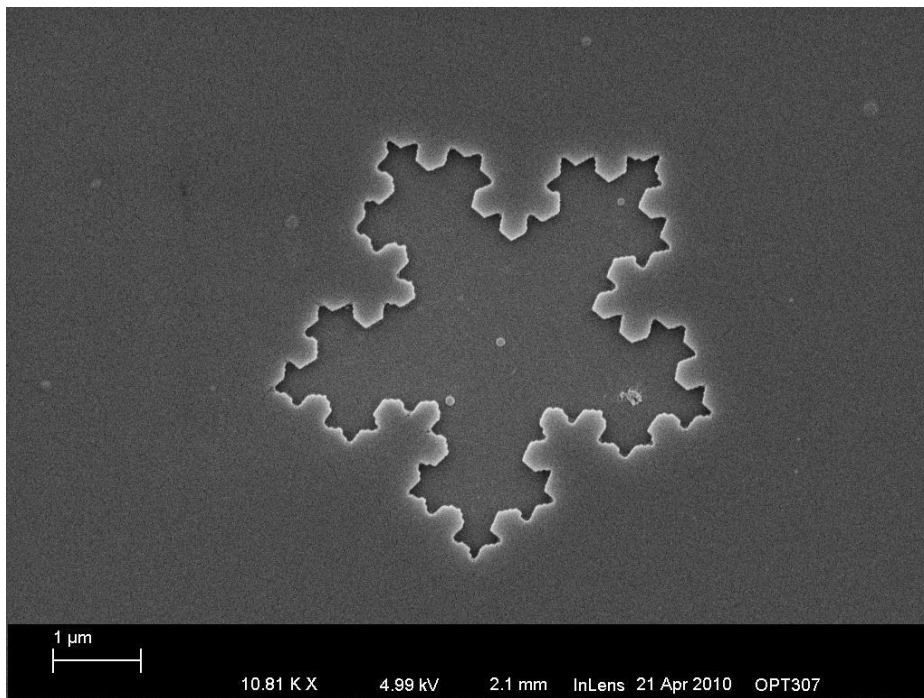


Figure 3. 7 Snowflake like structure produced by Electron Beam Lithography

To get high resolution and sensitive structures like Figure 3.7, the characteristics and quality of electron source. To make an adjustment on it, substrate and resist type, electron beam energy and dose, the development time and temperature parameter highly effective. Therefore, to optimize the process is more difficult than expected [27].

3.2 Bottom-Up Approach

The working principle of bottom-up approach nanoarchitecture is based on atom or molecular units. These units are combined with each other and build blocks with the size of atomic to nanometer scale (Figure 3.8). Unlike “Top-Down Approach”, bottom-up approach is more close to the chemical and biological research areas. At first, self-assembly nanoparticles are generated inside the colloidal solution. Then, they applied to the sample surface. This colloidal particles coated substrate can be used not only as final structure but also as mask.

In recent years, with synthesis method improvements, it is easy to control desired particles types. Not randomly oriented particles is generated. People can take under control not only in specific diameter range. They also control the shape of structures such as spherical, cubic, hexagonal etc depending on methods and the crystal structures of material. Moreover, dispersive quantity can be adjust. Nowadays, monodisperse, highly disperse and the combination of both can be generated by simple ways. These all structural and physical properties are necessary to both close pack and non-close pack sample preparation [28].

To sum up, controllable size, dimension and dispersive quantity of small particles can be easily applied to surface. Furthermore, the preparation of them is easy and they don't need highly priced precision machines. Therefore, this approach can be applied large surfaces in a short period of time. Because of the structural sizes, 3D structures can be created cheaply with reaching sub-10 nm dimensions.

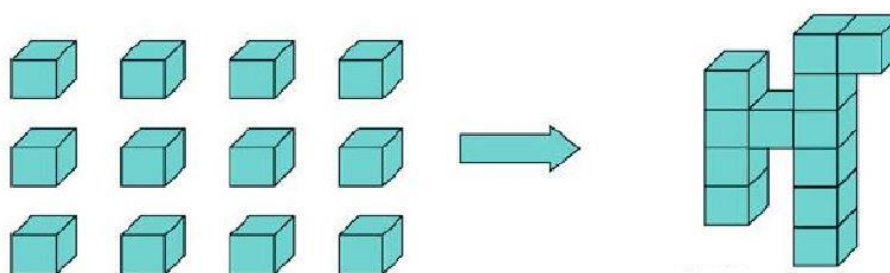


Figure 3. 8 Schematic diagram of Bottom-up approach

3.2.1 Self-Assembly of Nanoparticles

With nanotechnological improvements, nanoparticles is one of widely used tools for nano devices. By considering thermodynamical and other constraints, turning spontaneously generated self-assembly particles into well-ordered blocks get its importance. Nevertheless, working with nanosized structures is required controllable processes. Finding new synthesis methods for nanoparticle creation, self-assembly nanoparticles got their position into nanotechnological applications.

Self-assembly system includes five main characteristics for determination of the structure. The first characteristic called as components. This terms describe to create well-defined and stable configuration by means of the combination of sub-units. The second characteristic is interactions. Interaction determine states between two or more than two components. Molecular interaction is not strong and covalent in molecular level while magnetic, capillary, electrostatic and gravitational forces affect structural value of self-assembly system on meso-scale. The third characteristic is that self-assembly system should be reversibility. It is almost impossible to generate stable and desired final structure out of the blue. For this reason, it is necessary to break some bonding between molecules to reconfigured and readjust molecules' positions. Therefore, at intermediate level, the interaction between components should not be totally strong or weak to apply reversibility process. Moreover, environment, the forth characteristic, is another parameter to control the movements and interactions of components. The last characteristic is mobility. Mobility plays an essential role whether or not components aggregate with each other. While Brownian motion has an impact at molecular scale, gravity and friction forces point up at larger scale.

Considering manpower and money, working with nanoscale structure get its importance. Basic principle underlying this situation is that the smaller the size, the more operating speed system have. Furthermore, the energy consumption descends while computing every function due to smaller size structures [29].

In top down approaches, the working process is sustained by mostly resist dependent. Therefore, there exist some limitation for its resolution and speed. Considering the resolution parameter, wavelength of light source have great impact on minimum size

of features. Moreover, the mean slope of the curve between resist film thickness and zero thickness defines the contrast property of resist. If the wavelength is adjusted to small size features generation, the contrast value of image deposition.

However, the most important advantage of self-assembly is regularly created component turn into ordered form in desired size (Figure 3.9). Except from other type of technics, it can be defined as key especially in biological applications. For example, the combination of living cells created living organism that is used in DNA sequences. These living organisms act as a biological circuits to control biological and chemical systems [30].

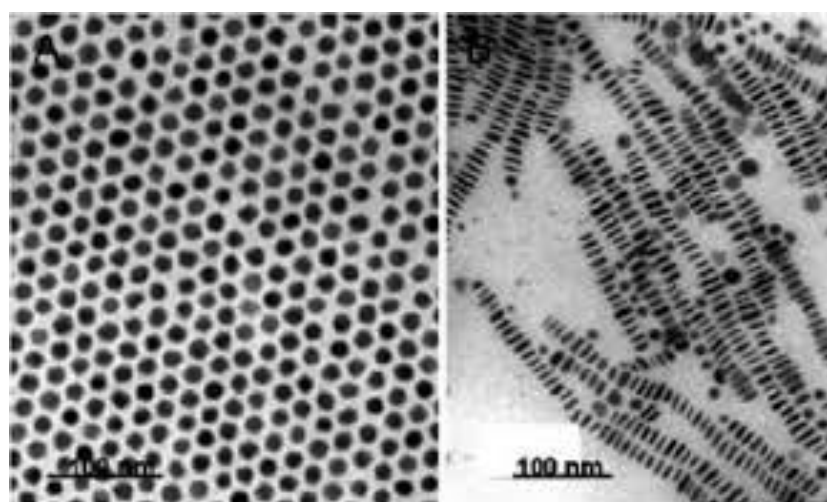


Figure 3. 9 Examples of self-assembled magnetic nanoparticles

3.2.2 Chemical Vapor Deposition

It is a kind of technique to deposit nanometer scale thin film over the substrate surface. The process starts with source gases flows into reaction chamber. To form a film, energy have to be applied to the system. Mostly, this energy transfer can be performed through heat or high frequency high voltage (RF Power) to decompose the source gas and chemical (Figure 3.10). On the contrary to other kind of deposition techniques that

phenomenon based on physical circumstances, chemical vapor deposition technique can be described as chemical process that is important to produce high purity and high performance solid materials.

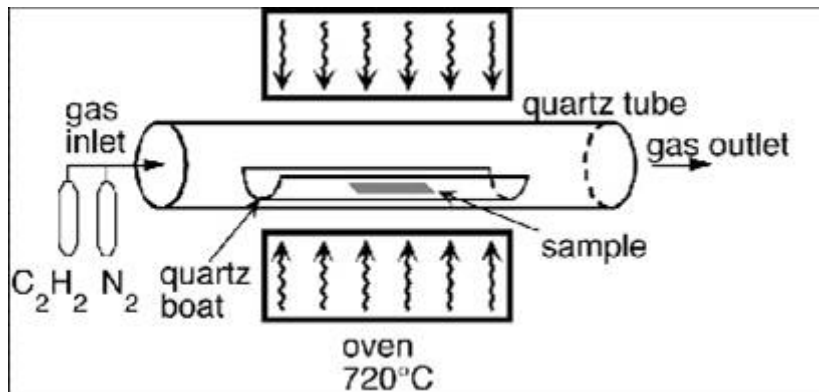
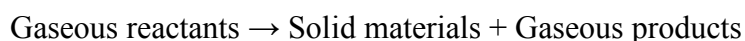


Figure 3. 10 Schematic drawing of Chemical Vapor Deposition System

The most powerful characteristics of chemical vapor deposition technique is to produce uniform thickness coating especially for complex shaped substrates. Moreover, it enable us to deposit selectively on patterned substrate. It is not restricted one type of film preparation. On the contrary, it is possible to make films as dielectrics, conductors, passivation layer, oxidation barrier and epitaxial layers.

In chemical vapor deposition, reactants which are in gaseous phase are allowed to enter into a reactor. Then, the chemical reaction shown in below happens on the surface of hot substrate.



During chemical process deposition process, there are five different reaction zones plays an essential role. In this reaction zone periods, CVD material identification is finalized. Homogeneous reaction in the vapor may occur in reaction zone 1. Sometimes these homogeneous nucleation reactions have bad impact on coating

quality. In detail, flaky and non-adherent coating is created. If these reaction are not applied by homogeneous nucleation, heterogeneous reactions in zone 2 get its role in the phase boundary vapor that is vulnerable condition. The deposition rate and coating quality is adjusted and identified during these reactions. In zone 3 and 5, like phase transformation, precipitation, recrystallization and grain growth processes, solid state reactions are formed due to high process temperature value. In zone 4 described as diffusion zone, to increase the stickiness between coating and substrate, several intermediate phase levels occur [31].

CHAPTER 4

NANOSPHERE LITHOGRAPHY

4.1 Introduction

According to the previous chapter, it can be collected most of the lithography methods into two main approaches as top-down and bottom-up. While top-down approaches focus on destroy big structure into smaller part, bottom-up approaches use sub-nano particles to build desired size nano and micro structures. Moreover, due to the process complexities that need high price special tools, most of the conventional lithography methods such as PL and EBL is not suitable for many researches.

Up till now, like masks or masters, most of the unconventional lithography techniques need intermediate tools. Also, it cannot be denied that soft lithography techniques are fast and easy methods even though they need single mask that produced by conventional lithography methods. With the help of Electron Beam Lithography technique, it is possible to reach small size nanoparticles due to not applying for large areas because of its speed. For the bottom approach, the repeatability and complexity are two main challenges to give identity to nanostructures with respect to density and shape although it has ability to produce sub-10 nanometer parts.

As mentioned in Figure 4.1, the dimensions can be adjusted by either approaches. This means that, it is possible find new method which is the combination of both top-down and bottom-up approaches called as hybrid method. One of the most convenient hybrid method is Nanosphere Lithography. In the following section, the detailed information of NSL will be mentioned.

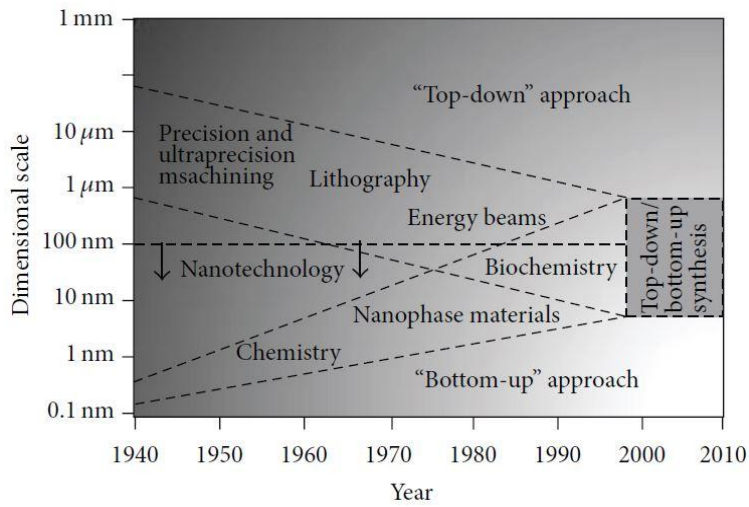


Figure 4. 1 The convergence of top-down and bottom-up approaches

4.2 Nanosphere Lithography Method (NSL) and History

As mentioned in part 4.1, researchers try to find a low cost and suitable way to generate nanometer scale regular or well-ordered pattern structures. For this reason, this method should be not only high repeatability and easy way like top-down approach but also achieve the size particle limitation like bottom-up approach. In other word, method should be combination of both approaches. Towards this need, NSL technique provide great opportunity to produce such structures.

As mask preparation and thin film preparation, NSL method can be divided into two main steps.

In mask preparation step, flat substrate surface that the most commonly used substrates are glass and silicon wafer is deposited with monodisperse spherical colloids in suspension by applying it over sample surface. This spherical shape colloid particles are also called as nanospheres. In this step, preparing surface chemically ready is very important parameter to get desired separation on nanospheres over surface. The detailed information of surface preparation will be given in Section 4.4.2. Moreover, the dilution of suspension containing spherical colloids affects the formation of

colloidal crystal mask preparation as monolayer or multilayer. After drying of suspension, the spherical colloids takes their final formation.

Before depositing thin film on substrate surface, the spaces between colloidal beads are used as desired pattern. Then, thin film is coated over surface. After applying ultrasonic to the sample including enough solution or using tape, all of the nanospheres are lifted-off. Then, desired nanodots structure is formed. If it is need to crystalize the sample or deposited thin film or crystallographic phase change, annealing process can be performed after removal of nanospheres. This annealing process is an optional step.

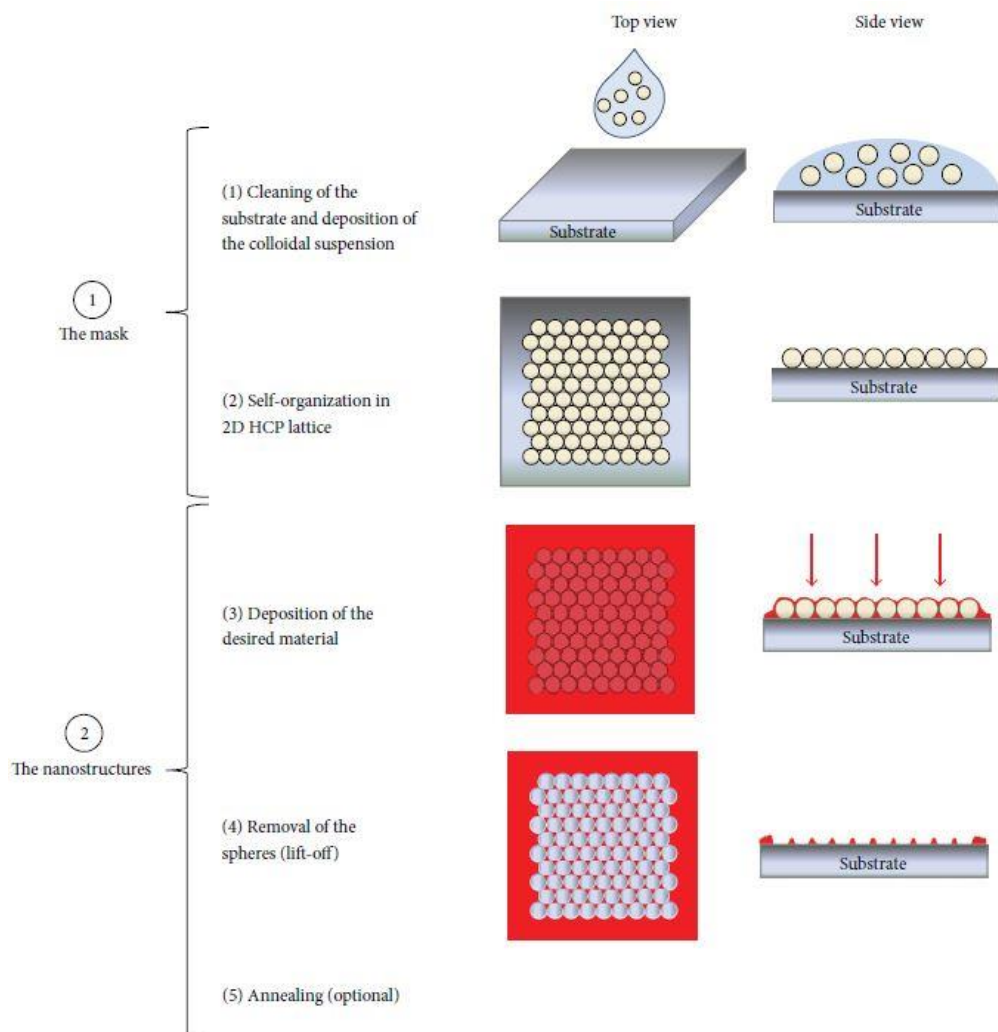


Figure 4. 2 Schematic process diagram of NSL

Since hexagonal close pack formed colloidal particles are used like bottom-up approach and this particles are used as a mask like top-down approach, NSL technique can be described as hybrid technique.

In 1981, well-ordered closepack monolayer structure is formed on glass substrate by Fischer and Zingsheim. For this reason, triangular shaped nanoparticles that are formed as hexagonal structure called as Fischer pattern. In their research, they used 312 nm diameter nanospheres. To get small-area particle formed as monolayer, they apply nanospheres over surface and wait until dry. Nevertheless, their main purpose is not use them as a mask, they are interested in copying pattern by using visible light.

In 1982, Deckman and Dunsmuir upgraded Fischer's idea. In other words, they tried to use colloidal particles as deposit material and lithographic mask. The deposition process can be divided into two with respect to their orientations as randomly and well-ordered. Unlike photolithography, mask is prepared by self-assembly phenomenon by using spin coating technique. For this reason, it is possible to face with some defects in tens of micrometer scale.

In 1990s, Hulteen and Van Duyne finalized the name of the method as "NSL". On the contrary to "Fischer and Zingsheim" and "Dechman and Dunsmuir" groups, they were focusing on well-ordered single layer and double layer structures as mask to produce nano structures. While single layer mask can generate triangular shape structure, double layer mask is used to get smaller dots.

In addition to produce nanoparticles over surface, Hulteen and Can Duyne studied in plasmon resonance properties of metallic pattern. This property also provide a bases for biosensor which is based on surface enhanced Raman spectroscopy. Moreover, the group also work on the mask formation mechanism both theoretically and experimentally.

Year after year, NSL take its position into nanotechnological structure formation methods and get its importance to produce wide variety of nanostructures.

4.3 Pattern Formation Equipments

4.3.1 Cleanroom environment

The smaller the particle size, the more sensitive procedure we should apply. Cleanroom environment is very important parameter for nanotechnological applications because working on nanometer scale needs cleaner environment. Considering the outside environment, there are so many dust particles that can be described in micrometer scale which is much bigger than generated structures. For this reason, it is almost impossible to work in such kind of environment for nanotechnological issues. Therefore, all of the experiments are done in GÜNAM clean room environments in Physics Department in Middle East Technical University (METU).

4.3.2 Surface cleaning and treatment chemicals

Almost all nanotechnological applications, final properties of surface before starting is very essential to get good experimental results. For this reason, sometimes chemical treatments are applied to sample to develop identity. These properties can be varies ranging from surface cleanness to surface hydrophilicity. In this project, deionized water (H_2O), sulfuric acid (H_2SO_4), hydrogen peroxide (H_2O_2), ammonium hydroxide (NH_4OH) and ethanol (C_2H_5OH), which purchased from Merck company except from deionized water, are used to surface modification and cleaning procedures. The details of these procedures will be given in Section 4.4.2

4.3.3 Nanosphere solution

Nanosphere Solution is main tool for lithography technique used as mask material. The solution contain 1.4×10^{11} particle having 750 nm diameter per ml and purchased from Polysciences. The second solution contains 450 nm polystyrene nanospheres

which was purchased from Invitrogen. In this study, both solutions were used by diluted with water.

4.3.4 Centrifuge

For the solution containing nanospheres, some special application needs to change solvent material without declining number of nanoparticle per ml. These special applications can be protected from aggregation of nanospheres or changing the surface modification of nanoparticles. In this project, centrifuge was used to decrease the aggregation value by changing the solvent material.

4.3.5 Thermal evaporation coating system

In this project, the main purpose is to describe the controllable size metal nanoparticles generation. To get it, metallic thin film coating process plays an essential role. For this reason, thermal evaporation method can be described as a suitable way for metal deposition. In our experiment, %99.99 percent purity of silver pellets (Ag) and tungsten boats purchased from *Kurt J. Lesker Company* are used for deposition process inside coating system.

4.3.6 Oxygen plasma device

It is an essential device that is used to clean surface, modify the surface hydrophilic and to adjust the size of nanosphere into desired size...etc. For this project, it is required to decrease the diameter of nanospheres. This device, *Femto Science: Cute Plasma Cleaning System*, is placed in Metallurgical and Materials Engineering Department at METU.

4.3.7 Furnace

For NSL techniques, annealing process plays an essential role to get smaller particles from bigger parts like dewetting technique. Moreover, it is important to crystallization processes. However, in this study, furnace is used for annealing process to change triangular shaped nanoparticle into spherical shaped and to decrease the size of spaces between spherical beads by melting them a little bit.

4.4 Procedure And Results

4.4.1 Nanosphere Selection

NSL is a kind of method that nanospheres is used as a main tool for lithographic mask. As described in Section 4.2, spherical shaped nanoparticles are deposited on substrate surface as close pack. The gap between nanospheres describe the size of the nanoparticles and the distance between nanoparticles. For this reason, it is essential to choose correct size of the nanosphere depending on desired nanoparticle size.

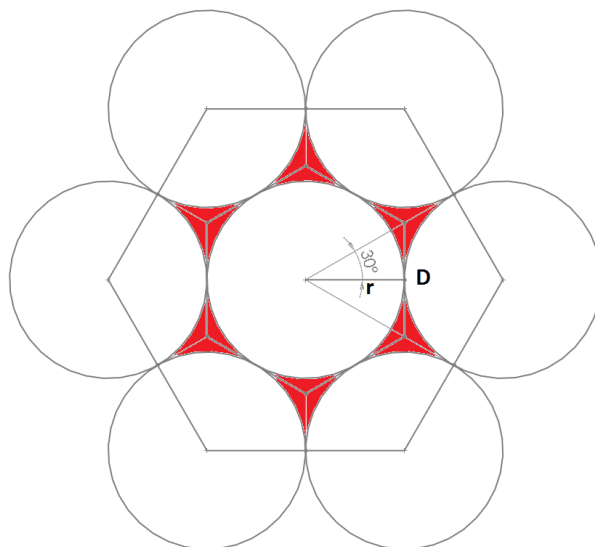


Figure 4. 3 Schematic diagram of particle distance and size calculation

According to the Figure (4.3), the area of triangle can be calculated $\frac{D^2\sqrt{3}}{4}$. “D” is the length of equilateral triangle. It is also equal to the diameter of the sphere. If one of six of each there sphere area is subtracted from total area of triangle, the area of the triangular shape like nanoparticle size can be calculated. The area of one of six sphere is $\frac{\pi R^2}{6}$. R is the radius of the sphere. Then, the area A of nanoparticle is described.

$$A = \frac{3D^2\sqrt{3}}{4} - \frac{\pi R^2}{2} \quad (4.38)$$

Furthermore, the distance between two nanoparticles are related with radius of nanosphere. The relationship between two particle distance “D” and radius of nanosphere is described as

$$D = \frac{2R}{\sqrt{3}} \quad (4.39)$$

Considering the total area surface coverage, average value is not related with diameter of the nanosphere. Whatever size is used, total surface coverage can be calculated as

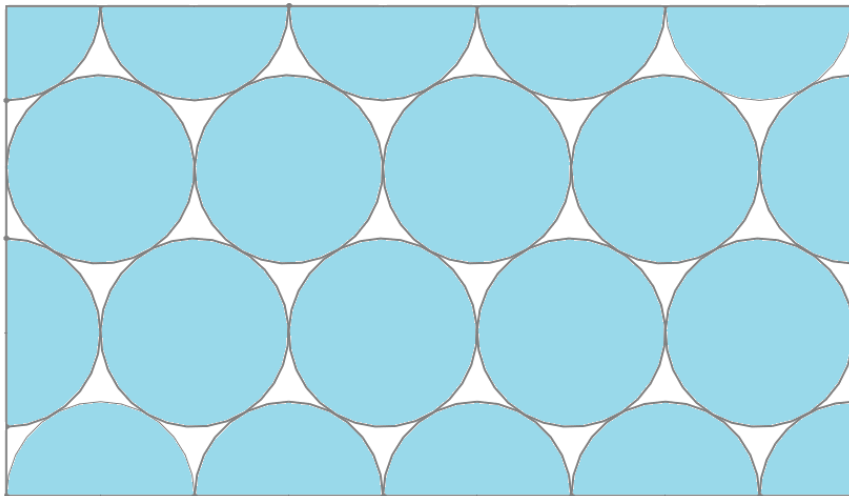


Figure 4. 4 Surface coverage of close-pack nanosphere structure

According to the equation 4.1 and 4.2, nanoparticle size and distance between nanoparticles are related with each other, it cannot be adjusted one parameter without changing the other in standard NSL method. Total surface coverage value, ratio of white area to whole rectangle, is also 10% always. However, with applying some expansions to Standard NSL process, all of the parameters can be discussed separately. Such expansions will be mentioned in Section 4.5

There are lots of nanosphere sizes and type. Depending on the application, size, chemically surface modification and material types plays an important role. If nanoparticles will be generated by standard NSL techniques, size and surface modifications are essential. While size of nanosphere determine the size of nanoparticle, surface modification should be considered for substrate material to get monolayer structure. In addition to these parameter, nanospheres can be used as nanoparticles except from lithographic mask. For that kind of specific applications, nanosphere material type gets its position.

Furthermore, to be protected from aggregation effect and to get well ordered structure, particle sizes should be same. The irregularity between particles' size damages orientation of structure. That situation creates some defects on substrate surfaces.

In this project, nanospheres have been used as lithographic mask for polished silicon wafer. For this reason, size, chemically surface modification, monodispersity are important for well-ordered structure.

4.4.2 Surface Treatment and Cleaning

Substrate surface cleaning plays an important role for nanotechnological application. Especially for bottom up techniques, small particles is used to build bigger structure. For this reason, nanometer scale particles are affected by micrometer scale dusts. Since NSL technique is applied by nanometer sized spherical particles, cleanness of substrate surface gets its necessary.

In this study, 4 inch one sided polished silicon wafer are broken into 2x2 cm small samples. Before starting cleaning process, extreme care is needed because it is a very

dangerous acidic and basic process. Chemical resistant gloves, covers and mask should be dressed.

At first, all of the wafer pieces rinsed with deionized water to remove micrometer scale silicon wafer pieces which comes from during breaking. Then, they are dried by blowing nitrogen. Then, cleaning solution is prepared by 3:1 mixture of 96% sulfuric acid (H_2SO_4) and 30% hydrogen peroxide (H_2O_2). This mixture is called *Piranha Solution* and during preparation, hydrogen peroxide must added to the sulfuric acid not reverse. After boiling samples for 2 hours, they are rinsed with DI water and transferred into 5:1:1 solution of water (H_2O), ammonium hydroxide (NH_4OH) and hydrogen peroxide (H_2O_2), base piranha treatment, for 30 min. Then, substrates are rinsed with DI water and dried with nitrogen. Finally, substrates have hydrophilic property that enables small amount of hydrophilic solutions to separate over large surfaces. Moreover, after base piranha treatment, there exist OH groups on substrate surface that charges the surface. Therefore, nanospheres can stack surface easily without aggregation [32-34].

If many substrates are prepared, unused ones should be stored in water to prevent hydrophilicity decreases and use for future works.

4.4.3 Nanosphere Deposition

4.4.3.1 Drop Casting

Mono dispersed nanoparticle plays an essential role for to build blocks. Each individual nanoparticles can be assemble into larger well-ordered particles. This sensitivity of this orientation depends on perfection of each nanoparticle and dynamic equilibrium processes. Normally, there are not so many assembly techniques to generate blocks for spherical particles due to their shape. However, their suitable technique capabilities are extensively countless. One of the most widely used method is drop casting method. The basic working principle of this method based on the evaporation on solvent including nanoparticles on flat substrate surface. For this study, spherical shaped nanoparticles is used; therefore, the shape of the packing pattern is

described as hexagonal. With the help of new improvements in drop-casting method, controlling evaporation rate and carrier solutions creates opportunities for large area close pack assemble structures.

For the drop casting method, the most frequently used assembly type is evaporation. This method is firstly monitored ferrofluid solution by TEM. In general, small amount of solvent containing nanoparticles and described as microliter is dropped on flat surface of the substrate. Then, the solvent slowly evaporates and creates well-ordered structure on the substrate surface to minimize the free energy. During evaporation period, like electrostatic interaction, Van der Waals Force and capillary force, weak interaction forces take their effects among nanoparticles. Furthermore, some kind of evaporation parameters such as concentration of solution, solvent type, evaporation rate are important for large area assembly. In this part, evaporation parameters and their effects will be discussed.

Depending on desired nanostructure, the position of nanosphere structure can be adjusting by changing the concentration of solution including nanospheres. While the higher concentration is used for bilayer or higher order builds, it is possible to get separated single layer structures by means of low concentration. However, in this study, the main goal is to generate single layer hexagonal close pack nanostructure by using drop casting method. For the drop casting method, one of the most important parameter is find suitable concentration of solution. Optimum concentration value can change a little bit because of environmental issues like temperature of environment, hydrophilicity of substrate and solvent type. For this reason, drop casting method should be applied in same environmental issue for its repeatability.

In this study, 750 nm diameter polystyrene nanospheres is used. To find suitable concentration for it, the starting point should be optimizing the total number of nanoparticles in solvent. It is very important especially for how large area is wanted to cover. When small areas needs to small number of nanospheres, much more nanospheres is required for larger areas. Moreover, different concentration value of solution can have same amount of nanospheres but it can give different results. For this reason, both of issues should be handled at the same time.

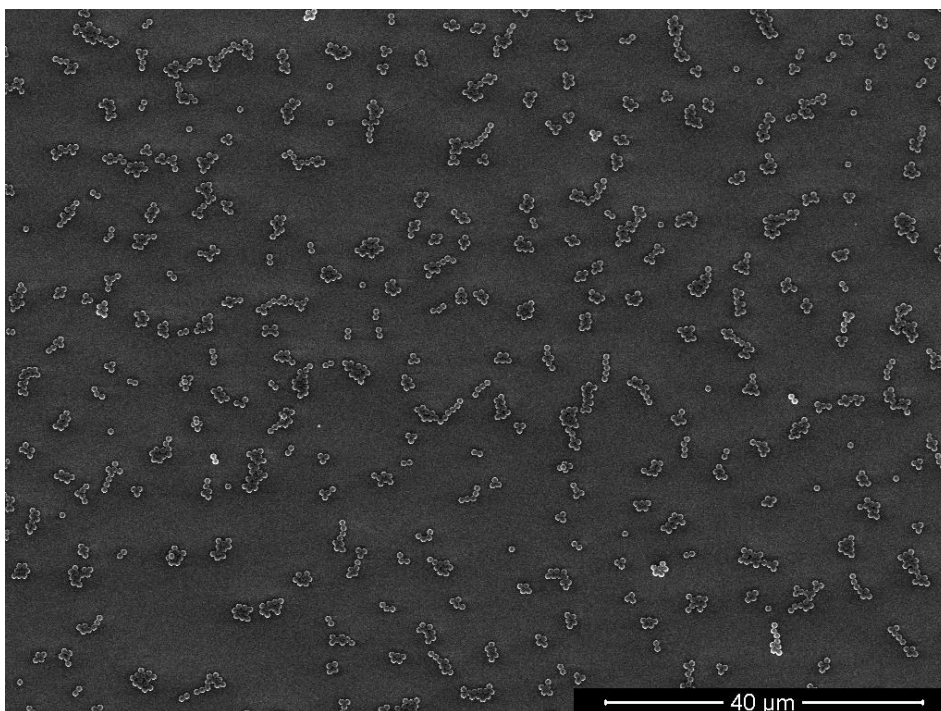


Figure 4.5 Low concentration single layer nanosphere array

Another essential parameter is solvent type because both surface and solvent should have same bonding type. In other words, both are either polar or nonpolar. By this way, substrate surface and solvent get their identity as hydrophilic and hydrophobic. While hydrophilic means “water loving”, hydrophobic means “water repelling”. And “hydro” means water. If both surface and solvent are hydrophilic or hydrophobic, one drop of solvent is enough to cover large area surface as thin layer. Figure (4.6). However, if they are different from each other solvent remains on the surface of the substrate as drop. In this study, this causes nanosphere aggregation and multilayer nanosphere structure on small area. For this reason, it is necessary to make them same chemical property to have single layer close pack structure. Due to our nanospheres diluted in water, surface modification should be hydrophilic. The detailed information to make the surface hydrophilic mentioned in (Section 4.4.2). Moreover, except from hydrophilicity, the viscosity is another factor that changes the hydrophilic property. With higher viscosity, solvent can move freely over surface and increase surface

wettability. Therefore, it creates an opportunity that nanosphere spread over surface as randomly oriented single layer and collect as single layer close pack while drying.

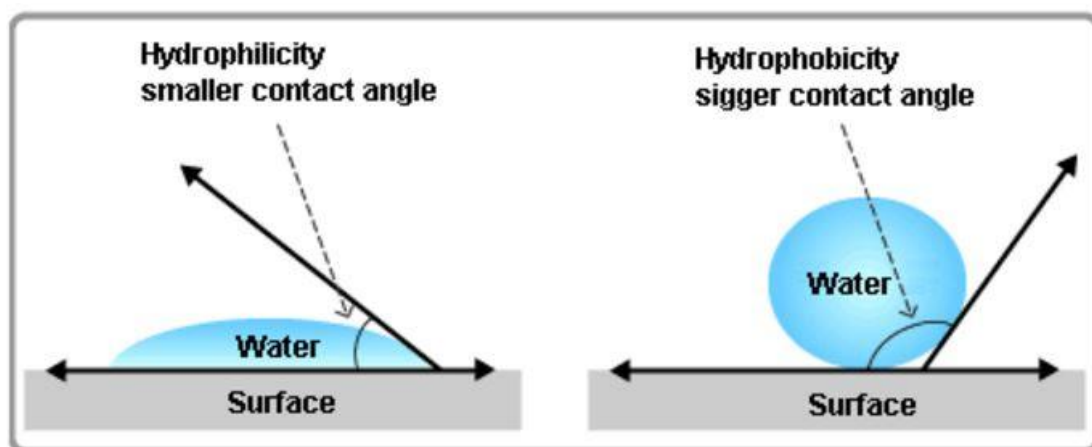


Figure 4. 6 Formation of single drop of water on hydrophilic and hydrophobic surface

Evaporation rate is another parameter that affects packing type altering. Under the same concentration and chemical property of substrate and solvent, evaporation rate differences change the building structure. Even though it is possible to get multilayer structure with the help of higher evaporation rates, it is also possible to get single layer structures by means of lower rates. This situation relates with the movements of nanospheres and whether or not nanospheres are in contact with the surface at the beginning. If the rate is high, nanospheres can be picked from the surface and put together because the force attracting them is very big and the electrostatic force between the surface and nanosphere cannot resist it. On the contrary, if the rate is low, during the evaporation period, there cannot exist enough force to move from the original state. Therefore, it can be resulted from a single layer but it is not well ordered close pack [35] (Figure 4.7).

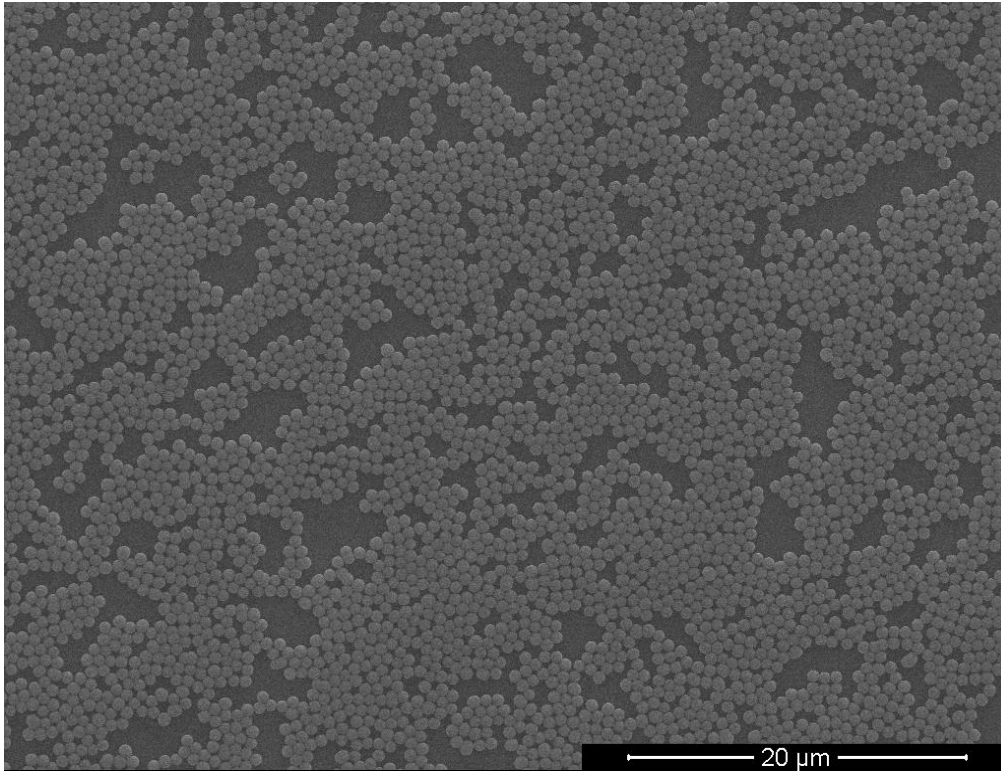


Figure 4. 7 *Single layer non close-pack nanosphere structure*

As a result, 750 nm diameter polystyrene nanospheres are diluted with water and ethanol in ratio of 1:1:1. The total amount of solution is 30 μl . Then, the solution is mixed in ultrasonic bath in 5 minutes and applied to the silicon wafer surface by using micropipette slowly. During solvent evaporation process, silicon wafer is heated to the 30 $^{\circ}\text{C}$ to increase evaporation rate. Finally, hexagonal close pack nanosphere structure was created [36] (Figure 4.8).

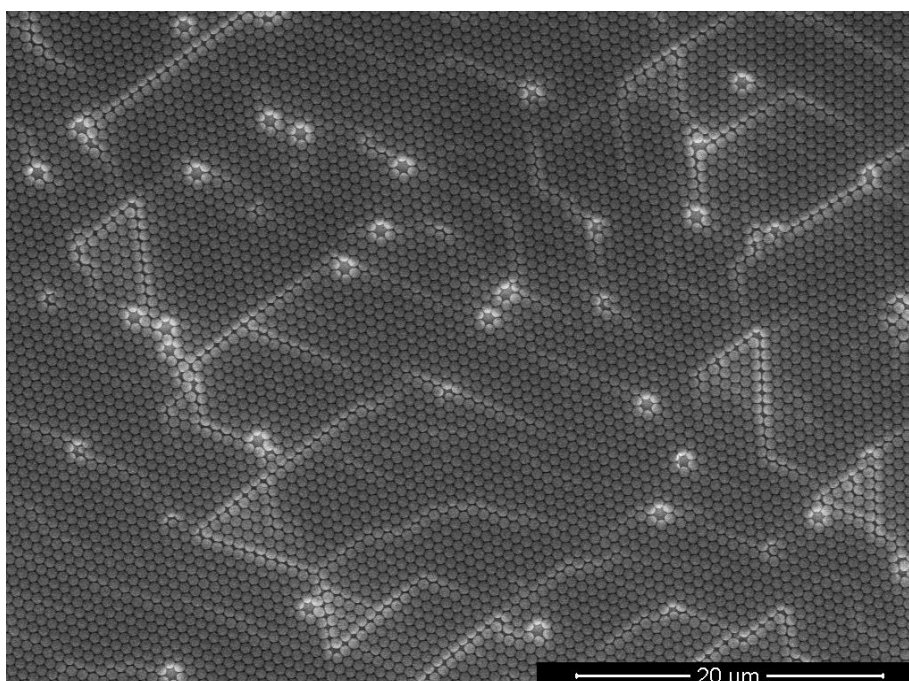


Figure 4. 8 Monolayer hexagonal close pack nanosphere structure

4.4.3.2 Langmuir Blodgett Like

In section 4.3.1, drop casting procedure is described to get hexagonal close pack structure in large. Although drop casting is very effective especially for flat surfaces, it is difficult to control over surfaces having high roughness value. Because spherical shaped particles cannot move freely over surface. That causes not only non-close pack structure but also aggregation in holes. For non-flat surfaces, a simple method Langmuir Blodgett has been developed.

At first mono dispersed nanospheres has been prepared by Stöber Method. Then, polystyrene particles are centrifuged. The main purpose of centrifuge process is transferring nanosphere into new solvent material, ethanol. At first, solution is transferred into eppendorf and centrifuged 30 min with 12000 rpm to precipitate nanospheres at the bottom of the eppendorf. Then, some part of the water is drawn by using micropipette and added same amount of ethanol to the eppendorf. After that, the solution is mixed by means of vortex. This procedure is repeated a few times to

decrease the amount of water inside the solution. By this way, all of the nanospheres can be moved to the ethanol solution.

The basic working principle of this method is based on creating single layer close pack structure on air-liquid interface then transferred onto substrate surface. At first, nanosphere suspension is dropped to the water surface slowly. This suspension widely separates over wafer surface and organized as a close pack due to capillary action between neighboring nanospheres. All of the nanospheres does not mixed to the water because surface tension of water is high. Finally, substrate material is dipped inside the solution and withdrawn slowly through up direction. As a result, close pack monolayer structure is transferred on substrate surface [37] (Figure 4.9).

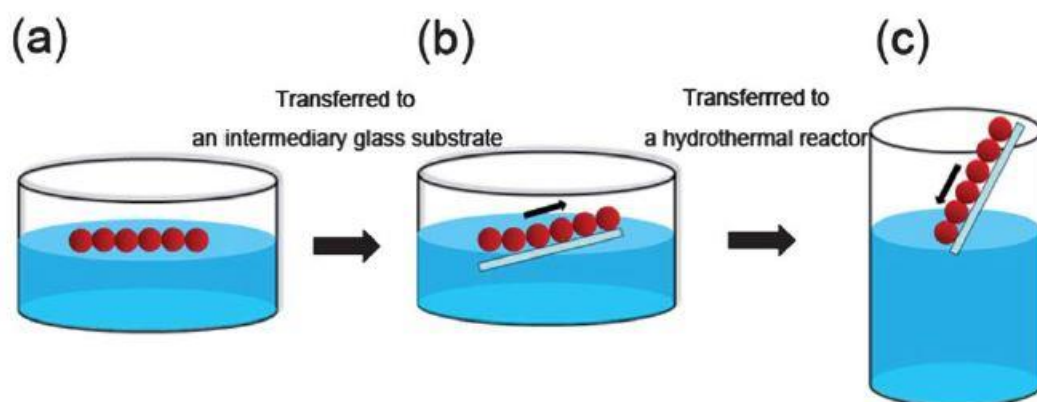


Figure 4. 9 Process steps of Langmuir Blodgett like surface coating

In this study, 50 μ l 1:4 ratio 450 nm diameter nanosphere and ethanol mixture is applied to the surface of the water. Then, silicon wafer is dipped inside the solution and slowly withdrawn inside the solution. Finally, well-ordered close pack nanosphere structure was generated [38,39] Figure (4.10).

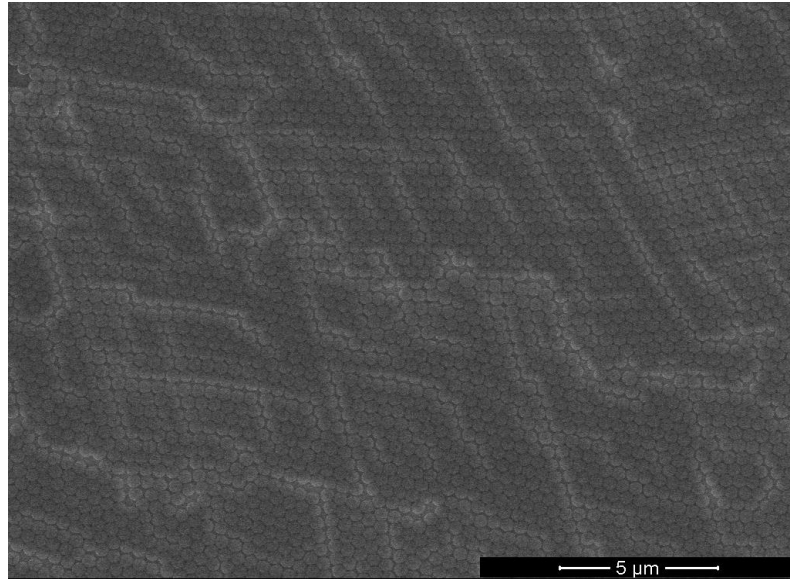


Figure 4. 10 Monolayer hexagonal close-pack nanosphere structure created by Langmuir Blodgett Like method

4.4.4 Thin Film Deposition

In advance thin film coating technology, one of the most frequently used way of physical vapor deposition technique is Thermal Evaporation. As other kind of deposition techniques, thermal evaporation system can be described as vacuum technology that desired pure coating material is coated to the surface of the substrate. This technology called as thin film because the thickness of the layer is defined as angstrom to micrometer scale.

Thermal evaporation system is preferable especially for pure metal deposition processes but it is also used for non-metal or oxides and nitrides molecules. In this study, thermal evaporation system is used for Silver (Ag) thin film deposition. In plasmonic applications, scattering of incoming light plays an essential role. For this reason, choosing low absorption and having high free electron density material are necessary for collective oscillation of free electrons. Drude model describe the interaction between metal nanoparticle and incident electromagnetic field as the dielectric function of free electron.

$$\varepsilon_{Drude}(\omega) = 1 - \frac{\omega_p^2}{\omega^2 + i\gamma\omega} \quad (4.40)$$

While real part of dielectric function shows scattering cross-section, imaginary parts of the dielectric function defines the absorption. High absorption value is not be preferable for plasmonic application. Considering other metals, silver has high scattering and low absorption cross-section. Therefore, it is suitable to use silver as target material to generate plasmonic nanoparticle.

For the substrate material, there is no strict rule to deposit with thermal evaporation system (Figure 4.11). The point that should be careful is which resistance value against heat. Except from this point, it has wide variety of substrate coating such as optical glass components, silicon wafers or any other possibilities.

The basic working principle of thermal evaporation system is heating target material inside high vacuum chamber. At first, target material is placed on filament. Then, by applying voltage through filament, the temperature value of value reaches a few thousand Celsius degree. This increasing also increases the temperature of target material and there exist some vapor pressure inside the vacuum chamber. It is very important parameter that low vapor pressure is needed to get sufficient vapor cloud. Finally, evaporated target material rises up through the target material and combined with substrate as thin film.

Normally, target material is heated above its melting point to get uniform vapor. Due to direction of vapor though up, the crucible is located at the bottom of the vacuum chamber and the substrate is mounted as face downwards.

Depending on precision of coating, there exist many coating parameter of thermal evaporation system that enable users to get desired results such as thickness, uniformity, adhesion strength, stress, grain structure, optical and electrical properties.

In this study, the thickness of the thin film and coating uniformity is two main issue. For this reason, the deposition rate and deposition time should be considered. In Figure 4.12, there exist some coating defects. This defects is caused by low vacuum chamber pressure, low deposition rate and low thickness values. If starting vacuum chamber

pressure is not well enough higher than 10^{-4} torr and deposition rate described as a few angstrom per second, target material interact with other molecules in environment. Therefore, the thickness of deposited target material over surface decreases and uniformity cannot be supplied. This situation leads to coating defects over surface.

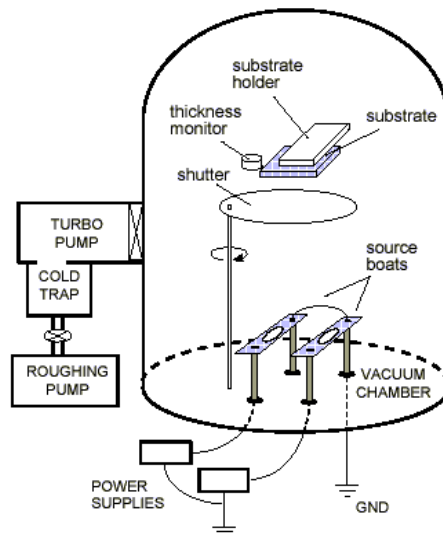


Figure 4. 11 Schematic diagram of thermal evaporation coating system

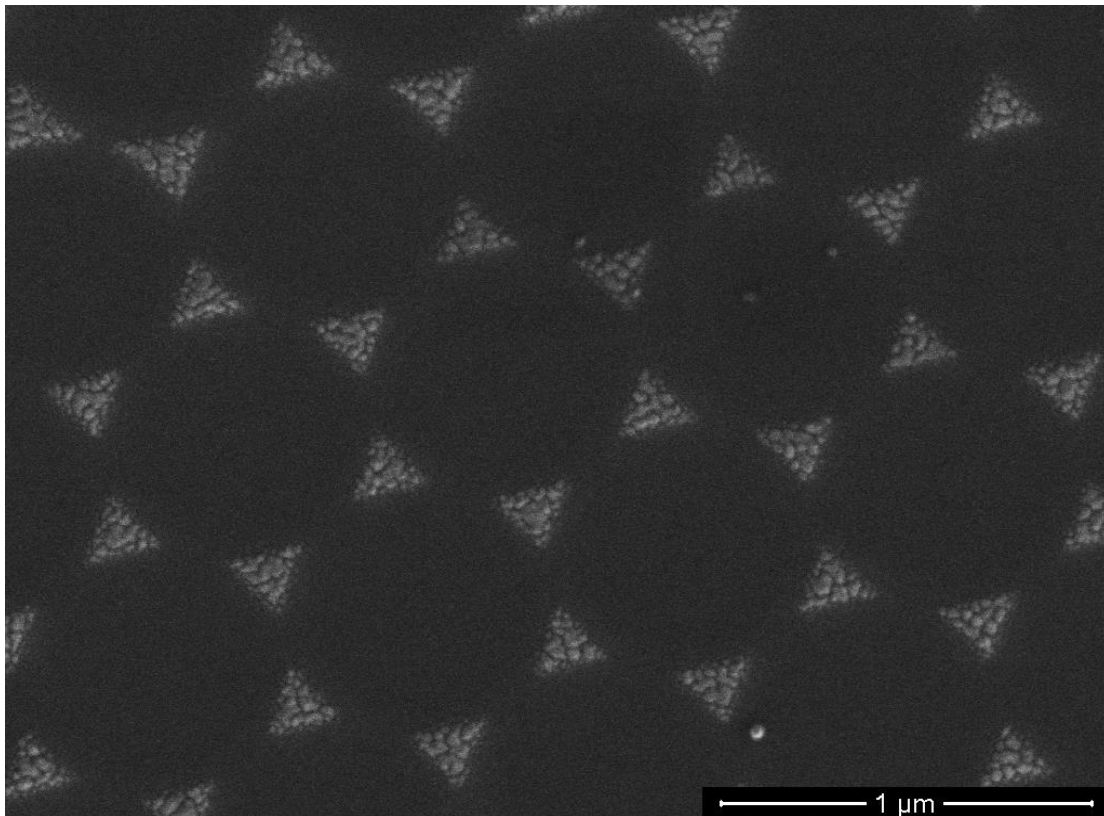


Figure 4. 12 Triangular silver lattices with defects

However, it is possible to get more uniform coating if the chamber pressure is lower than 10^{-5} torr and deposition rate is increased to a few nanometer. With the help of lower chamber pressure and higher deposition rate, the target material does not interact with air molecules and goes to substrate act more directional. In this study, desired thickness value is about 20 nanometer. For this reason, it is hard to control the expected thickness value by increase the deposition rate higher. Therefore, it was not work on higher deposition rate.

4.4.5 Lift –Off

After successful deposition of silver to the surface of the substrate, to get the triangular shape nanostructures, lift-off process plays an essential role to remove whole

nanospheres from the surface without striking thin film. For this reason, there are two main methods to apply this procedure.

The first method is using transparent tape. It is a mechanical way that transparent tape is stuck to a nanosphere-coated surface. Then, it is separated from the surface, taking the nanospheres with it. This can be an easy and costly method, but it is possible to encounter problems during the lift-off process with no return. In other words, it is very difficult to stick transparent tape over the surface without bubbles. Therefore, not all nanospheres can be removed in the first attempt. Moreover, it is not possible to use transparent tape a second time because it is inevitable to remove the thin film during the process. Another problem is that some areas may be coated with multilayered nanospheres. Each transparent application only removes one layer. Again, the second attempt is a risky application due to thin film removal.

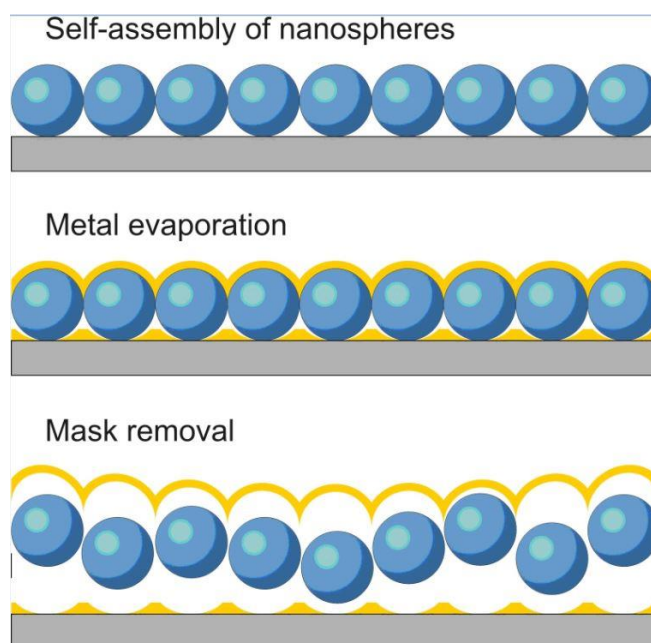


Figure 4. 13 Chemical nanosphere mask removal process

The second method is sonication in solvent (Figure 4.13). Depending on the adhesion between nanosphere and surface, it can be applied into two way. Both ways are carried out by ultrasonic bath. If chemical bonding is not strong enough, main issue to remove whole particle is physical vibration inside ultrasonic bath [40]. Sonication in ethanol is suitable way. If not, it is needed to dissolve polystyrene nanosphere in solvent like toluene. In this study, same result is obtained by using both chemical (Figure 4.14).

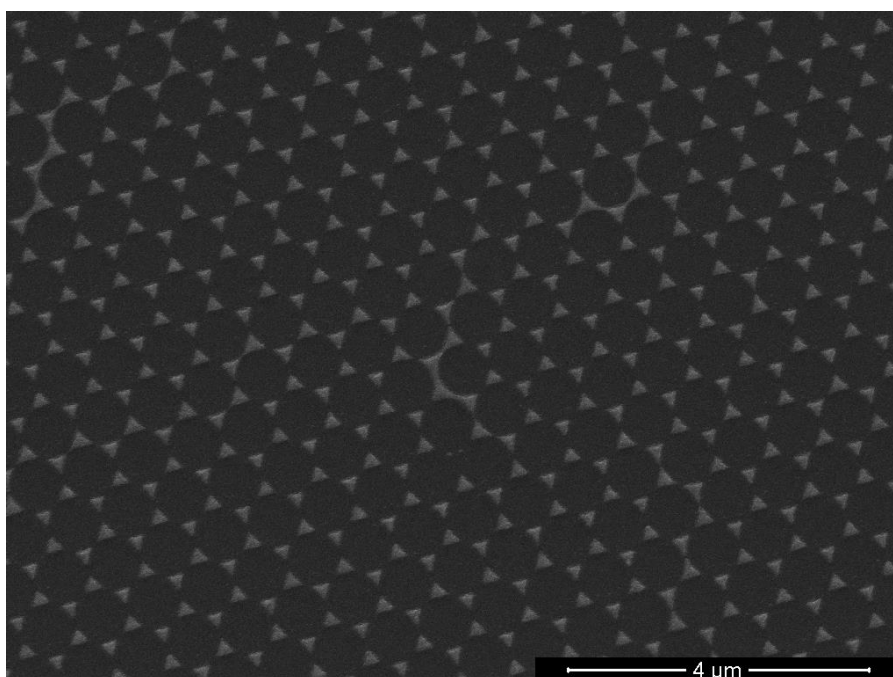


Figure 4. 14 Well-ordered triangular silver nanoparticles after lift-off

4.5 Beyond the Capabilities of Classical Nanosphere Lithography

4.5.1 Double Layer Structures

In addition to monolayer close-pack nanosphere structure, it is possible to transform it into double layer. By doing this, one of the main parameter depends on the increase in

concentration of the solution. At first, close-pack monolayer is generated. Then, the second layer lie in depressions of the first layer.

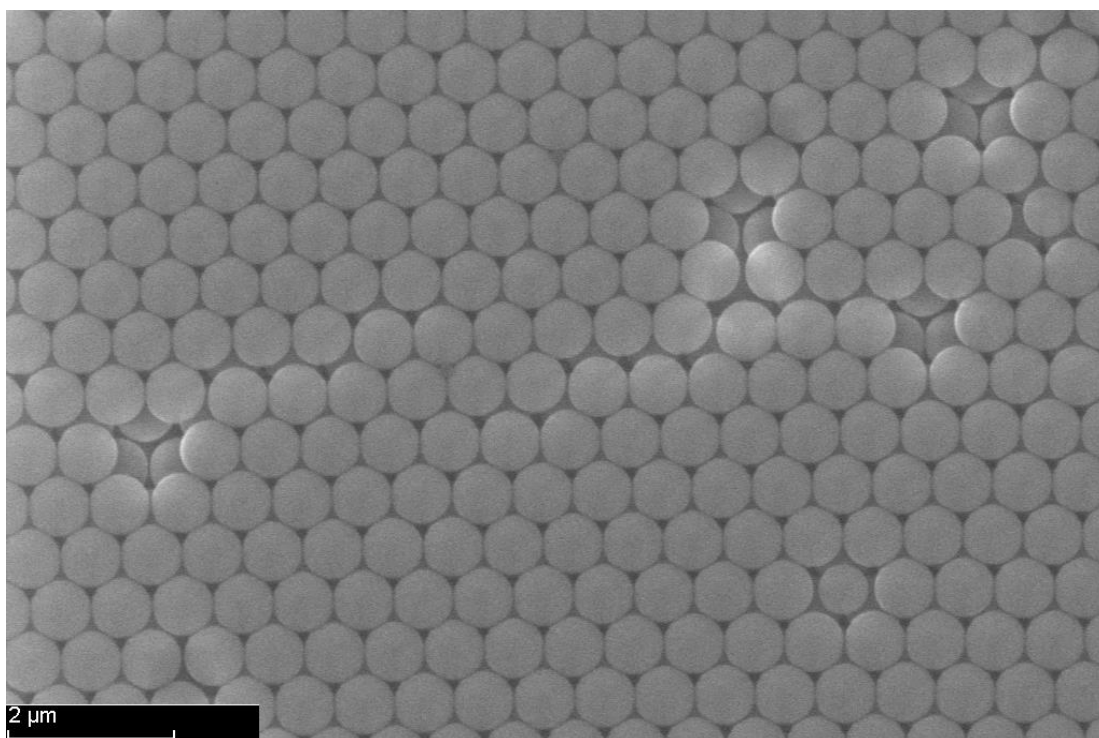


Figure 4. 15 Double layer well-ordered hexagonal close-pack nanosphere structure

As seen in Figure 4.15, double layer was produced as well-ordered like single layer structure because one sphere find its way to the gap between three spheres. This act is especially related with the curvature structure of the sphere and height of the gaps. Furthermore, hexagonal like nanostructure can be built by means of second layer instead of triangular shape. The reason of change in structure type is that some of the gaps are blocked by the second gaps as reverse (Figure 4.16).

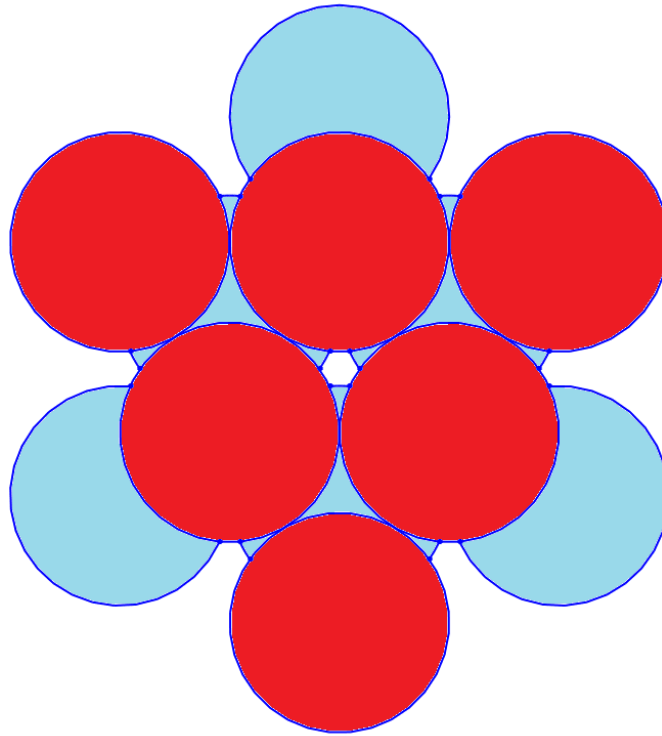


Figure 4. 16 Schematic diagram of double layer structure and transformation of gap between nanospheres

As a result, total nanoparticle surface coverage reduces almost one forth by comparing to classical nanosphere lithography method. In detail, half of the surface coverage is decreased by second layer nanospheres the rest half of the reduction is caused by the gaps formed by second layer [41].

To sum up, double layer nanosphere lithography method creates an opportunity to produce well-ordered, smaller and more separates nanostructures.

4.5.2 Annealing Nanoparticles

It is a last step that triangular shaped silver nanoparticles get their final structure with thermal annealing. As clearly seen in Figure 4.14, the beginning shape profile of silver nanoparticles is triangular due to NSL method. Which means, size and triangular shape of nanoparticles match the spaces between three nanospheres before thermal

annealing. In this study, main focus is transform triangular shape into rounded one. For this reason, substrate material was annealed at 200 °C which is lower than the melting point of silver. Although, it does not reach to temperature that melts silver nanoparticle completely, it is effective to reform of surface at the apexes of triangular silver nanoparticles. Therefore, the surface tension of silver nanoparticle leads to retraction of these softened apexes. Then, it get final rounded shape state [42] (Figure 4.17). Moreover, it should be considered that if the particle size is not big enough described as nanometer to few micrometer, the melting point is lower than the melting point of bulk material.

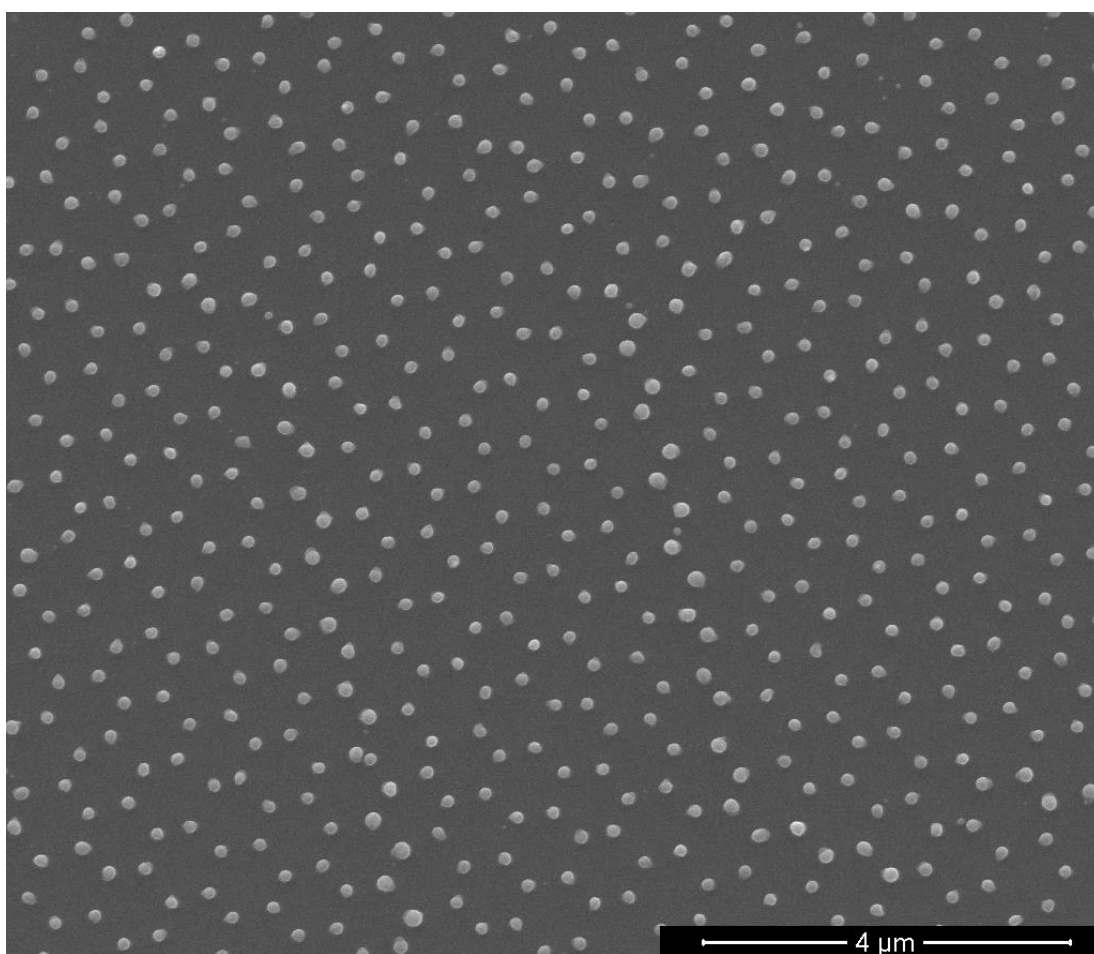


Figure 4. 17 Rounded shape silver nanoparticles after annealing at 200 °C for 1 hour

Moreover, this situation can be explained by capillary instability. It is probability that the film does not contain any defects but there always exist some non-homogeneity in thin film. By means of thermal effect, groves are formed inside thin film as a result of low interfacial energy. Then, these groves determine the final shape of nanoparticles.

4.5.3 Oxygen Plasma Treatment

NSL technique uses ranging from nanometer to micrometer scale spherical shaped particles as lithographic mask for material deposition systems, wet and dry etching processes or any other combination of other lithographic techniques and methods. In standard Nanosphere Lithography techniques, colloidal spherical nanoparticle are separated over the sample surface as hexagonal close pack by drop coating, spin coating or any other coating techniques. To modify close pack structure, one of the most convenient way is oxygen plasma etching. It decrease the size of the polystyrene nanoparticles without affecting the position of nanoparticles. In other words, all of nanospheres don't change their position, the only changed situation is the creation of larger gaps between nanoparticles due to reduction in nanospheres' diameter. This new modified well-ordered nano pattern creates opportunities especially for size dependent optical, plasmonic and magnetic applications. Moreover, it can be used as template for generating the growth of multiwalled carbon nanotubes or nanometer scale holes.

In this study, *Femto Science: Cute Plasma Cleaning System* in Metallurgical and Materials Engineering Department at METU is used to modify 400 nm diameter polystyrene nanosphere to lower diameter ones. This modification is applied by the oxygen plasma treatment. It is a kind of physical dry etching process which the mixture of argon and oxygen is used as main sources. By applying the RF source to the system, plasma is occurred. Then, it is used as a physical etching source that decreases size of nanospheres [43-46].

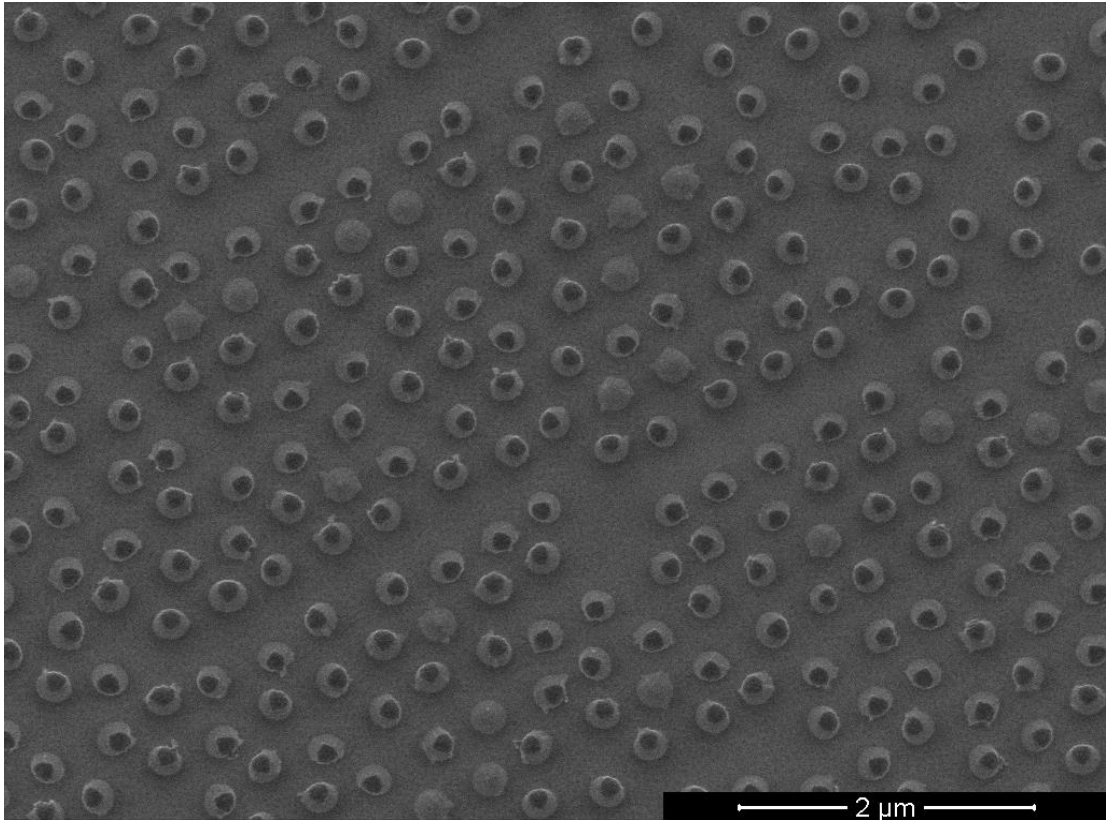


Figure 4. 18 *Reduction in size of 400 nm polystyrene nanosphere after oxygen plasma treatment*

For this process, focusing point is to prove whether or not it is possible to decrease the diameter of spheres without altering their position. As clearly seen in Figure 4.18, periodic hexagonal close-pack structure turn into non close-pack periodic structure.

However, it is a very critical process that there are several parameter affecting plasma generation. These parameters can be described as total gas flow, etching duration and chamber pressure and substrate material. For this process, total gas flow and chamber pressure adjust the power of plasma and homogeneity of it. Then, each substrate material show different responses against the plasma because every material have their own molecular bonding energy. For this reason, different power values are need for different materials. Finally, etching duration is necessary for reduction percentage of nanospheres' sizes. Moreover, if it is needed to modify the distances between spheres, choosing correct size is important mentioned in Section 4.4.1.

In previous, it is mentioned the capabilities of oxygen plasma over the size reduction of nanospheres and parameter that affect the homogeneity of plasma. To better understand situation, it is clearly seen in Figure 4.19 that whole surface is covered by same size diameter nanospheres and the beginning size of the sphere determine the distance between each pair. In this study, process nanosphere diameter is 400 nm so the distance is 400 nm excluding the inhomogeneity. This homogeneity problem causes the effectiveness to decline and some part of the area is different from other areas.

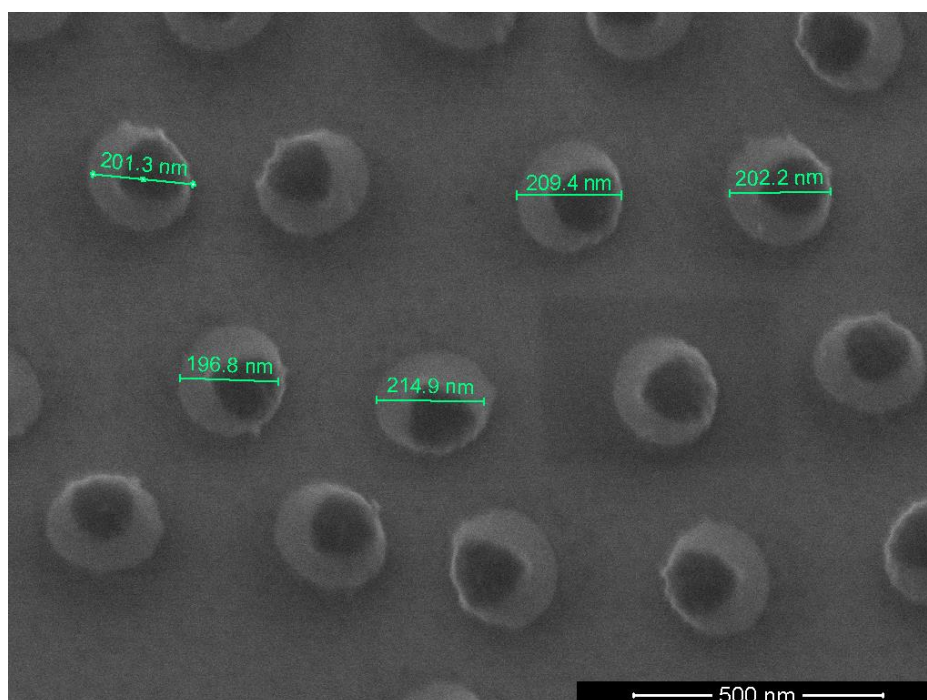


Figure 4. 19 Size distribution of 400 nm polystyrene nanosphere after oxygen plasma treatment

4.5.4 Annealing Nanospheres

In classical Nanosphere Lithography, the gap between polystyrene nanospheres serves as a mask to produce nanoparticle. The shape of these nanoparticles is close to

triangular. Moreover, there is a relationship between size of the particle and distance between any of two. In other words, all of the particle dimensions and central distance strongly depends on the size of the nanospheres. These two parameters cannot be adjusted as two independent parameter by using classical Nanosphere Lithography method.

However, with the help of thermal annealing, it is possible to overcome polystyrene nanosphere diameter dependency particle size limitations. In detail, the particle distances is determined by size of the nanospheres which is described in Section 4.4.1. Then, polystyrene nanospheres is annealed to deform them controllably. The deformation reduces the gap between spheres. As a result, smaller particles can be generated by bigger spheres.

In this study, the important point is to determine the optimum temperature and time values for controllable deformation of nanospheres. As a result, 120 °C was found adequate point without shock effect. Then, by altering annealing time values, reduction in gap sizes was observed [47, 48].

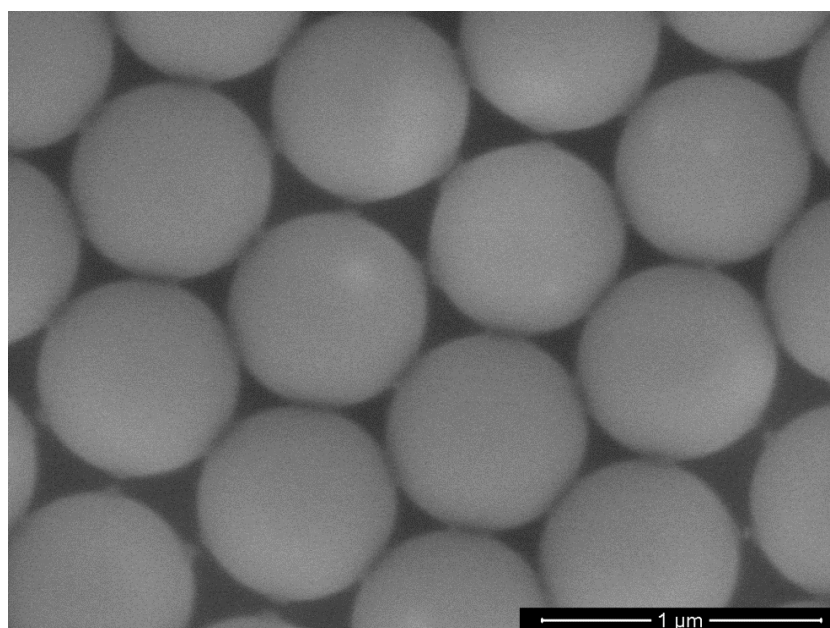


Figure 4. 20 Close-pack structure of 750 nm polystyrene nanosphere before annealing

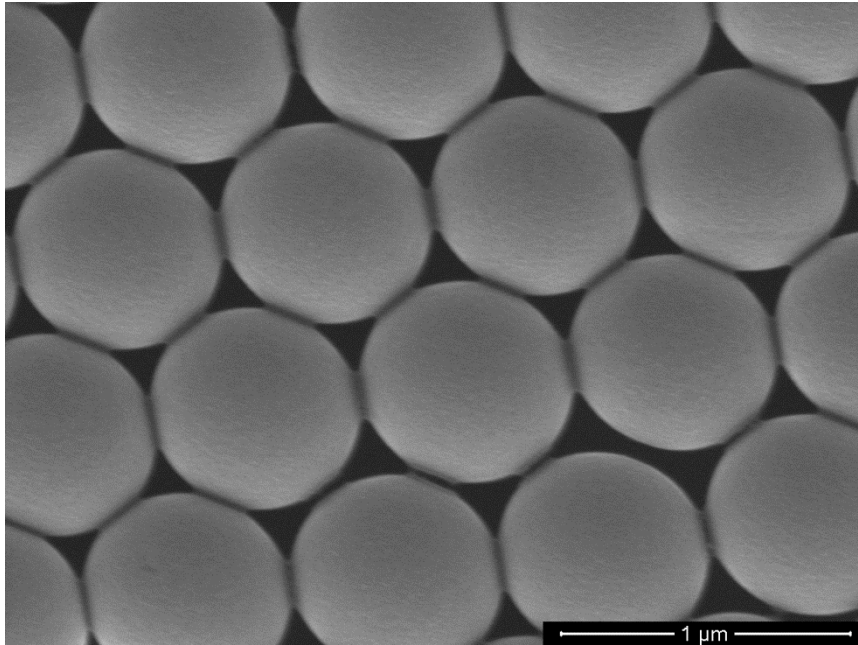


Figure 4. 21 Close-pack structure of 750 nm polystyrene nanosphere after annealing at 120 °C for 5 min

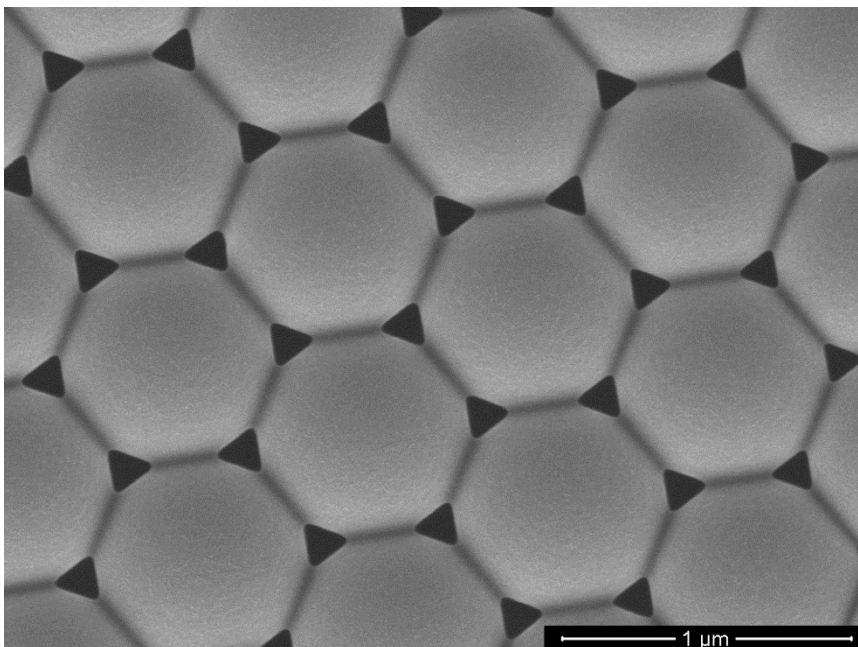


Figure 4. 22 Close-pack structure of 750 nm polystyrene nanosphere after annealing at 120 °C for 8 min

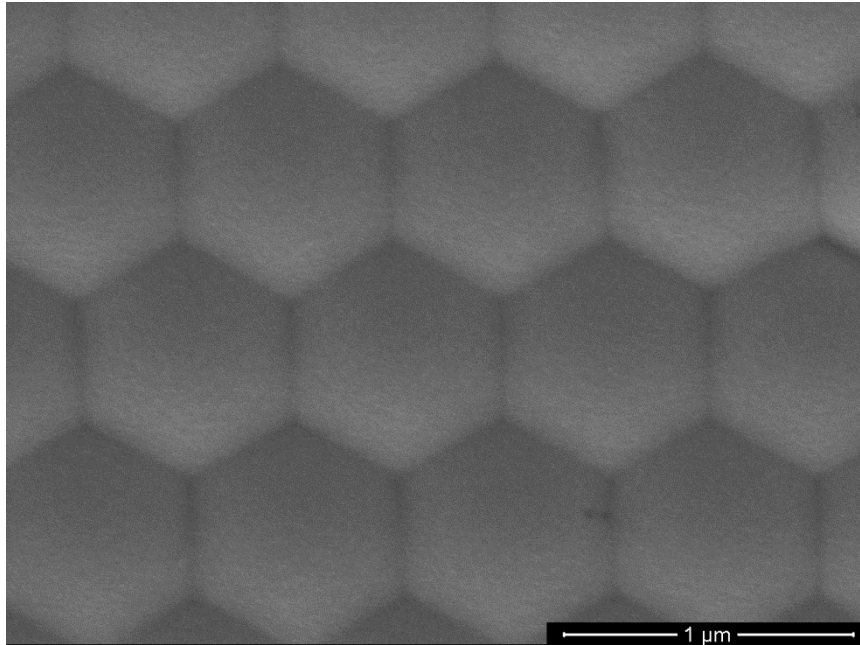


Figure 4. 23 Close-pack structure of 750 nm polystyrene nanosphere after annealing at 120 °C for 12 min

Except from Figure 4.20, all of 3 samples shown in Figure 21,22 and 23 are annealed at 120 °C for 5, 8 and 12 minutes respectively. It is clearly seen that overall shape of the spheres does not fully deformed. The only thing is melting them a little bit leading to reduction in gap size. Which means, increase in annealing time decreases gap sizes. After 12 minutes, they can be fully closed and hexagonal pattern was obtained.

As a result, annealing process can be described as an enhancement of classical NSL method that makes distance and particle size two independent parameter. That situation reproduces new lithographic mask which can be used for many processes ranging from composing different size nanoparticles to surface manufacturing combining with etching processes.

4.6 Image Analysis

Image analysis can be described as giving meaning to image by extracting it. In today's world, most of the images are taken by digital ways. In other words, all images are

made up of pixels. The color of these pixels are the combination of three main colors which are red, blue and green. The intensity of value of each colors determine each pixel's color and shade. Since size of the pixels are so small, the combination of every pixel create one big image without noticing transition between pixels. Moreover, unlike colorful, pixels are identified specific scales such as black to white or yellow to black. In this study, the transition between black to white, grayscale, is used to analyze images.

As desired target material size is between nanometer to micrometer scale, special visualization techniques is needed to transform it as an image. Because of diffraction limit of visible light, it can be almost impossible to take an image for smaller particles. For this reason, like Scanning Electron Microscope (SEM) or Atomic Force Microscope (AFM), focused electrons or sharp tips is used to get it. In this study, the main purpose is to generate nanoparticles especially in lateral way. Therefore, SEM is main tool for qualitative and quantitative image analysis. It gives grayscale images that the contrast difference is used to take images with a few nanometer resolution. Furthermore, by using magnification value and length scale, how large area and particle sizes are analyzed is determined.

Image analysis plays an essential role for detailed information. Some kind of samples have randomly distributed size many nanoparticles. And it is almost impossible to determine the size of the each nanoparticles, surface coverage and histograms of all particles. It takes much time for each images and the possibility is high for wrong calculation. For this reason, special techniques should be applied for it. In this study, Gwyddion software is used for image analysis. The basic working principle of the software based on the contrast differences inside SEM image. Every pixel has own grayscale shade. By means of this contrast difference, it is possible to make barrier between pixels. Barrier separate image into two different parts as selected and unselected. Moreover, if selected pixels are adjacent, software calculate them as a part. By this way, selected part can be analyzed with respect to each other and total area. As a result, every particle analysis can be applied by single measurement in a short period of time.

In this study, Gwyddion software is used to calculate nanoparticle size, distribution and total area coverage. All of the particles was generated by NSL and its extension.

In Figure 4.24, particles are generated by standard NSL Method. Then, substrate was annealed with 200 °C to make triangular shape nanoparticles into spherical shape particles. By using contrast differences between particles and the surface, all of the nanoparticles are selected. After that, Gwyddion software gave detailed information of the image. According to the analysis, it is found that the total area coverage is 7.7%. Moreover, histograms shows that the average particle size is about between 110 and 130 nm (Figure 4.25).

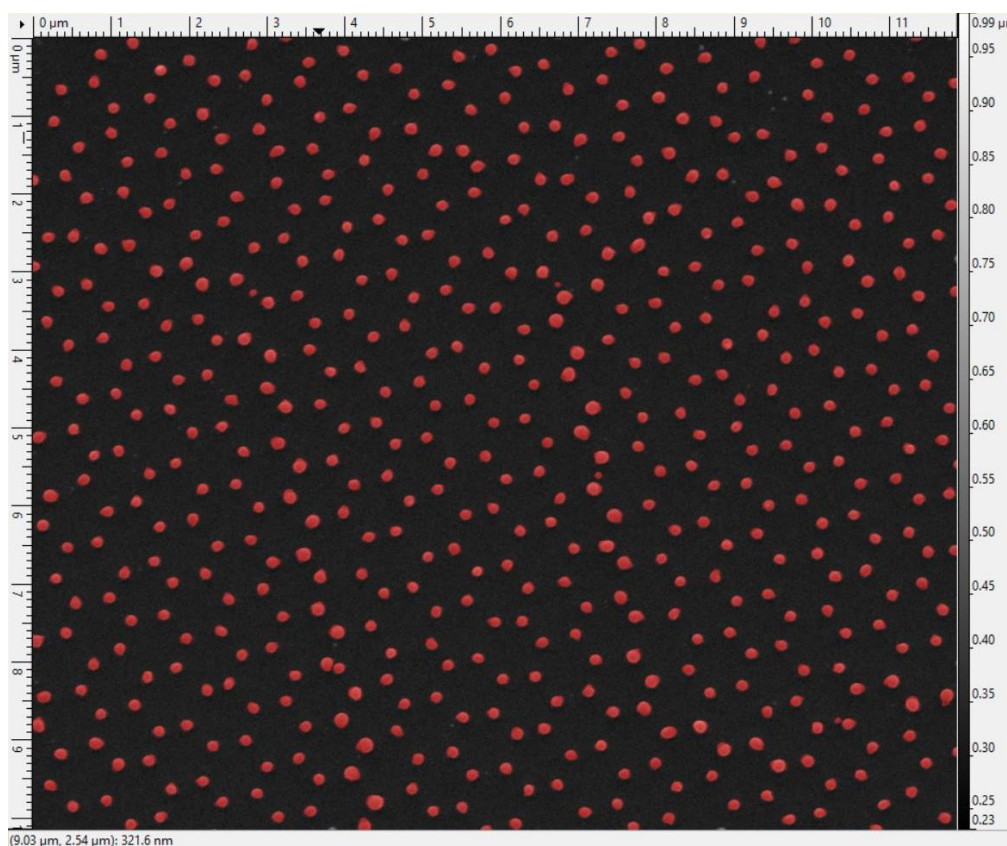


Figure 4. 24 Gwyddion particle selection of spherical particles after annealing triangular ones

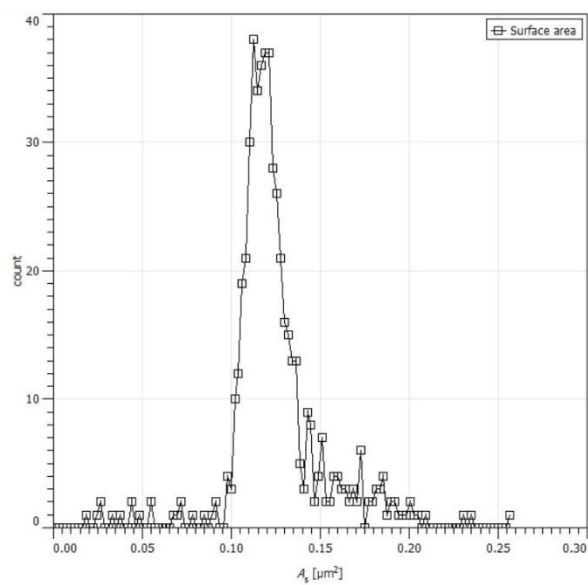


Figure 4.25 Particle size distribution of Figure 4.24

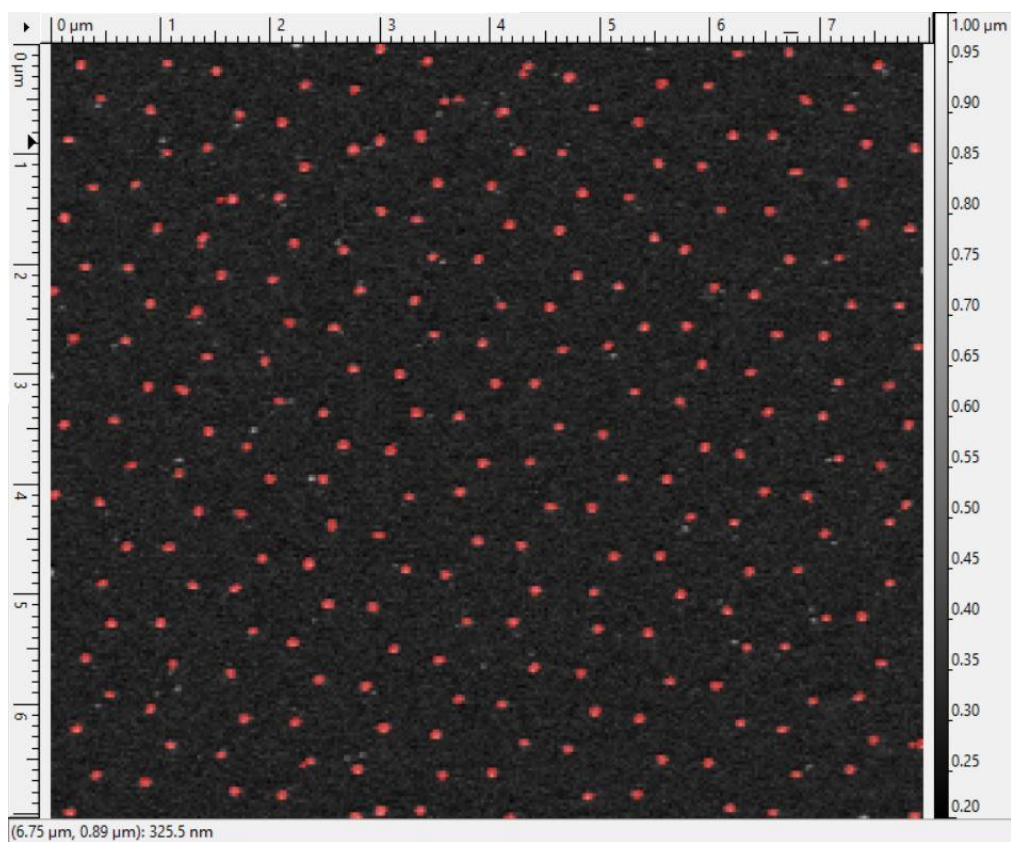


Figure 4.26 Gwyddion particle selection of spherical particles after reducing triangular gaps and annealing triangular ones

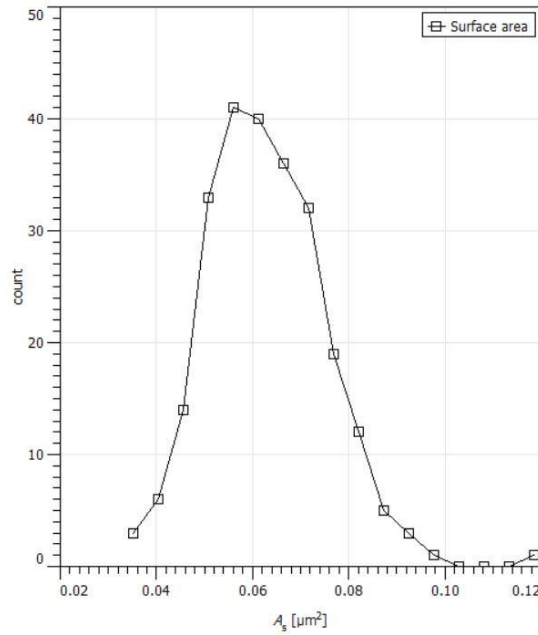


Figure 4. 27 Particle size distribution of Figure 4.26

In Figure 4.26, in addition to the standard NSL process, polystyrene nanospheres are annealed with 120 °C in three minutes before thin film coating. After this annealing process, the gap between nanospheres was reduced. By this way, as mentioned in Section 4.5.4, it can be generated small nanoparticle by using bigger nanospheres. According to the Gywddion analysis for this study, it is found that the total area coverage is 3% and the average particle diameter is 70 nm (Figure 4.27)

To sum up, it is easily understand that NSL Technique is a powerful and controllable method. All of the particle diameters, surface coverage and particle distances can be adjusted and generated with the combination of other techniques.

4.7 Numerical Calculation

All metallic nanoparticles contains free electrons. These electrons under some boundary conditions such as particle geometry, material types oscillate in the metal nanoparticle. The oscillation condition related to the surface charge density is called

as Localized Surface Plasmon's (LSPs). One of the most effective issue of LSPs is near field coupling as a result of the interaction of two close nanoparticles. Every single particle has its localized modes. With the effect of the Coulomb interaction, localized modes are couple to each other. Then, that leads to generate new hybridized modes. Considering two spherical particles with a distance r which have α_1 and α_2 polarizability, coupling can be defined by dipole approximation. The approximation gives an effective polarizability α_{eff} that can be investigated into two separated parts as longitudinally and transversally aligned dipoles. Both dipoles can be described respectively as

$$\alpha_{eff}^{long} = \frac{\alpha_1 + \alpha_2 + \frac{\alpha_1\alpha_2}{\pi r^3}}{1 - \frac{\alpha_1\alpha_2}{4\pi^2 r^6}} \quad (4.41)$$

$$\alpha_{eff}^{trans} = \frac{\alpha_1 + \alpha_2 - \frac{\alpha_1\alpha_2}{2\pi r^3}}{1 - \frac{\alpha_1\alpha_2}{16\pi^2 r^6}} \quad (4.42)$$

For the longitudinal coupling, if the distance between two spherical particles decreases, the effective polarizability value increases. Moreover, Drude-like response is analyzed in lower frequency. This is called as redshift. However, the situation is a little bit different from longitudinal mode for transversally coupled dipoles. It shows blueshift with decreasing distance.

If the two particle as close enough, both particles are expressed as dimer. The resonance shift of metallic dimers strongly related with the distance. In other words, the closer dimers are, the stronger interaction there exists. This near-field interaction generates high LSPs modes, or bonding dimer mode (BDP). Therefore, large electric field enhancement can be produced by altering the distance between two particles. The point where strongest electric field can be measured is called as *hot spot*.

In addition to the spherical particles, nanoparticles having different shapes can also exhibit coupling. One of the most well-known coupling type is bowtie antenna which is generated by two triangular shaped nanoparticles. If the gap between the particles decreases, the electric field is enhanced dramatically. This value can reach 100 times

higher than the incident electric field due to sharp edges of particles. In other words, the electrons collect more at sharp edges than smooth ones. For this reason, the stronger enhancement are analyzed [49].

To analyzed electric field enhancement as numerically, one of the most convenient software is *Comsol Multiphysics*. This software has capability to simulate large usage of areas ranging from mechanical to electromagnetics issues. As it can be easily understand from its name, electromagnetic calculation can be applied by electromagnetic related module. For this reason, all of the analysis was done by *Wave Optics Module*. The basic working principle of the module can be handled into three main parts as geometry, wave definition and results.

In geometry part, space and shape of nanoparticle are defined. Due to nanoscale particle sizes, the optimum space area should be chosen as micro scale to speed up the calculation. Then, triangular mesh structure is generated to solve electric field distribution and materials are added for environment and particles. For the wave definition, propagation direction, polarization, incident intensity and wavelength of the electric field is determined. Finally, numerical design is started. Results shows desired values by selecting it from result tabs.

In this study, three main studies were considered. Two of them are related with electric field enhancement between single and two particles as spherical and triangular shapes. The last one is about using polystyrene nanospheres as submicron lens system.

As mentioned before, high free electron density material like silver plays an essential role for plasmonic applications. For this reason, silver was chosen as material for experimental and numerical studies. To show dipole moment and coupling efficiency, spherical and triangular shaped nanoparticles having (120 nm) and (200) nm size respectively was created in air environment. By applying electric field propagating along y direction, down to up, with x-polarized, the electric field distribution over whole area was analyzed. The wavelength value of the wave was chosen 532 nm due to compare it by Raman measurement result.

For the one single spherical silver nanoparticles, free electrons are spread over the surface homogenously. When electric field is applied to it, the resonance between

incident wave and electrons happen. This situation creates electric field enhancement close to particles. As seen in Figure 4.28, normalized electric field gets its maximum values at left and right of the sphere. This situation can be explained by polarization of light. In this simulation, the polarization of incident light is along x direction; therefore, enhancement exist along x direction.

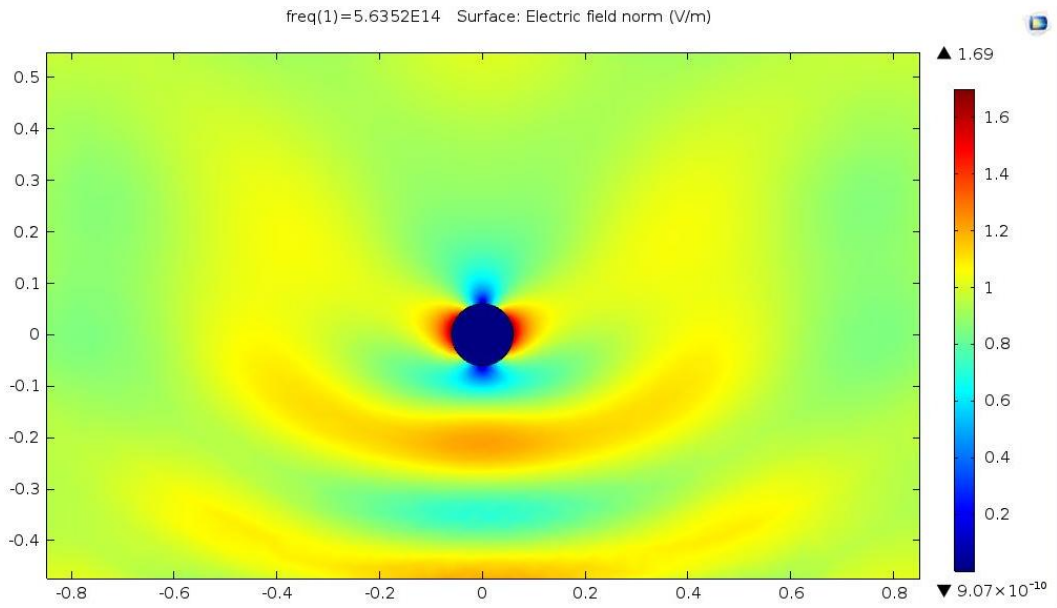


Figure 4. 28 Normalized electric field distribution caused by the interaction between 120 nm spherical single nanoparticle and x polarized electric field propagating along y direction

According to the Figure 4.29, (120) nm size spherical nanoparticles exhibit small coupling effect. The reason of this situation is that both particles are not close enough. If the distance between two particles, having same sizes, is small, there exist strong electric field enhancement due to coupling of two particles as seen in Figure 4.30.

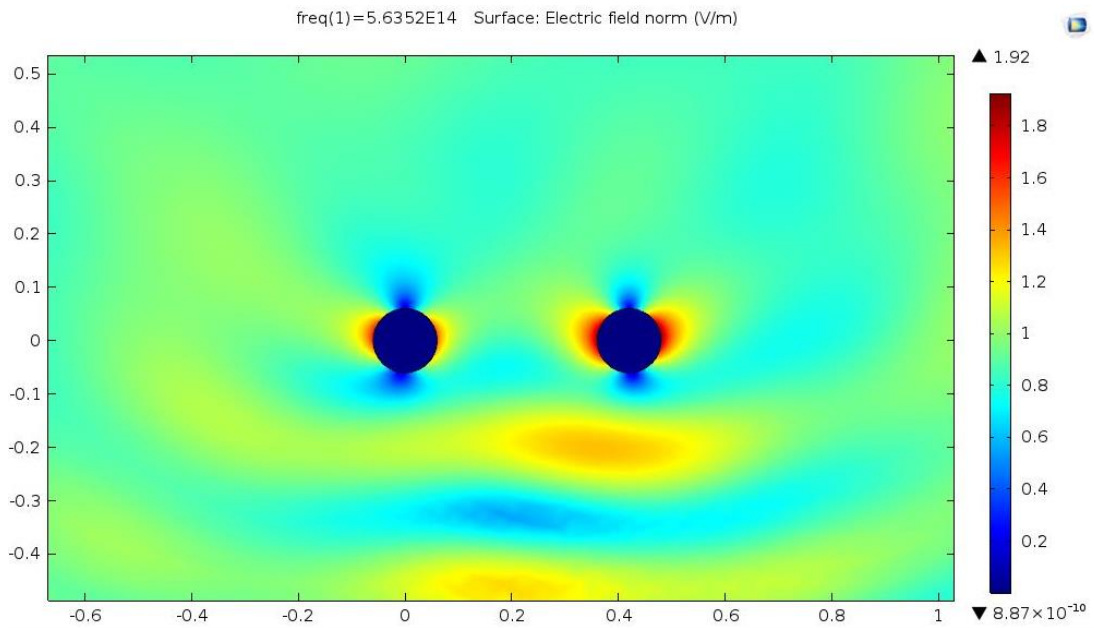


Figure 4. 29 Normalized electric field distribution caused by the interaction between two 120 nm spherical nanoparticles and x polarized electric field propagating along y direction

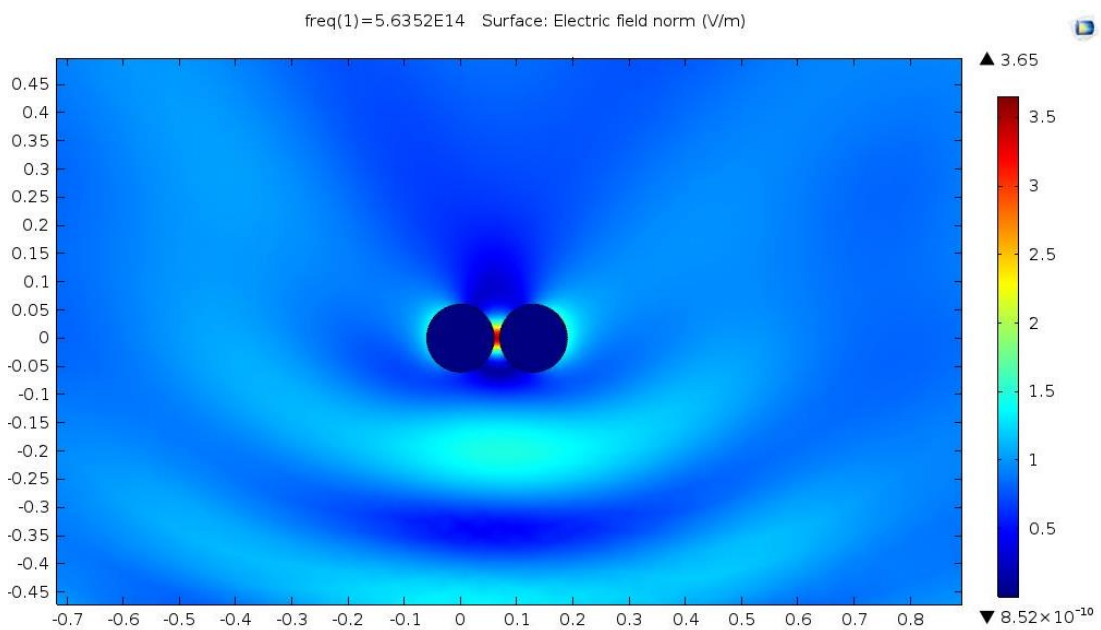


Figure 4. 30 Coupling and normalized electric field distribution caused by the interaction between two 120 nm spherical nanoparticles and x polarized electric field propagating along y direction

For the second case, instead of spherical particles, triangular shaped particles was demonstrated with holding all of the wave parameters steady. The results are clearly impressive. In other words, the electric field enhancement reaches to 3 times higher values than incident wave. This situation can be explained by two main reasons. The first one is that most of the free electrons are collected at the sharp edges of the particles. Therefore, it is high possibility that more electrons interact with each other and higher field enhancement can be obtained at that points (Figure 4.31). Another reason is about the distance between the particles. By using standard NSL techniques, triangular shaped nanoparticles are very close to each other at the beginning. This situation leads to strong electric field enhancement (Figure 4.32). As a result, it is quiet normal to get higher enhancement before annealing the triangular nanoparticles generated by NSL.

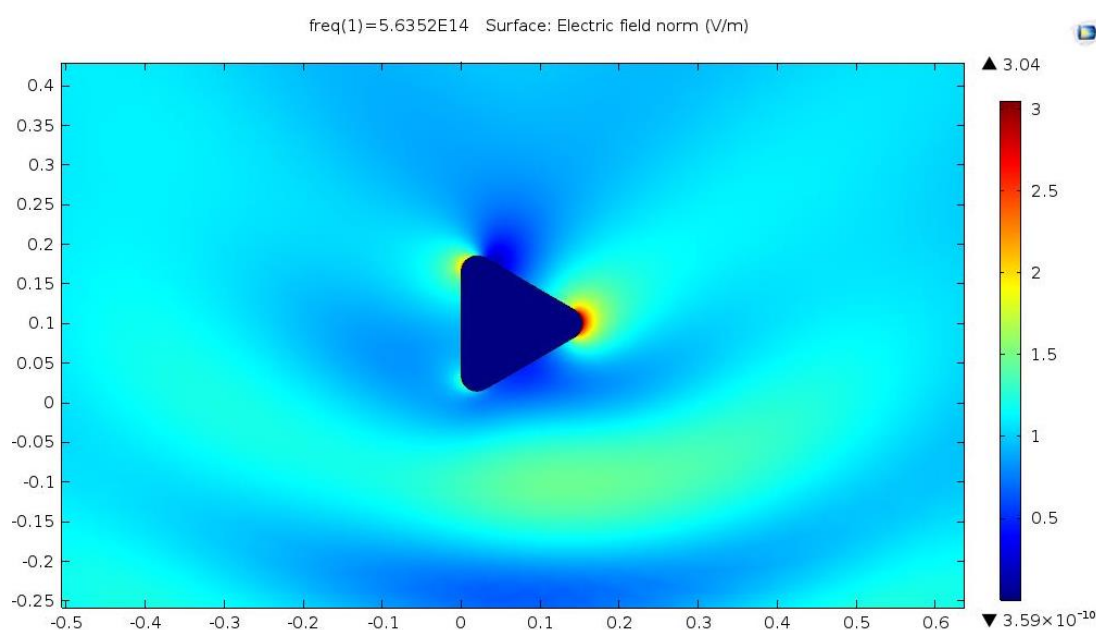


Figure 4. 31 Normalized electric field distribution caused by the interaction between 200 nm triangular single nanoparticle and x polarized electric field propagating along y direction

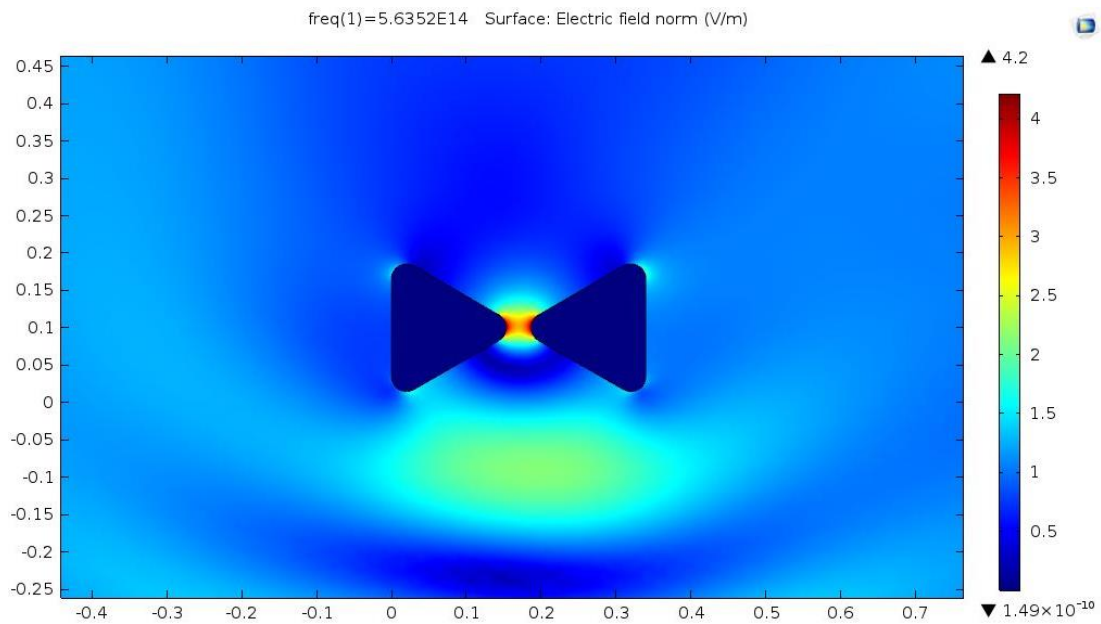


Figure 4. 32 Coupling and normalized electric field distribution caused by the interaction between two 200 nm triangular nanoparticles and x polarized electric field propagating along y direction

In addition to the coupling effect, polystyrene nanospheres can be used as submicron lens array. As mentioned in Section 4.5.4, it is possible to close all gaps between nanospheres by annealing nanospheres. This situation generates hexagonal shaped lens like systems that both surfaces are convex. Which means, their shapes resemble biconvex lens. Top surface of this structure can be used as desired pattern with Nanoimprint Lithography technique. If transferred this pattern to substrate surface, curved honeycomb lens array like structure but seemed as convex in 2D can easily be generated.

According to the Figure 4.33, 532 nm light source was applied to 2 μm periodicity curved interface between air and silicon. As clearly seen in simulation, the electric field gets its maximum values at some points inside the silicon substrate. This means that wave is focused on some certain points depending on the wavelength, size of the lens array and substrate types. Therefore, it can be said that NSL technique is suitable for other kind of applications rather than plasmonics.

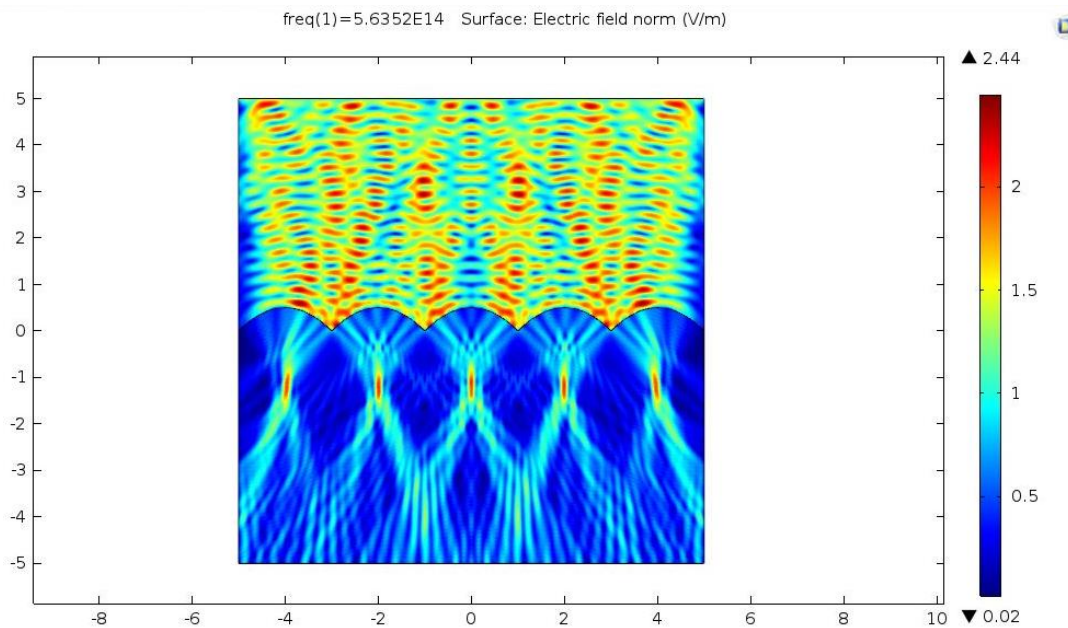


Figure 4. 33 Refraction of light from air-silicon interface

4.8 Optical Measurements

4.8.1 Surface Enhanced Raman Measurement

By using 750 nm polystyrene nanospheres as a deposition mask, triangular shaped particles are formed all the surface of polished silicon wafer surface. The material of the particles are chosen silver due to its high electron density. Then, light source was applied to the sample to measure field enhancement rate.

According to the Figure 4.34, surface enhanced raman spectroscopy measurement are taken both silicon wafer and triangular silver islands coated silicon wafer. For both samples have one single peak coming from silicon. Moreover, it is clearly seen that the intensity value was increase about 15% higher than initial one. This means that metal nanoparticles enhances total electric field near sharp corners of triangles.

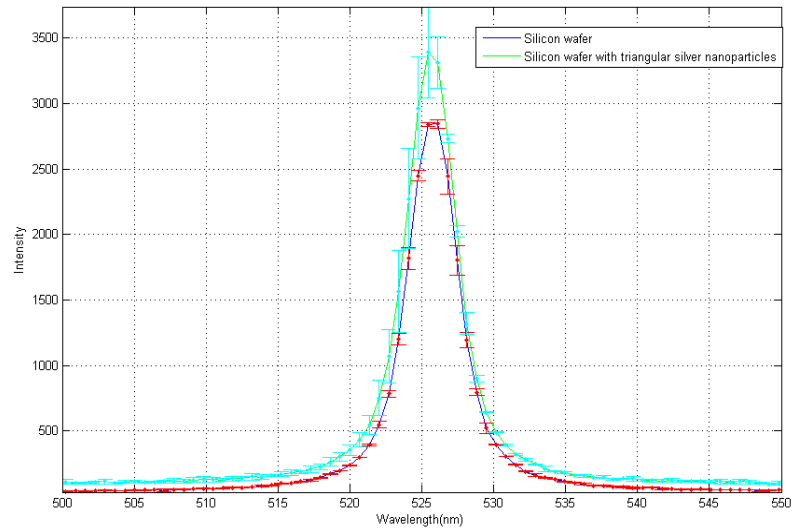


Figure 4. 34 Raman measurement of silicon wafer and 200 nm triangular silver nanoparticle coated silicon wafer

Considering the triangular nanoparticles, they cover almost 10% of all surface. As a result of interaction between metal particle and wave, electric field enhancement occur at sharp edges of them depending on polarization and particle position. High field enhancement is observed close to each particle but that affect whole system. According to the raman measurement (Figure 4.34), the total enhancement was measured 15%. In order to calculate the enhancement factor of each particle

$$\left(Enhancement\ factor \times \frac{10}{100}\right) + \left(1 \times \frac{90}{100}\right) = \frac{115}{100}$$

Then, enhancement factor can be found as 2.5 which matches simulated value (Figure 4.31) regardless of coupling, defects, particle position or polarization.

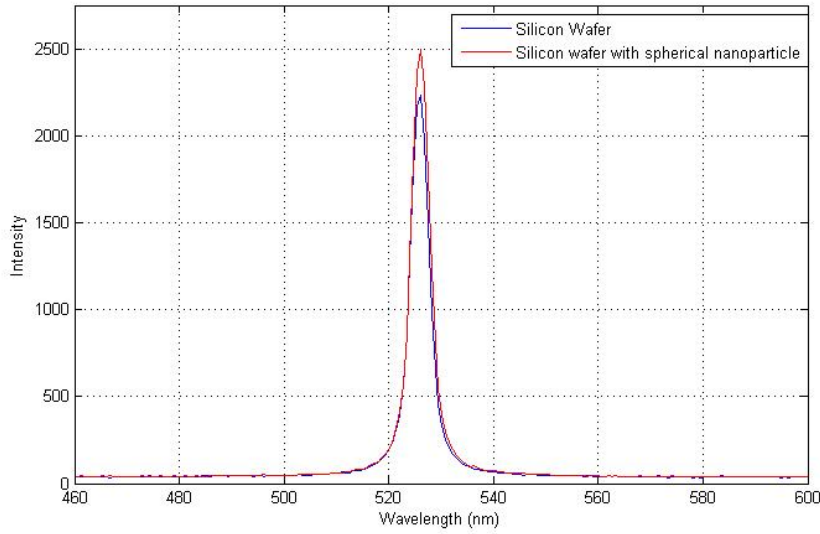


Figure 4. 35 Raman measurement of silicon wafer and 120 nm spherical silver nanoparticle coated silicon wafer

For the second case, Figure 4.35, triangular shaped nanoparticles were annealed at 200 °C for 1 hour. After annealing process, nanoparticles were rounded; in other words, triangular nanoparticles were transformed into spherical particles. After that, the same measurement procedure was applied for it. As a result, about 13% electric field enhancement was observed.

For the spherical particle, same calculation can be applied in order to calculate the enhancement factor. According to Figure 4.24, surface coverage of spherical particles was calculated about 7.7% of total area. Then, enhancement factor can be measured by considering the raman measurement result (Figure 4.35) as

$$\left(\text{Enhancement factor} \times \frac{7.7}{100} \right) + \left(1 \times \frac{92.3}{100} \right) = \frac{113}{100}$$

As a result, enhancement factor is found 2.81. Each spherical particle act as a dipole moment when interact with electric field. Therefore, simulated value (Figure 4.28) should be multiplied by two. As a result calculated and measured value close to each other regardless of coupling, defects or polarization

As mentioned in Section 4.6, the electric field is enhanced in both conditions due to plasmonic effects of metallic nanoparticles. Furthermore, the enhancement percentages are seen close to each other or reduced. However, it does not mean that annealing triangular metal nanoparticles decreases the field enhancement. The physical concept behind this situation can be explained by Surface Enhance Raman Spectroscopy (SERS) and its particle shape and size dependency. In other words, the resonance frequency change its position with altering particle size and shape [50, 51]. To sum up, for this measurement, the correct result can be explained as metallic nanoparticles produced by NSL exhibit plasmonic effects that enhanced the electric field.

4.8.2 Reflection Measurement

NSL is a special tool that deposited spherical particles to the substrate surface as close-pack acts a 3D photonic crystal. As a result of this structure, whole system behave as diffraction grating [52]. To better understand this situation, analyzing constructive and destructive interference peaks coming from reflection measurement can be used. Therefore, nanosphere deposited and nondeposited silicon wafer reflection measurement were taken.

According to the Figure 4.36, it is clearly seen that reflection values fluctuates with increasing wavelength value for coated sample. This circumstance prove that system acts as diffraction grating.

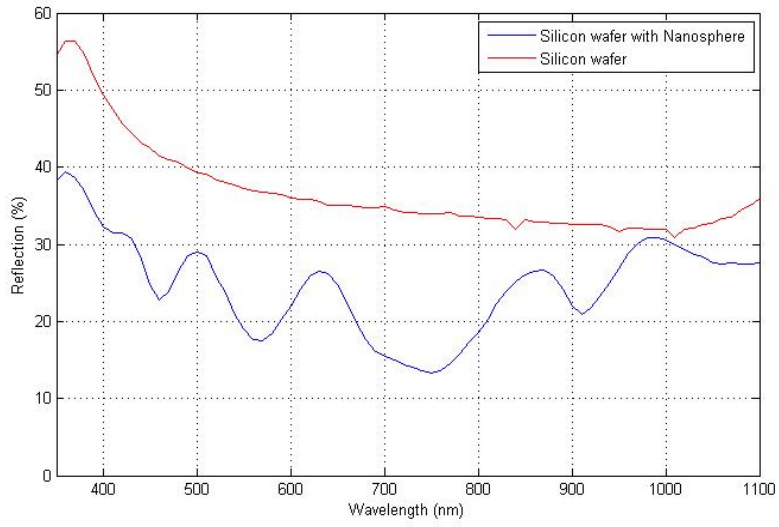


Figure 4. 36 Reflection measurement of uncoated and close-pack nanosphere coated silicon wafer

CHAPTER 5

CONCLUSIONS

In this study, the main aim is to implement special nanostructuring technique called NSL and try to extend its capabilities. Most of the commercial lithography methods can be divided into two different subtitles as top-down and bottom-up. While top-down approach based on break bigger parts into nanometer to micrometer scale smaller parts, bottom-up approach uses smaller particles to produce bigger ones. Moreover, depending on their capabilities, most of these methods can be implemented specific area of usage. Like applicability for large area, high cost, special tool demand or resolution, some features causes depreciation of their importance. For this reason, it is very essential to constitute new method like NSL containing valuable features for production. This special method can be described as a combination of both approaches due to their capabilities. In detail, it is cheap, easy to implement, inherently parallel and high throughput material nano manufacturing method which is versatile tool for large variety of nanoparticle buildings and well-ordered 2D and 3D arrays. This theses describe our last studies to extend the scope of NSL to include fabrication processes of different shape nanoparticle motifs, their characterizations and beyond the capabilities of classical NSL.

In classical method, periodic well-ordered metal nanoparticles can be generated by three main steps which are close-pack nanosphere structuring, thin film deposition and lift-off. These steps that detailed procedures were given in Chapter 4 play an essential role for particle generation. In other words, there exists some defects during production if spheres are not arranged well-ordered, thin film is not deposited in correct parameters or wrong lift-off chemical is chosen. The detailed of each steps were optimized and rearranged by means of the SEM image characterizations. After optimized production parameters, the metallic nanoparticles were successfully fabricated for large area as possible as without defects. For the deposition material, silver were chosen as a suitable material due to its high free electrons density. This is

very important especially for plasmonic applications; however, dielectric or other metallic materials can be used as target material for any other applications. It depends on in which application worked on. As a result, well-ordered triangular shaped metal nanoparticles were produced successfully. Nevertheless, whatever size nanosphere is used, the shape of the particles and total surface coverage do not alter. The variable parameters are the size of the particle and the distance between the particles related to the size of sphere. But the real problem is that these parameters cannot be handled as separate parts due to their linear relationship. For this reason, classical NSL method is not enough for desired pattern exactly but it is necessary for plasmonic applications.

To better understand their plasmonic effects, at first, 750 nm diameter polystyrene nanospheres are deposited on silicon substrate surfaces. Therefore, approximately 220 nm triangular metal islands were fabricated successfully. When applied electric field to these metallic particles, almost %20 to %25 the electric field enhancement coming from resonance between electromagnetic wave and electrons was observed from Raman Spectroscopy Measurement. This result was also supported by Comsol simulations for one single particle and coupling effect between two particles.

In addition to material type and size of the particle, particle shape, surface coverage and distance between the particles can be described important parameters for plasmonics. As discussed in Chapter 4, classical NSL method do not have any capability to change these parameters separately. For this reason, it is needed to improve the method by means of some external impacts. One of most power powerful tool for it is thermal annealing by means of oven. This process can be applied to metallic particles or nanosphere itself. Annealing triangular shape metallic particles causes shape transformation into spherical ones because of low interfacial energy. Therefore, spherical nanoparticles having lower diameter were achieved in this study. On the other hands, heating close-pack polystyrene nanosphere structure at 120 °C melts them and leads to decrease the gap between three nanospheres. This temperature is the optimized value to adjust reduction of gaps sized with respect to time. The more time it is applied, the more reduction it exist. Finally, it is possible to close whole spaces with higher implementation time. This circumstance especially important to produce smaller triangular particles that the distance between them are greater. After

thin film deposition and lift-off processes, if the particles annealed again, the particles having same distances but spherical shape ones can be generated. As a result, two particle distance can be controlled by the chosen nanosphere diameter while the particle size can be adjusted by annealing. In other words, this study carried out successfully one step further beyond the classical NSL technique.

Another powerful concept is double layer NSL method. By using this, it is possible to reduce particle sizes and total particle surface coverage since the second layer not only close half of the triangular gaps coming from first layer totally but also blocks half size of the remaining gaps. Therefore, hexagonal like smaller nanoparticle can be produced as mentioned in Section 4.2.

All of these extensions to the classical method are related to the decrease the size of the particle and total surface coverage. By combining all with tilted evaporation, close-pack nanosphere structure acts as the mask which is a little bit further to the surface. This creates an opportunity to produce more than one single particle from one single hole. Therefore, the surface coverage can be obtained by the multiplication factors of both number and the angle of depositions.

Beyond nanoparticle generation for plasmonics, nanospheres can be used as 3D photonics crystal as a diffraction grating as discussed in Section 2.1.5. Furthermore, NSL method is capable of surface modification and also it can be recombined with other lithography methods and physicochemical processes. For example, as mentioned above, the gap between spheres was totally closed by annealing. Then, periodic honeycomb structure having curvature curve was produced successfully in this study. The recombination of this surface with nanoimprint lithography and transfer it to another substrate creates an opportunity for surface texturing. This texturing is challenging problem by using other kind of lithography methods and needs special tools. However, it is easy to succeed it by a few steps by NSL. On the contrary to closing holes, oxygen plasma have an influence on polystyrene nanosphere to reduce their sizes without changing their original positions. In this study, with the effect of it, diameter of polystyrene nanosphere was decreased to 200 nm from 400 nm. Therefore, well-ordered but separate nanosphere structure was achieved successfully. For this process, diameter of spheres at the beginning determine the distance between two

spheres while oxygen plasma duration indicate how much reduction in size exist. As a result, this kind of structure can be used to produce either periodic nanowire or nanohole as desired size and periodicity with the combination of physical or chemical etching mechanisms. In the future, NSL can be combined with Hole Mask Lithography system to produce well-ordered and complex plasmonic structures.

REFERENCES

- [1] S. Horikoshi and N. Serpone, "Introduction to Nanoparticles," *Microwaves Nanoparticle Synth. Fundam. Appl.*, pp. 1–24, 2013.
- [2] T. Quirk, "There's plenty of room at the bottom," *Australas. Biotechnol.*, vol. 16, no. 3, p. 36, 2006.
- [3] Å. Thidell and P. Arnfalk, "Nanoparticles : A Closer Look at the Risks to Human Health and the Environment Perceptions and Precautionary Measures of Industry and Regulatory Bodies in Europe Åsgeir Helland," *Environ. Manage.*, no. October, 2004.
- [4] V. L. Kumar, "STUDY OF MAGNETIC NANOSTRUCTURES FABRICATED BY NANOSPHERE LITHOGRAPHY," 2007.
- [5] M. A. AGAM, "An Investigation of physical processes in nanosphere lithography," 2006.
- [6] L. N. Ng, "Manipulation of Particles on Optical Waveguides," 2000.
- [7] M. Kolwas, "Scattering of Light on Droplets and Spherical Objects: 100 Years of Mie Scattering," *Comput. Methods Sci. Technol.*, 2010.
- [8] C. Mätzler, "MATLAB Functions for Mie Scattering and Absorption," 2002.
- [9] B. García-Cámara, "On Light Scattering by nanoparticles with conventional and non-conventioanl optical properties," 2010.
- [10] C. Gruber, "Photonic Metal Structures via Self-Assembly Processes," 2010.
- [11] "Optical Properties of Solids." [Online]. Available: http://ocw.mit.edu/courses/mechanical-engineering/2-58j-radiative-transfer-spring-2006/readings/chap6_solid_prop.pdf.
- [12] M. Thoreson, Z. Liu, U. Chettiar, and P. Nyga, "Studies on metal-dielectric plasmonic structures," 2010. [Online]. Available: http://ocw.mit.edu/courses/mechanical-engineering/2-58j-radiative-transfer-spring-2006/readings/chap6_solid_prop.pdf.

- [13] P. Di Sia, “Modelling at Nanoscale,” pp. 3–22, 2012.
- [14] E. C. F. García-Santamaría, Nelson and P. V Braun, “An optical surface resonance may render photonic crystals ineffective,” no. 111, pp. 1–6.
- [15] Z. Hao, S. Han, J. Wang, and Y. Luo, “2D Photonic Crystal Structures Fabricated by Nanosphere Lithography,” *Lasers Electro-Optics, 2005. CLEO ...*, pp. 235–236.
- [16] A. Nuermairaiti, “Studies on the Self-organization of Colloidal Nanoparticles at Interfaces.”
- [17] N. Vogel, “Surface Patterning with Colloidal Monolayers.”
- [18] G. Trefalt and M. Borkovec, “Overview of DLVO Theory,” pp. 1–10, 2014.
- [19] S. J. Mejia-Rosales, A. Gil-Villegas, B. I. Ivlev, and J. Ruiz-García, “Predicting the phase diagram of two-dimensional colloidal systems with long-range interactions,” *J. Phys. Chem. B*, vol. 110, no. 44, pp. 22230–22236, 2006.
- [20] P. Colson, C. Henrist, and R. Cloots, “Nanosphere lithography: A powerful method for the controlled manufacturing of nanomaterials,” *J. Nanomater.*, vol. 2013, 2013.
- [21] G. Venugopal and S. Kim, *Advances in Micro/Nano Electromechanical Systems and Fabrication Technologies*. 2013.
- [22] A. Rosa, M. Yan, R. Fernandez, X. Wang, and E. Zegarra, “Top-down and Bottom-up approaches to nanotechnology,” *Portl. State Univ.*
- [23] M. Liu, J. Zhuoyu, and S. Liwei, “Top-Down Strategy,” vol. 8, 2010.
- [24] C. Wang, “Thermally annealed plasmonic nanostructures,” 2012.
- [25] S. Landis, *Nano Lithography*. .
- [26] B. D. Lucas, J. S. Kim, C. Chin, and L. J. Guo, “Nanoimprint lithography based approach for the fabrication of large-area, uniformly oriented plasmonic arrays,” *Adv. Mater.*, vol. 20, no. 6, pp. 1129–1134, 2008.
- [27] S. Mohammad, Ali Mohammed, Mustafa, Muhammad, Stepanova, Maria, Dew,

- “Nanofabrication Techniques and Principles,” *Nanofabrication Tech. Princ.*, p. 344, 2012.
- [28] Q. Li, *Anisotropic Nanomaterials*. .
- [29] N. A. Kotov and P. S. Weiss, “Self-assembly of nanoparticles: A snapshot,” *ACS Nano*, vol. 8, no. 4, pp. 3101–3103, 2014.
- [30] A. S. Iyer and K. Paul, “Self-assembly: a review of scope and applications,” *IET Nanobiotechnology*, vol. 9, no. 3, pp. 122–135, 2015.
- [31] J.-O. Carlsson and P. M. Martin, *Handbook of Deposition Technologies for Films and Coatings: Science, Applications and Technology*. 2010.
- [32] A. Frommhold, A. P. G. Robinson, and E. Tarte, “High aspect ratio silicon and polyimide nanopillars by combination of nanosphere lithography and intermediate mask pattern transfer,” *Microelectron. Eng.*, vol. 99, pp. 43–49, 2012.
- [33] A. Tsigara, A. Benkhial, S. Warren, F. Akkari, J. Wright, F. Frehill, and E. Dempsey, “Metal microelectrode nanostructuring using nanosphere lithography and photolithography with optimization of the fabrication process,” *Thin Solid Films*, vol. 537, pp. 269–274, 2013.
- [34] W. Y. Ji, I. S. Jae, M. A. Ho, and G. K. Tae, “Fabrication of Nanometer-scale Pillar Structures by Using Nanosphere Lithography,” *J. Korean Phys. Soc.*, vol. 58, no. 42, p. 994, 2011.
- [35] K. Sparnacci, D. Antonioli, S. Deregibus, G. Panzarasa, M. Laus, N. de Leo, L. Boarino, V. Kapeliouchko, and T. Poggio, “Two-dimensional non-close-packed arrays of nanoparticles via core-shell nanospheres and reactive ion etching,” *Polym. Adv. Technol.*, vol. 23, no. 3, pp. 558–564, 2012.
- [36] F. Járαι-Szabó, S. Aștilean, and Z. Néda, “Understanding self-assembled nanosphere patterns,” *Chem. Phys. Lett.*, vol. 408, no. 4–6, pp. 241–246, 2005.
- [37] E. M. Akinoglu, A. J. Morfa, and M. Giersig, “Nanosphere lithography-exploiting self-assembly on the nanoscale for sophisticated nanostructure

- fabrication,” *Turkish J. Phys.*, vol. 38, no. 3, pp. 563–572, 2014.
- [38] S. J. Barcelo, S. Lam, G. A. Gibson, X. Sheng, and D. Henze, “Nanosphere lithography based technique for fabrication of large area , well ordered metal particle arrays,” 2012.
- [39] C. Geng, L. Zheng, J. Yu, Q. Yan, T. Wei, X. Wang, and D. Shen, “Thermal annealing of colloidal monolayer at the air/water interface: a facile approach to transferrable colloidal masks with tunable interstice size for nanosphere lithography,” *J. Mater. Chem.*, vol. 22, no. 42, p. 22678, 2012.
- [40] C. M. Zhou and D. Gall, “Surface patterning by nanosphere lithography for layer growth with ordered pores,” *Thin Solid Films*, vol. 516, no. 2–4, pp. 433–437, 2007.
- [41] A. Mohammadkhani and K. Jiang, “Fabrication of dual patterned nanocavities using double layer nanosphere lithography,” *Proc. IEEE Conf. Nanotechnol.*, pp. 9–12, 2011.
- [42] B. J. Y. Tan, C. H. Sow, T. S. Koh, K. C. Chin, A. T. S. Wee, and C. K. Ong, “Fabrication of size-tunable gold nanoparticles array with nanosphere lithography, reactive ion etching, and thermal annealing,” *J. Phys. Chem. B*, vol. 109, no. 22, pp. 11100–11109, 2005.
- [43] M. D. Ionita, D. Kontziampasis, B. Mitu, A. Smyrnakis, E. Gogolides, and G. Dinescu, “Management of polymeric spheres diameter in colloidal lithography by low and atmospheric pressure plasma treatments,” 2015.
- [44] Y. Zhang, X. Wang, Y. Wang, H. Liu, and J. Yang, “Ordered nanostructures array fabricated by nanosphere lithography,” *J. Alloys Compd.*, vol. 452, no. 2, pp. 473–477, 2008.
- [45] C. L. Cheung, R. J. Nikolic, C. E. Reinhardt, and T. F. Wang, “Fabrication of nanopillars by nanosphere lithography,” *Nanotechnology*, vol. 17, pp. 1339–1343, 2006.
- [46] K. Ellinas, A. Smyrnakis, A. Malainou, A. Tserepi, and E. Gogolides, “‘Mesh-assisted’ colloidal lithography and plasma etching: A route to large-area,

- uniform, ordered nano-pillar and nanopost fabrication on versatile substrates,” *Microelectron. Eng.*, vol. 88, no. 8, pp. 2547–2551, 2011.
- [47] W. Li, W. Zhao, and P. Sun, “Fabrication of highly ordered metallic arrays and silicon pillars with controllable size using nanosphere lithography,” *Phys. E Low-Dimensional Syst. Nanostructures*, vol. 41, no. 8, pp. 1600–1603, 2009.
- [48] A. Kosiorek, W. Kandulski, H. Glaczynska, and M. Giersig, “Fabrication of nanoscale rings, dots, and rods by combining shadow nanosphere lithography and annealed polystyrene nanosphere masks,” *Small*, vol. 1, no. 4, pp. 439–444, 2005.
- [49] P. Patoka, “Tunable plasmonic properties of nanostructures fabricated by shadow nanosphere lithography,” 2011.
- [50] H. Guo, W. Xu, J. Zhou, S. Xu, and J. R. Lombardi, “Highly efficient construction of oriented sandwich structures for surface-enhanced Raman scattering,” *Nanotechnology*, vol. 24, no. 4, p. 045608, 2013.
- [51] H. Im, K. C. Bantz, S. H. Lee, T. W. Johnson, C. L. Haynes, and S. H. Oh, “Self-assembled plasmonic nanoring cavity arrays for SERS and LSPR biosensing,” *Adv. Mater.*, vol. 25, no. 19, pp. 2678–2685, 2013.
- [52] J. Eisenlohr, J. Benick, M. Peters, B. Bläsi, J. C. Goldschmidt, and M. Hermle, “Hexagonal sphere gratings for enhanced light trapping in crystalline silicon solar cells,” *Opt. Express*, vol. 22 Suppl 1, no. January, pp. A111–9, 2014.
- [53] H. A. Lorentz, “Versuch einer Theorie der Electricischen und Optischen Erscheinungen in Bewegten Körpern” 1906.